AD NUMBER

AD472539

NEW LIMITATION CHANGE

TO

Approved for public release, distribution unlimited

FROM

Distribution authorized to U.S. Gov't. agencies only; Administrative/Operational Use; 7 Oct 1965. Other requests shall be referred to Department of Defense [DoD], Attn: Public Affairs Office, Washington, DC 20301.

AUTHORITY

Boeing Co. ltr, 17 Mar 1975

SECURITY MARKING

The classified or limited status of this report applies to each page, unless otherwise marked.

Separate page printouts MUST be marked accordingly.

BOEING

SEATTLE, WASHINGTON

THE BOEING COMPANY

REV LTR

CODE IDENT. NO. 81205

NUMBER D2-90683-1

TITLE: CRATERING CHARACTERISTICS OF WET AND DRY SAND

FOR LIMITATIONS IMPOSED ON THE USE OF THE INFORMATION CONTAINED IN THIS DOCUMENT AND ON THE DISTRIBUTION OF THIS DOCUMENT, SEE LIMITATIONS SHEET.

MODEL _____ CONTRACT _____

ISSUE NO. _____ ISSUED TO: _____

PREPARED BY C. V. FULMER 10-7-65

SUPERVISED BY D. M. YOUNG 10-8-65

APPROVED BY J. A. BLAYLOCK

APPROVED BY G. L. KEISTER 10/9/65

SHEET 1

U3 4802 1430 ORIG. 4/65

ABSTRACT

Thirty-seven 1-pound spheres of TNT were individually exploded at various depths of burst in a sand test pad. Of these, 19 detonations were conducted in a dry-sand medium and 18 in a wet-sand medium at comparable depths of burst. The craters produced were accurately surveyed by using a bridge and probe assembly. The results of these crater surveys are shown on topographic maps. In addition to topographic measurements, volumetric measurements of the craters, ejecta measurements, and medium density, moisture content, and grain size distributions are presented.

The experimental procedures, equipment, test area, and sand medium are discussed in detail. The comparison of crater characteristics of wet- and dry-sand environments are discussed and the results presented in tables and graphs. In addition to the crater characteristics, the formation of intracone structures, shock-agglutinated missiles, and the reduction in size of the sand grains composing the medium are discussed.

KEY WORDS

Mass distribution	Intracone structure	Uplifted ground surface
Apparent crater	Lip crest	Original ground surface
True crater	Apparent lip crest height	Ejecta
Fallback material	Surface burst	Crater characteristics

TABLE OF CONTENTS

LIST OF ILLUSTRATIONS

LIST OF ILLUSTRATIONS (Continued)

LIST OF ILLUSTRATIONS (Continued)

LIST OF TABLES

1 INTRODUCTION

1.1 BACKGROUND

1.1.1 Lampson's empirical calculations and many subsequent studies using chemical and nuclear explosions have demonstrated that crater size can be used as a criterion for predicting damage to existing structures from ground shock and ejected debris. Yet, despite numerous investigations undertaken since World War II, the phenomenology of crater formation by explosive detonation is not well understood. To date, nuclear surface detonations have been confined to two natural media: (1) the desert alluvium of the Nevada test site and (2) the saturated and sometimes submerged coral formations of the Pacific test site. Cratering experiments using a chemical explosive have been undertaken in various media: desert alluvium, glacial alluvium, weathered soils, sand, clay and gravel, as well as in sedimentary, igneous, and metamorphic rock.

1.1.2 Detailed studies of crater dimensions obtained from these tests show the formation of significantly larger craters in near-saturated media. One possible explanation for this result is that wave action causes erosion and downward slippage of the crater walls, which is followed by the filling of these craters with sea water; moreover, the moisture content and chemical composition of the coralline medium may have also influenced the crater dimensions.

1.1.3 Specific experiments have not been performed to evaluate the effects of soil moisture on crater parameters; therefore, information relating to the influence of moisture content on explosive crater formation is scarce.

1.2 OBJECTIVES

The primary purpose of the experiment described in this document was to determine the influence of moisture content on the physical dimensions of explosive craters in sand. A secondary objective of this experiment was to determine the amount of grain size reduction in the sand medium caused by the detonation of the explosive charges.

2 EXPERIMENTAL PROCEDURE

2.1 DESCRIPTION OF THE EXPERIMENT

2.1.1 Thirty-seven 1-pound spheres of TNT were exploded in a sand-filled test pit. The test area used for this experiment is located in Area 5 of The Boeing Company Tulalip test site, Marysville, Washington. The experiment was conducted in two parts: The first part consisted of 19 detonations with the charge placed at various burial depths in a dry-sand medium; the second part consisted of 18 detonations at similar burial depths but in a wet-sand medium. The burial depths for charges used in the dry-sand medium were 0, 50.8, 76, 102, 152, 228, 305, 381, 457, 533, 610, 686, and 762 millimeters below the surface of the test pad. Charges were also detonated at 50.8 and 76 millimeters above the surface of the test pad. Burial depths used in the wet-sand medium were 50.8, 102, 228, 381, 508, 533, and 686 millimeters below the surface of the test pad. Additional detonations took place at 0 and at 50.8 millimeters above the wet-sand surface.

2.1.2 For all shots in the dry-sand medium, the moisture content was less than 0.5 percent by weight. Maintaining a uniform moisture content throughout the sand medium for the wet-sand shots proved difficult. Several different methods were used in the attempt to achieve a standard and uniform moisture content. The most satisfactory method involved wetting the surface of the sand pad with a fine spray of water until the entire pad and underlying pit were saturated. A sump, located at the base of the test pit, was pumped throughout the wetting operation, and the water level in the sump was held at a minimum. Additional water was sprayed on the test pad while the sump was being emptied. This prevented drying out of the pad's surface. The pump and water were turned off before the charge was placed in position and armed.

2.1.3 The original surface of the test pad was carefully restored by backfilling the shot hole with tamped wet sand. A small wood block was used to tamp and level the surface area of the filled shot hole. When overhead motion pictures were taken, the shot position was marked with an X painted on the restored surface of wet sand. The entire operation of loading and backfilling the shot hole required approximately 5 minutes. During this time, water was not sprayed on the surface of the test pad not pumped from the sump.

2.1.4 Five shots of the wet-sand series (W2.5A, W3.5A, W4.5A, W5.5A, and W6.4A) were repeated because of a hard, impervious, dense horizon and a perched water table that formed approximately 20 inches below the surface of the test pad.

2.2 SEQUENCE OF EVENTS

2.2.1 Field testing followed the sequence listed below:

1. Firing site prepared by compacting the test pad to a uniform density and leveling the surface of the pad to ±2 millimeters.

2. Pretest survey made to establish topographic datum.

3. Debris-sampling pads located and emplaced; geometric patterns painted on the test pad surface.

4. Sand pad wetted and the sump pit pumped as required.

5. Test instruments, firing circuits, and photographic equipment checked.

6. Charge emplaced and burst depth verified. Backfilling accomplished to maintain a uniform density.

7. Area evacuated.

8. Countdown completed and charge fired.

9. Firing site checked.

10. High-speed motion-picture equipment removed. Postshot crater photographs taken as required.

11. Postshot crater survey made; debris samples recovered.

12. Debris samples dried and weighed.

13. Shock-comminuted material removed.

2.2.2 Generally, this sequence of events required 2 or 3 days work to complete a single detonation. No shots were detonated when prevailing weather conditions could influence the validity of the results. (A large vinyl-coated nylon tarpaulin was used to cover the pad when it was not in use.)

2.2.3 The usual sequence of events during the preparation and detonation of the dry-sand series is shown on Figure 1, Views E through R. This sequence was modified for the wet-sand series to include a wetting and pumping operation to maintain the desired moisture content of the sand medium.

2.3 EXPLOSIVE

A 1-pound sphere of TNT was the explosive device used in these experiments. These charges contained 50 grams of pentolite (cap sensitive core) with a shallow cap well and a concentric covering of cast TNT. Each sphere weighed 1 pound (±5 percent) and developed an approximate energy of 2.09×10^{13} ergs when detonated. All charges were fired with a No. 8 commercial blasting cap.

VIEW A

TEST PIT SHOWING SUMP AND LOWER PLASTIC LINER. WATER PUMP LINE IS SHOWN IN LOWER LEFT CORNER.

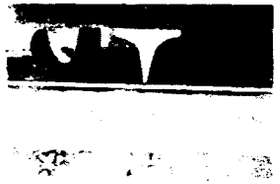

VIEW D

TRACK COORDINATE SCALE (Y).

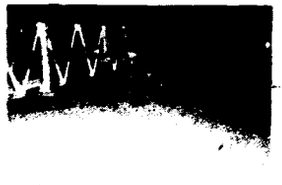

VIEW G

PLACING THE SAMPLE CATCH TRAYS USED IN COLLECTING THROWOUT DETRITUS.

VIEW J

INSTALLING THE OVERHEAD HIGH-SPEED MOTION-PICTURE CAMERA.

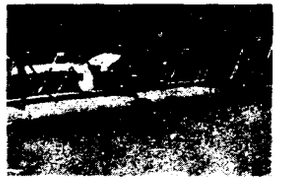

VIEW M

FILLING SAND-RETAINER TUBE PRIOR TO FINAL COMPACTION OF CHARGED HOLE.

VIEW P

SAMPLING THE DEBRIS FROM THE CATCH PADS.

VIEW B

FILLING AND COMPACTING TEST PIT SAND MEDIUM.

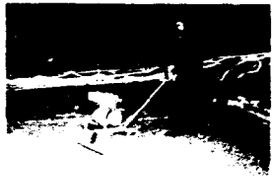

VIEW E

COMPACTING THE SURFACE OF TEST PIT.

VIEW H

PAINTING GEOMETRIC FIGURES ON THE PRESHOT SAND SURFACE.

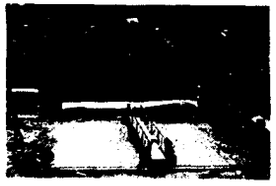

VIEW K

ALIGNING THE OVERHEAD CAMERA ABOVE GROUND ZERO.

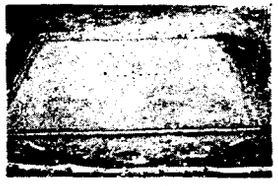

VIEW N

FINAL PRESHOT SAND SURFACE.

VIEW Q

SURVEYING THE CRATER LIP AND THROWOUT AREA.

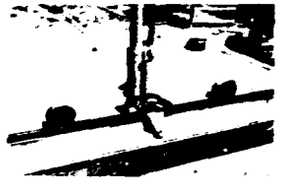

VIEW C

BRIDGE COORDINATE SCALE (X) AND THE VERTICAL PROBE (Z) USED IN SURVEYING THE CRATER.

VIEW F

LEVELING THE SURFACE OF TEST PIT.

VIEW I

REMOVING THE VINYL-COATED NYLON PIT COVERING.

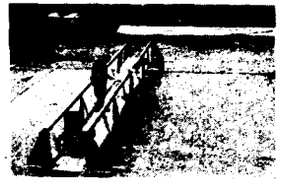

VIEW L

LOWERING CHARGE INTO THE SAND-RETAINER TUBE.

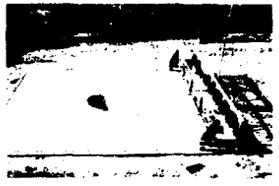

VIEW O

POSTSHOT CRATER AND THROWOUT.

VIEW R

TEST PIT RE-COVERED AFTER FIRING.

Figure 1 Construction of Test Pit Area and Preparation and Detonation of Charge

2.4 MEDIUM

2.4.1 All shots for this experiment were fired in well-packed, fine-grained, kiln-dried plaster sand. This sand had the following grade size characteristics: 100 percent smaller than No. 8 screen, 98 percent smaller than No. 16 screen, 66 percent smaller than No. 30 screen, 11 percent smaller than No. 50 screen, and 3 percent smaller than No. 100 screen. A cumulative curve for the sand medium used in these experiments is shown on Figure 2.

2.4.2 The test pit sand medium was compacted to an approximate uniform density of 1.70 with the aid of a Jackson Mechanical Compactor capable of delivering blows of 15 psi. After compaction of the test area, the entire pad area was leveled to a plane surface of ±2 millimeters. The compacting and leveling operations are illustrated on Figure 1, Views E and F.

2.4.3 After each shot, the disturbed and powdered sand matrix within the crater area was removed and replaced with sand of the original composition. The fine powdered sand was removed by winnowing the sand matrix with an electrically driven blower.

2.5 TEST PAD

2.5.1 The Tulalip test pad is a flat sand surface approximately 25 feet square, flanked by tracks used to support the survey bridge. A firing area occupies the central portion of this pad and overlays the pit and sump. The test pit is approximately 6 feet thick and is underlaid by a gravel-filled sump. The water level present in the sump or test pit is measured by inserting a dip stick into a pipe that terminates at the base of the sump pit.

2.5.2 Extraneous surface water is kept out of the pit by a 6-mil polyethylene-sheet lining. Installation of this liner is shown on Figure 1, Views A and B. The plan and cross-sectional views of the test pit are shown on Figure 3 and the entire facility is shown on Figure 4.

2.6 COLLECTION OF EJECTA

2.6.1 The ejecta sampling system used in these experiments comprised 54 stations located along 12 radial lines that extend outward from ground zero and are spaced 30 degrees apart. Individual collecting pads were located along these radial lines at distances of 180, 225, 320, 570, and 1,070 centimeters from ground zero. Each station sampled a radial sector of 5.6 degrees. The location of these stations is shown on Figure 3, and the sampling area of each station is shown on Table 1.

2.6.2 A sample-retainer tube was used to obtain ejected debris from the collection pad. This procedure is shown on Figure 1, View P.

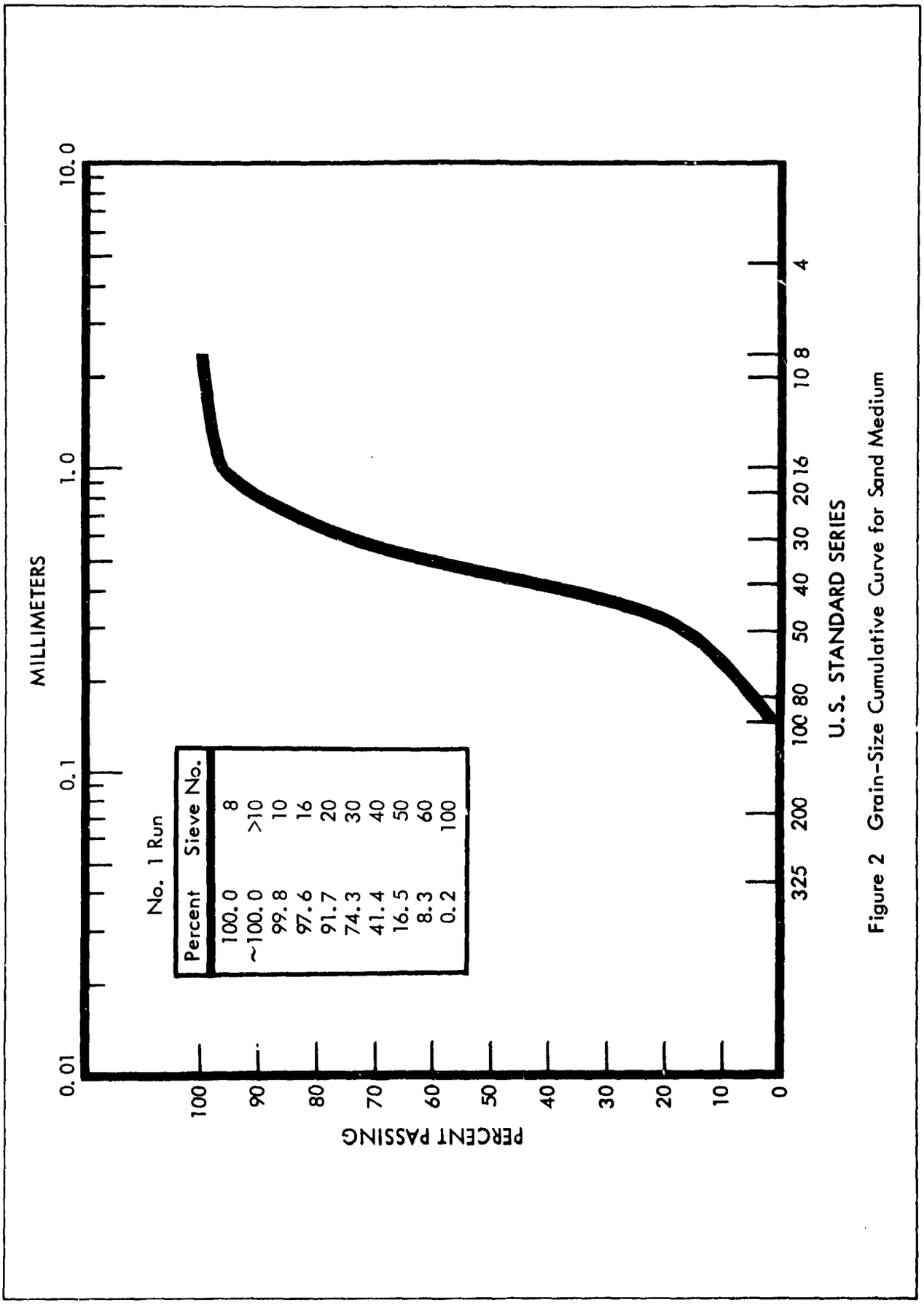

Figure 2 Grain-Size Cumulative Curve for Sand Medium

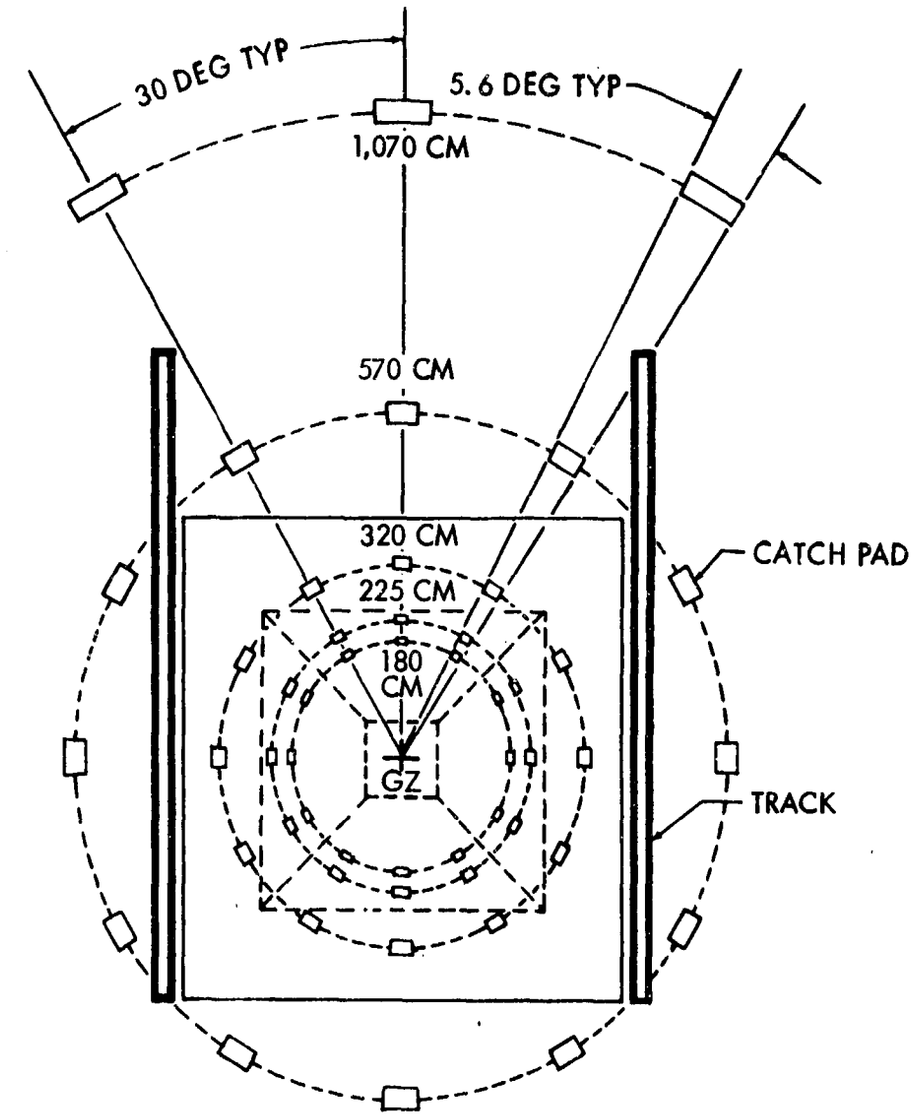

PLAN VIEW

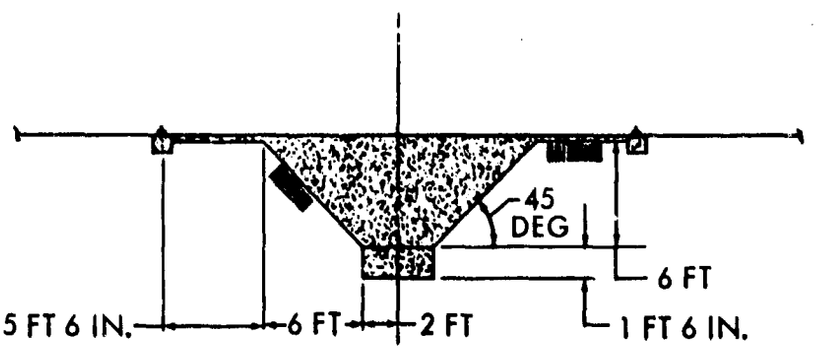

CROSS-SECTION VIEW

SCALE: 1 IN. = 10 FT

Figure 3 Plan and Cross-Sectional Views of the Test Area

Figure 4 Test Conditions

Table 1. Location of Sampling Stations

Concentric Ring	Number of Samples	Distance from Ground Zero (cm)	Sampling Area (cm^2)
1	12	180	140.0
2	12	225	180.25
3	12	320	228.0
4	12	570	498.25
5	6	1,070	798.0

2.7 PHOTOGRAPHIC DOCUMENTATION

Each crater was documented photographically. Generally a high-level and a ground-level oblique view were taken of each crater. In addition, many close-up photographs were taken to obtain details of selected features. High-speed motion-picture photography was used to document the sequence of events during crater formation. Motion-picture film speeds varied from 3,000 to 6,000 frames per second, depending on prevailing light. Two high-speed cameras were used to document the early history of crater formation. One camera was mounted on a bracked approximately 25 feet above ground zero. The other camera was mounted on a ground tripod for a low-level oblique view of the detonation. Installation of the high-speed motion-picture camera and camera locations are shown on Figure 1, Views J and K.

3 MEASUREMENTS

3.1 TOPOGRAPHIC MEASUREMENTS

Topographic measurements were taken with a graduated track, bridge, and vertical probe assembly. These devices are shown on Figure 1, Views C and D. The crater survey recorded the postshot relief by measuring along traverses parallel and normal to the tracks. Measurements outside the crater lip were made every 100 millimeters. Inside the crater lip, measurements were often made every 50 or 25 millimeters, depending upon inner crater topography. Postshot elevation values were recorded and used in the construction of contour maps. Two crater profiles or cross sections were also constructed by using survey data. One of these profiles was constructed parallel to the X or bridge axis, and the other was parallel to the Y or track axis. These contour maps and cross sections are included in Appendix C.

3.2 VOLUMETRIC MEASUREMENTS

Three methods were used to calculate crater volume: (1) calculation of the volume of the solid generated by revolving the average radial cross section about its axis; (2) use of the general cone formula, $1/3\pi r^2 h$; and (3) summation of the negative elevation values measured during the crater survey. Results obtained with these methods agreed within less than 5 percent; that is, the largest of three values did not exceed the minimum by more than 5 percent. The summation method was adapted for calculating crater volume because of its simplicity and ease of use.

3.3 DENSITY AND MOISTURE MEASUREMENTS

The ASTM sand-cone method was used to measure the sand density and moisture. These measurements were made after each shot for both the wet- and dry-sand experiments. Moisture content of the medium during the dry-sand series did not exceed 0.5 percent by weight. Moisture content was measured for sand removed from the charge hole prior to detonation for the wet-sand series. Preshot moisture measurements always yielded somewhat higher values than postshot measurements due to surface evaporation and downward percolation of the water once the wetting operation had been discontinued. Safety requirements prohibited watering and pumping operation once the charge was placed in firing position; therefore, an average of the recorded preshot and postshot moisture content was arbitrarily assumed to be the moisture content in the upper portion of the sand matrix at the time of detonation.

3.4 GRAIN SIZE MEASUREMENTS

Grain size was measured by screening the original sand matrix, fractured sand from the apparent crater, and ejected crater debris collected on sample trays. Screens were Tyler standard screen numbers 4, 8, 10, 16, 20, 30, 40, 50, 80, 100, 200, and 325.

3.5 EJECTA MEASUREMENTS

Ejected debris deposited from 180 to 1,070 centimeters from ground zero was sampled by using the radial net of stations shown on Figure 3. The ejected material deposited upon sample trays was dried, weighed, and the mass recorded in gm/cm^2. The debris deposited between the crater lip and 180 centimeters was estimated by using the difference between the postshot and preshot topographic survey elevations. This value includes debris thickness plus the crater lip uplift.

4 CHARACTERISTICS OF EXPLOSIVE CRATERS

4.1 BACKGROUND

4.1.1 The experimental work of Lampson (Reference 1) and the analytical work of Nordyke (Reference 2) and Murphey and Vortman (Reference 3) have shown that craters produced by surface and subsurface explosions have dimensions that depend upon many parameters. The most important of these factors are (1) the quantity of explosive energy released, (2) the physical properties of the medium in which the detonation takes place, and (3) the burial depth of the exploding device.

4.1.2 The crater studies reported here represent an effort to improve our knowledge of craters produced by chemical explosives. In these studies a 1-pound spherical charge of TNT was used as a standard of explosive energy. A medium-grained sand matrix of known density and moisture content was used to standardize the environment in which the detonations took place. When the quantity of energy released and the physical properties of the medium remain nearly constant, the effect of burial depth upon the crater's physical dimensions can be more accurately evaluated.

4.2 NOMENCLATURE

4.2.1 The nomenclature of explosive crater features recommended by Nordyke (Reference 4) has been used in this report. Similar terms, however, have been employed in the available literature with varied meanings and it seems advisable, therefore, to define the terms that are used here to describe the physical character of craters.

4.2.2 Definition of these terms is as follows:

1. Original ground surface: The original ground surface of the Tulalip experiments refers to the preshot level (±2 mm) of the test pad.

2. Apparent Crater: The apparent crater is the resulting void remaining in the test pad after the explosion has taken place.

3. True crater: The true crater is the actual crater developed by ejection, scour, and compression of the surrounding media, excluding later modification by the ejected material falling back into the crater.

4. Fallback material: The fallback material is that portion of ejected mass that falls back into the original true crater; it includes slide material, breccia, ballistic ejecta, and dust.

5. Lip crest: The lip crest is the highest topographic portion of the crater lip; it is always located outside the crater and may be either sharp or rounded in profile.

6. Apparent lip crest height: The lip crest height is the average difference in elevation of the lip crest and the original ground surface.

7. Uplifted ground surface: The uplifted ground surface is that portion of the original ground surface that has been uplifted and permanently displaced.

8. Intracone and crater: These are relatively small features confined to crater bottoms and result from surface or above-surface detonations. The Tulalip intracones differed from previously described similar features in that a smaller intracrater was inside the cone.

The above crater nomenclature is diagrammed on Figure 5 and is used throughout this report.

4.3 CRATER CHARACTERISTICS IN DRY-SAND ENVIRONMENT

4.3.1 Surface bursts on a dry-sand surface are characterized by shallow craters with relatively low crater lips. Approximately 38 percent of the crater volume is due to compression and uplift of the sand medium around the exploding charge; the remaining 62 percent of the volume is due to scour and ejection of sand grains from the crater area. As burial depth increases, the crater becomes somewhat wider, the depth increases markedly, and lip crest height increases. The diameter-to-depth ratio of the apparent crater decreases rather uniformly to a value of approximately 4 and remains so for moderate burial depths (20 to 40 mm). Within this burial depth range, the diameter and depth of a resulting crater increases at about the same rate as burst depth does until an optimum burst depth is reached. In other words, the optimum burial depth of a given charge will produce the largest crater dimensions. At Tulalip, the maximum radius, depth, and volume occurred at the same burst depth. The optimum burst depth for a 1-pound sphere of TNT was approximately 38.1 mm in both wet and dry sand. At burial depths greater than optimum, the crater diameter increased slowly and the crater depth decreased so that the ratio of diameter to depth increased to a value greater than 9 for a 76.2-mm burst depth. Figure 6 shows the relationship for crater diameter to crater depth ratio and charge burial depth. Shot D5.5A was detonated at near-optimum depth for a 1-pound TNT charge in a dry-sand matrix. Approximately 95 percent of the apparent crater volume resulting from this shot can be attributed to the ejected mass.

4.3.2 The lip crest height, lip-to-lip diameter, and crater radius represent average measurements observed along the four principal radii extending outward from ground zero. These four radii correspond to the X and Y directions of the rectangular

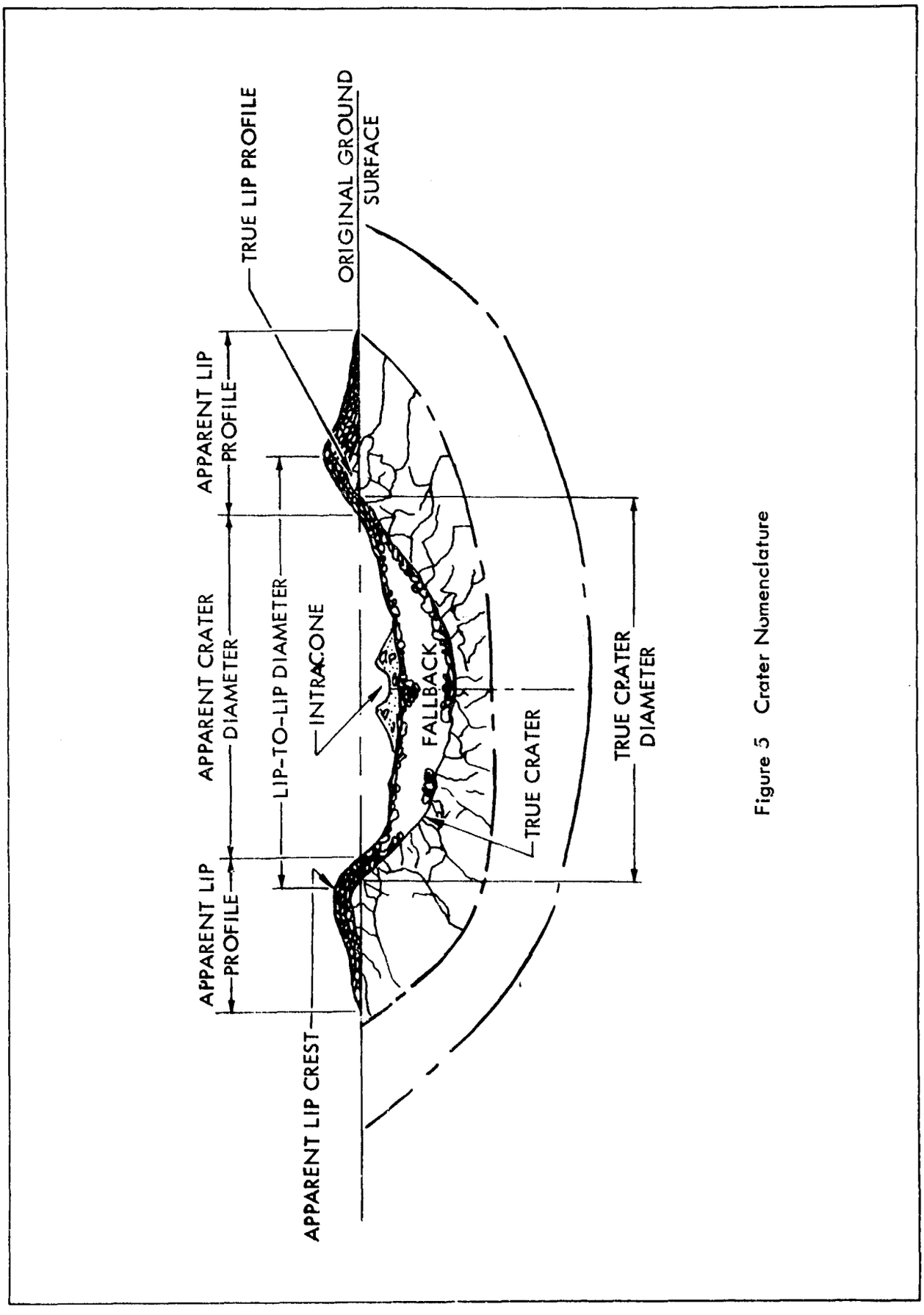

Figure 5 Crater Nomenclature

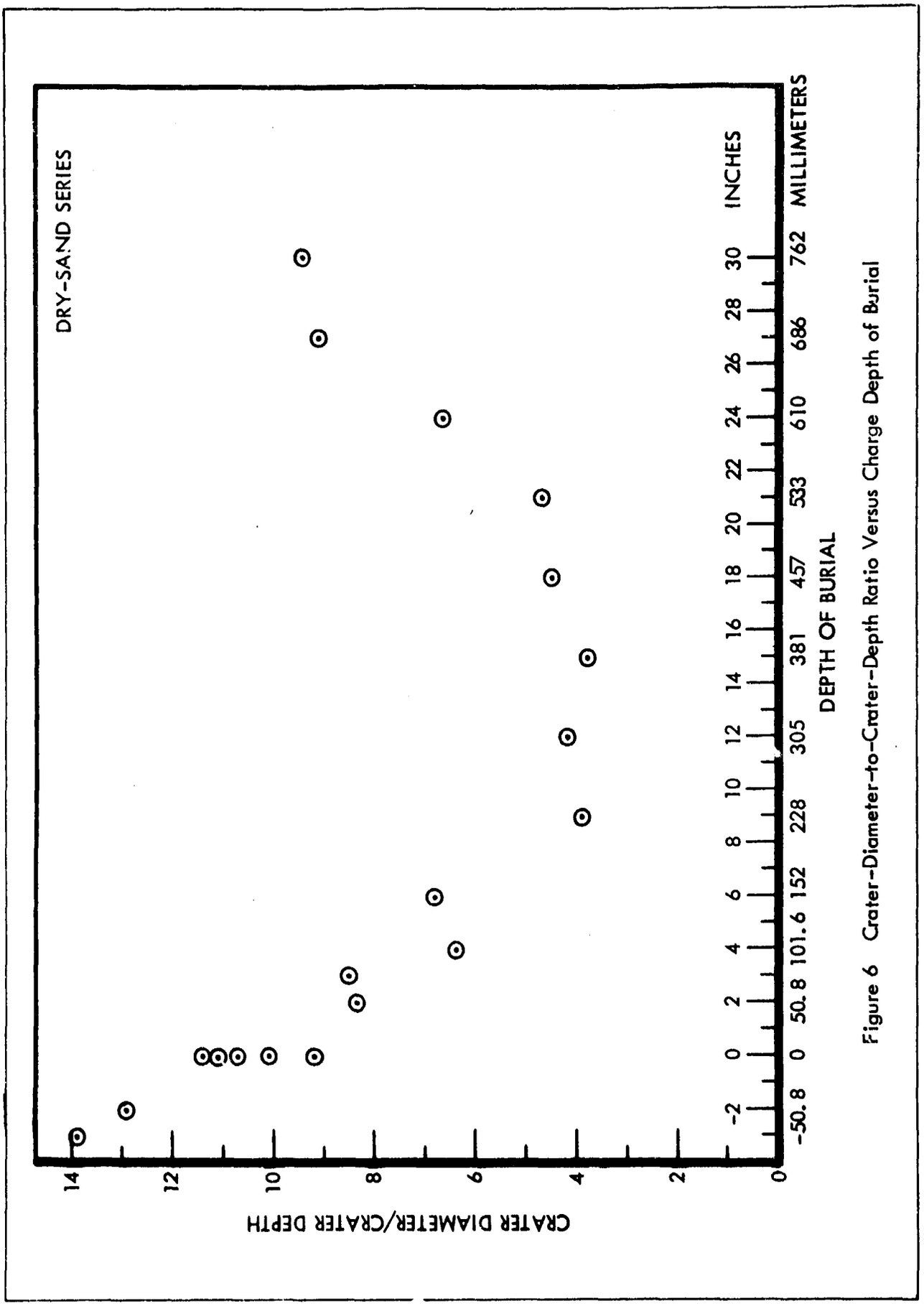

Figure 6 Crater-Diameter-to-Crater-Depth Ratio Versus Charge Depth of Burial

coordinate system and remained constant for all shots. The above crater parameters along with maximum crater depth, maximum crater radius, crater volume, moisture content of the medium, density of medium, burial depth of charge, and photography used are listed in Table 2 for all detonations in a dry-sand environment.

The relationship of crater radius, crater depth, and lip crest height to the burial depth of a 1-pound sphere of TNT detonated in a dry-sand matrix is shown on Figure 7. The plotted measurements of the average crater radius and the maximum depth of the crater follow similar parabolic curves. Both of these curves have a common maximum ordinate at a 38.1-mm burial depth. This represents the optimum burial depth for 1-pound spheres of TNT detonated in sand.

4.3.3 The average lip crest height measurements when plotted against the burst depth do not result in a parabolic curve similar to that of other crater parameters. The lip crest height appears to increase uniformly as the burial depth is increased from -76 to 762 mm. The ratio of lip crest height to crater radius appears to be approximately one-half the value for larger explosive craters. Roberts (Reference 5) has found that a reasonable lip crest height estimate for numerous craters formed by explosions at scaled burst depths of -0.05 to 1.03 is approximately equal to 0.1 of the crater radius.

4.3.4 The relationship of the average lip-to-lip diameter and crater volume to the detonation depth is shown on Figure 8. The resulting curves are similar to those plotted for crater radius and crater depth versus burial depth. The maximum ordinate for all these curves corresponds to the optimum burial depth for a 1-pound TNT charge detonated in sand.

4.4 CHANGES IN GRAIN SIZE IN THE SAND MEDIUM

4.4.1 A high-explosive detonation in dry sand modifies the size distribution of the affected sand medium and produces an increase in the frequency of certain grain sizes and a decrease in others. The shock-induced pressures produce a light-colored sand flour by crushing the sand grains surrounding the exploding charge; this crushing effect is confined to the true crater area and significantly reduces the grain size of the sand medium.

4.4.2 The measurement of grain size reduction was accomplished by screening four samples collected from the bottom of craters D1A, D2.5A, D5.5A, and D8A. These samples represent the fallback ejecta material composed of sand flour, broken and unbroken grains of sand, and pressure-agglutinated fragments of this material. Cumulative curves based on the screen analysis of the preshot sand medium and the postshot crater fallback material are shown on Figures 9 and 10. The mean diameter of the comminuted debris falling back into the crater is a function of the depth of burial of the exploding charge. This relationship is shown on Figure 11 and additional screen data are listed on Table 3.

Table 2. Crater Dimensions for Dry-Sand Series

Shot Number	Depth of Burial (mm)	Average X-Y Lip Height (mm)	Average X-Y Lip-to-Lip Diameter (mm)	Maximum Crater Depth (mm)	Average Crater Radius (mm)	Maximum Crater Radius (mm)	Crater Volume X 10^6 (mm^3)	Moisture Percent	Density	Photography	
										Motion	Still
D1A	-76	10	1,000	65	453	469	21.5	0.5	1.6		X
D1.5A	-50.8	17	1,150	71	459	500	22.0	0.5	1.6		X
D2A	0	32	1,250	90	515	517	28.9	0.5	1.6		X
D2B	0	26	1,300	91	506	555	31.6	0.5	1.6	X	
D2C	0	28	1,350	104	557	638	40.3	0.5	1.6		X
D2D	0	25	1,250	105	487	497	36.75	0.5	1.6		X
D2E	0	25	1,300	99	500	543	35.0	0.5	1.6		X
D2.5A	50.8	34	1,650	139	587	600	55.2	0.5	1.6		X
D3A	76	35	1,750	147.5	630	652	72.5	0.5	1.6		X
D3.5A	102	33	2,000	202	633	717	97.5	0.5	1.6	X	X
D4A	152	39	1,850	191	648	682	117.0	0.5	1.6		X
D4.5A	228	45	2,000	374	729	758	227.4	0.5	1.6	X	X
D5A	305	62	2,080	348	799	839	270.4	0.5	1.6		X
D5.5A	381	75	2,150	445	846	872	380.3	0.5	1.6	X	X
D6A	457	81	2,100	362	819	843	323.6	0.5	1.6		X
D6.5A	533	97	2,000	339	779	798	253.1	0.5	1.6	X	X
D7A	610	120	2,050	222	740	766	185.3	0.5	1.6		X
D7.5A	686	102	1,700	119	543	676	50.5	0.5	1.6		X
D8A	762	137	1,400	80	376	476	17.84	0.5	1.6	X	X

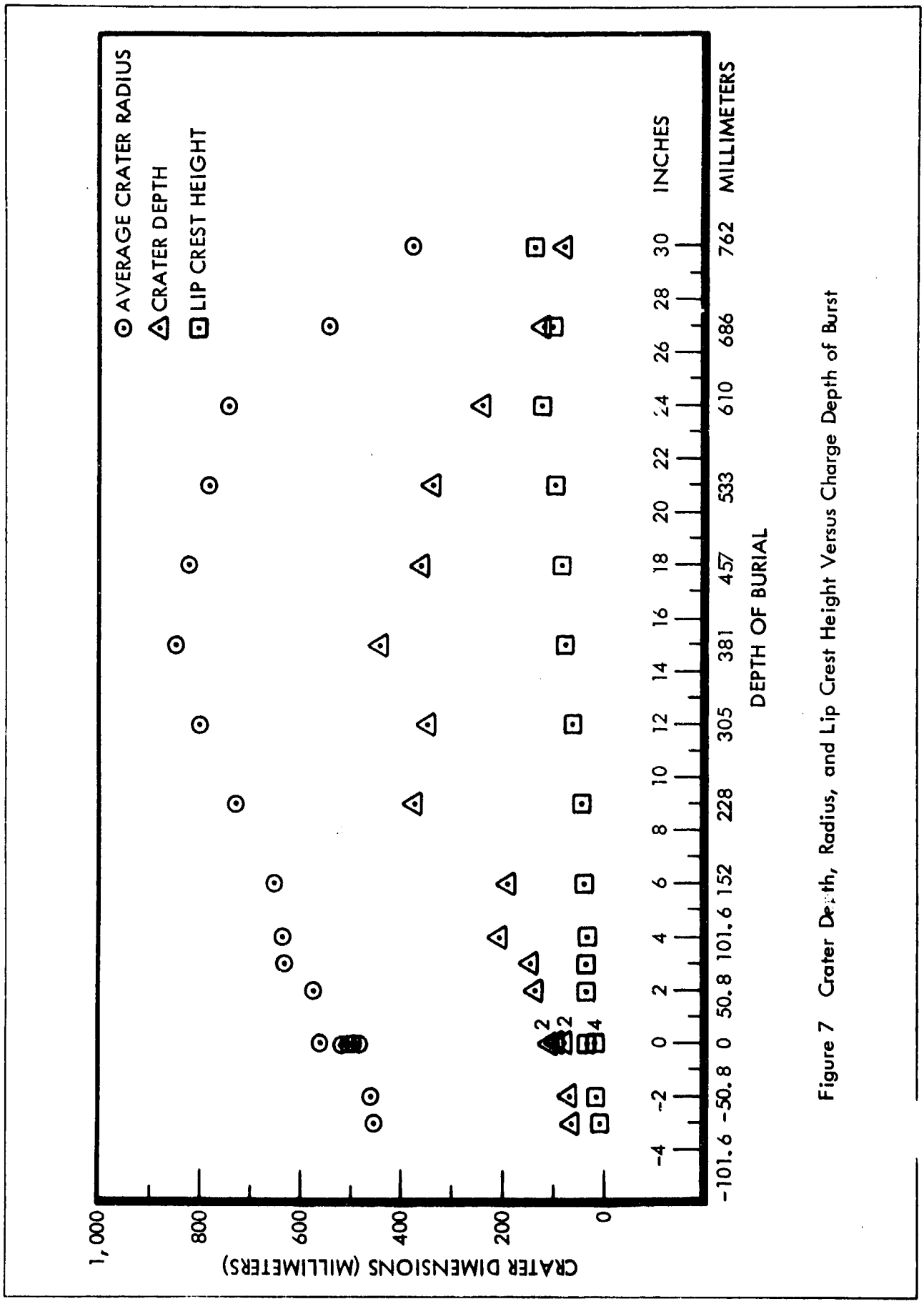

Figure 7 Crater Depth, Radius, and Lip Crest Height Versus Charge Depth of Burst

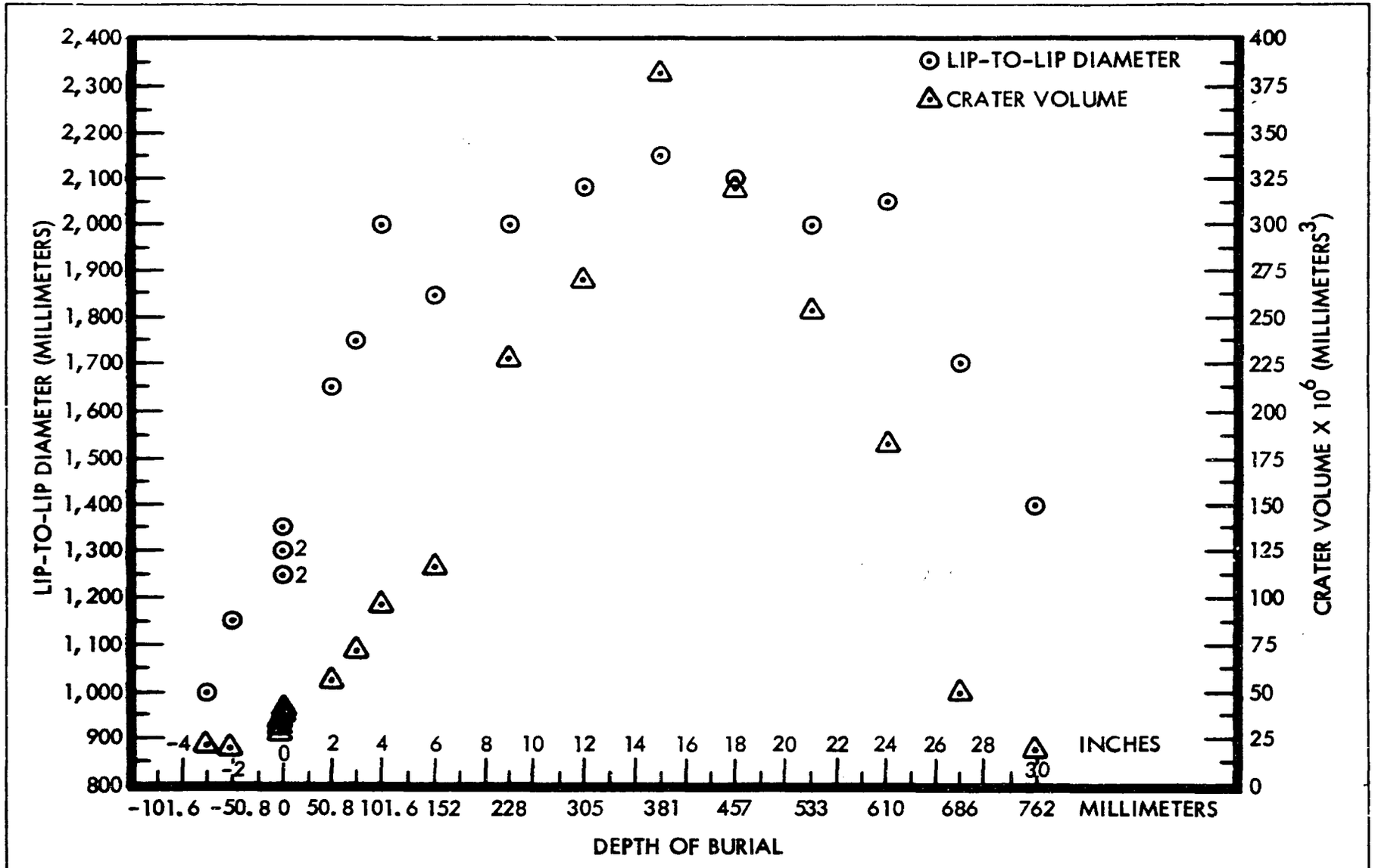

Figure 8 Lip-to-Lip Diameter and Crater Volume Versus Charge Burial Depth

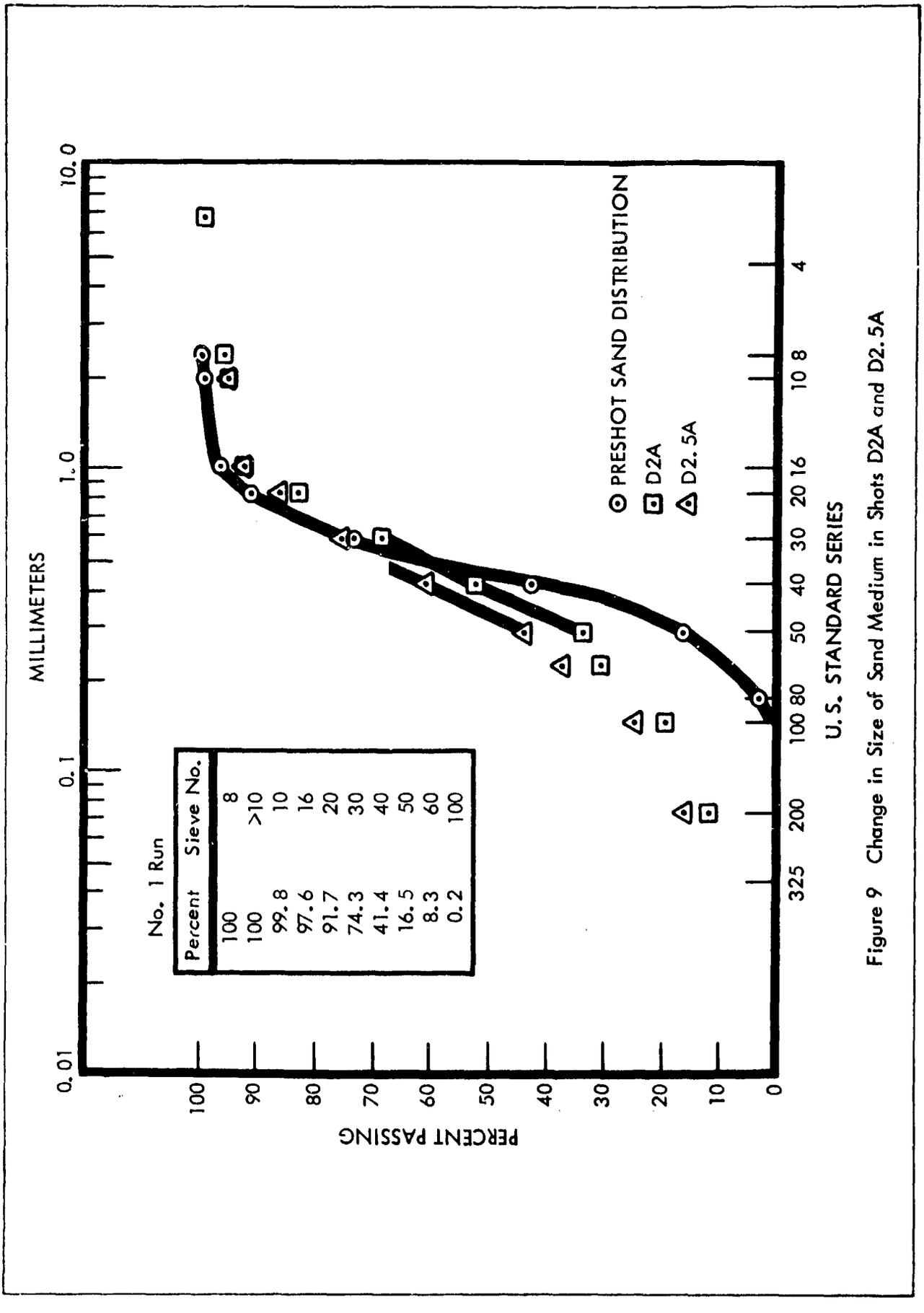

Figure 9 Change in Size of Sand Medium in Shots D2A and D2.5A

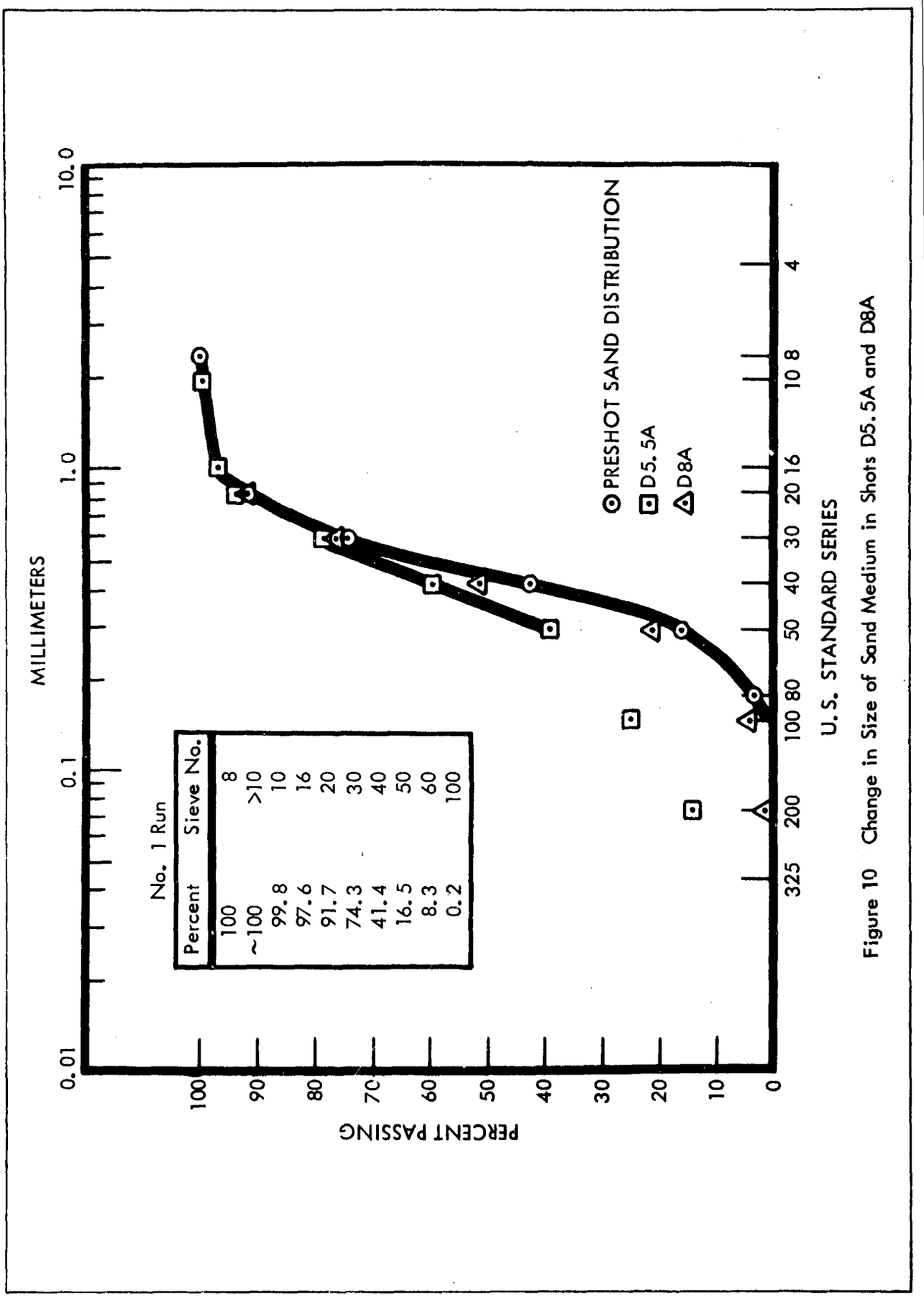

Figure 10 Change in Size of Sand Medium in Shots D5.5A and D8A

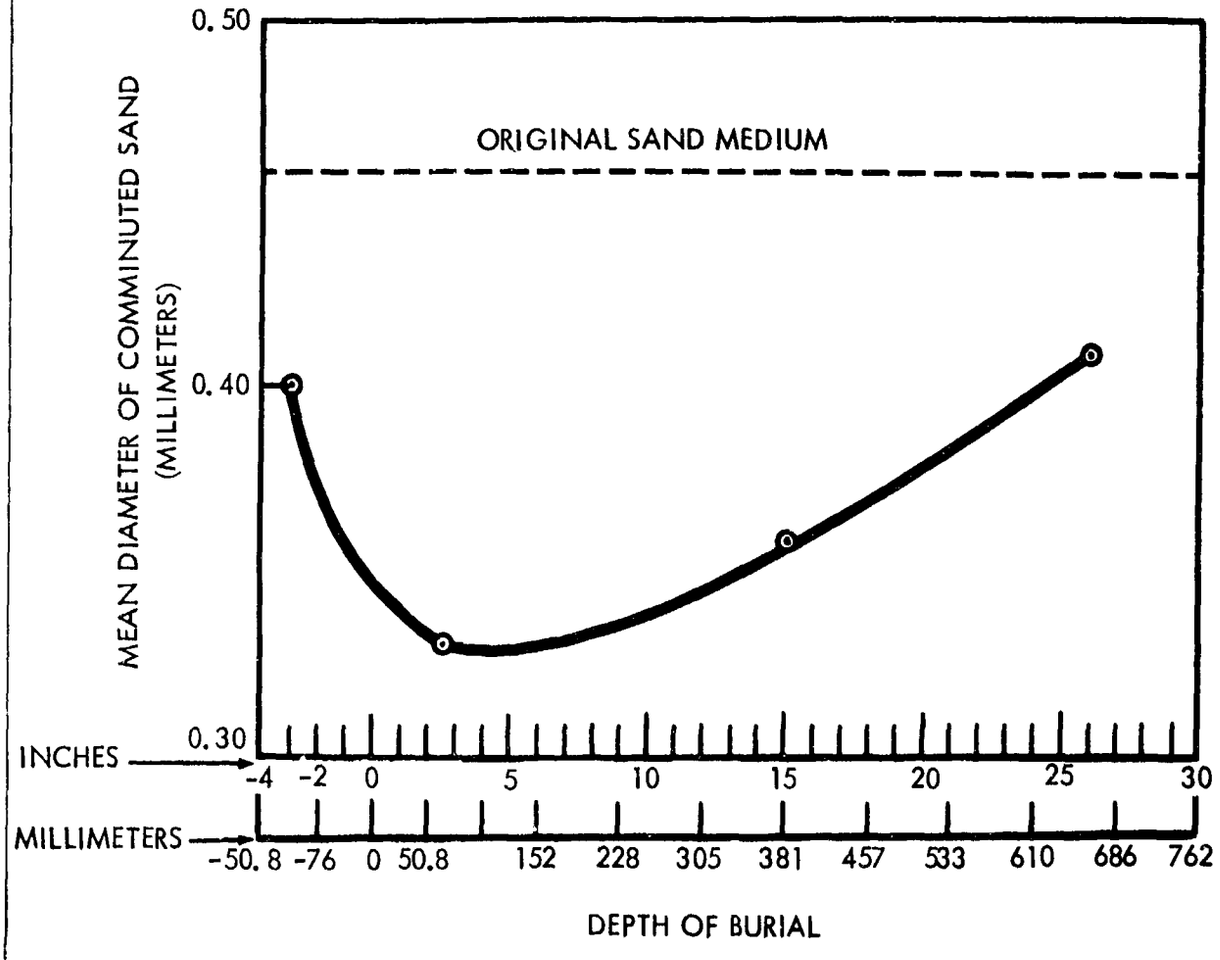

Figure 11 Mean Diameter of Comminuted Debris Falling Back into the Crater Versus Charge Depth of Burial

Table 3. Screen Analysis

Sample Number	Depth of Sample (mm)	Charge Depth (mm)	Mean Sand Diameter (mm)	Screen Number 3	8	10	16	20	30	40	50	60	100	140	200	Pan
				Screen Opening in Millimeters 6.680	2.362	1.981	1.168	0.833	0.589	0.417	0.295	0.246	0.147	0.104	0.074	<0.074
				Percent by Weight												
Preshot			0.465	0	0	0.2	2.2	5.9	17.4	32.9	24.9	8.2	8.1	0.2	0	0
D1A	69	76	0.400	0.1	3.15	0.95	4.1	8.5	14.25	17.85	16.1	5.0	10.3	4.2	3.45	11.5
% Fragments*				100	100	75	43.7	39.3	25.8	-						
% Decrease				+	+	+	+	+	17.6	45.4	36	39	+	+	+	+
D2.5A	137	50.8	0.330	0	0	3.96	3.55	5.8	10.8	14.9	16.8	6.4	12.65	5.0	3.88	16.3
% Fragments*						100	60	34	20	17	14	20	15	5	3	
% Decrease						+	+	1.7	35.3	54.5	32	+	+	+	+	+
D5.5A	445	381	0.360	0.6	0.35	0.25	1.8	6.5	12.4	18.3	21.0	3.8	12.4	4.4	3.3	10.7
% Fragments*				100	100	100	7	4	1							
% Decrease				+	+	+	18	9.2	28.7	45.4	16	4.8	+	+	+	
D8A	76	762	0.420	0.2	0.14	0.2	1.7	6.2	15.3	26.0	28.8	9.4	9.6	1.1	0.6	1.0
% Fragments*				100	100	100	8.5	3	2	2	0.7					
% Decrease				+	+	+	+	+	11.7	21.2	+	+	+	+	+	+

*Shock-agglutinated fragments.

4.4.3 The crushing strength of the individual grains of the sand medium is dependent upon size, composition, and crystalline cleavage. Each of these three parameters is known to vary considerably; therefore, their effect on the gross comminution cannot be evaluated. Explosion effects that reduce the mean diameter of the matrix will also reduce the frequency of the larger grain sizes with a corresponding increase in frequency of the smaller grain sizes.

4.4.4 Pressure-agglutinated fragments and missiles increase the proportion of the coarser size fraction for the postshot fallback. The fragments and missiles may represent broken fragments of a shock cone composed of pressure-agglutinated sand flour as well as fractured and unbroken grains of sand. The agglutinated or pressure-welded material forms easily friable, angular fragments varying in size from a few millimeters to more than 1 inch in length. These fragments do not appear to have been fused at the grain boundaries, but they are capable of withstanding the forces of ejection and impact. The microscopic characters of the agglutinated fragments are shown on the photomicrograph on Figure 12. Some of these fragments are ejected; others fall back into the crater, thus creating new sizes of material coarser than the original sand.

4.4.5 Fragments and missiles of the agglutinated or pressure-welded type were developed only in the dry-sand environment. These fragments were not formed by detonations in wet sand. The ejection of these "welded" fragments or missiles produced numerous secondary craters two to four crater radii from the point of detonation. Some of these missiles remain within the secondary crater formed by the impact, others were partly disaggregated or broken on impact. Some of the secondary splash craters produced by these agglutinated missiles are shown on Figure 13, Views P, Q, and R.

4.5 CRATERING CHARACTERISTICS IN WET SAND

4.5.1 The results of previous cratering experiments using both nuclear and chemical explosives have indicated that the moisture content of the host rock or soil medium may in some manner influence the size of the resulting crater. This hypothesis was supported by the significantly larger craters produced at the Pacific test site as compared with detonations of similar size in dry soil or rock.

4.5.2 The wet-sand experiment series consisted of 18 detonations of 1-pound spheres of TNT in a wet-sand medium that varied from 5.8 to approximately 22 percent moisture by weight. These charges were fired above the surface, on the surface, and below the surface of the test pad at the same depths used for the dry-sand series. The subsurface shots were positioned so that the center of gravity of the charge was located at 50.8, 101.6, 228, 381, 508, 533, and 686 mm below the surface of the test pad.

4.5.3 The moisture content of the sand was determined by weighing and drying sand removed from the charge hole prior to the detonation of the charge. In addition,

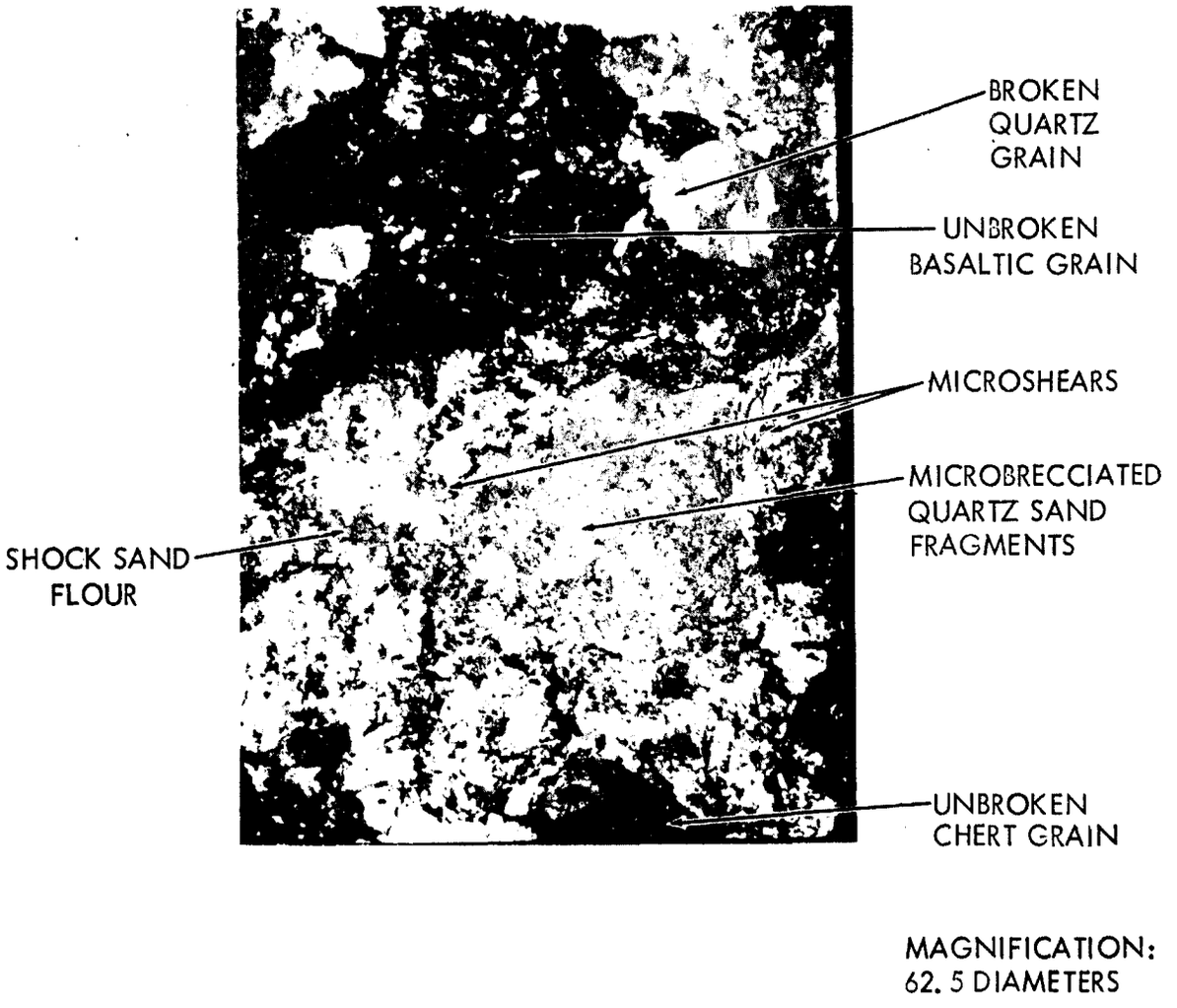

Figure 12 Photomicrograph of a Pressure-Agglutinated Missile

VIEW A

D1A (DOB -3 IN.)

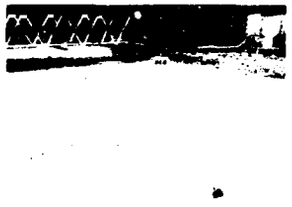

VIEW D

D2B (DOB 0 IN.)

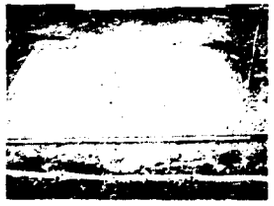

VIEW G

D3.5A (DOB 4 IN.)

VIEW J

D5.5A (DOB 15 IN.)

VIEW M

D7A (DOB 24 IN.)

SPLASH CRATERS
D6.5A
RULER = 6 INCHES

VIEW P

VIEW B

D1.5A (DOB -2 IN.)

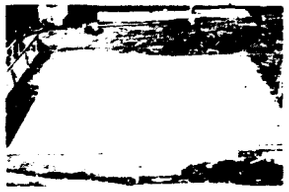

VIEW E

D2.5A (DOB 2 IN.)

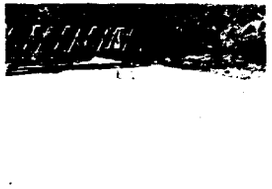

VIEW H

D4A (DOB 6 IN.)

VIEW K

D6A (DOB 18 IN.)

VIEW N

D7.5A (DOB 27 IN.)

VIEW Q

VIEW C

D2A (DOB 0 IN.)

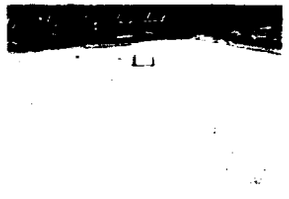

VIEW F

D3A (DOB 3 IN.)

VIEW I

D4.5A (DOB 9 IN.)

VIEW L

D6.5A (DOB 21 IN.)

VIEW O

D8A (DOB 30 IN.)

VIEW R

Figure 13 Crater [illegible] Dry Sand at Various Depths of Burial

density and moisture content of the test pad were also determined immediately after the test pad had cleared after the detonation. Moisture content of the sand medium at detonation time was approximated by averaging the preshot and the postshot moisture measurements.

4.5.4 After each experimental crater had been surveyed, the sand medium surrounding the crater area was removed to a two-crater depth and replaced with sand of original composition. The replacement sand and the entire pad surface was then compacted, leveled, and moistened in accordance with the previously described procedure. The medium below the two-crater depths remained more compressed than the peripheral areas of the test pad, and the permeability of the sand medium in this region was reduced because of the greater degree of packing. The wetting operations required for the subsequent shots washed the finely divided sand flour and carbon remaining in the medium from earlier detonations downward into the lower more compressed and less permeable horizon. In this manner, an impervious layer of fine sand flour and carbonaceous material was deposited approximately 635 mm below ground zero. The formation of the impervious horizon created a perched water table or a saturated horizon extending to approximately 508 mm below the surface of the test pad at ground zero. This situation was not discovered until the charge hole for shot W6.5A was prepared. The charge for this shot was placed at 508 instead of 533 mm below the surface of the test pad in order to have the center of gravity of the TNT sphere coincide with the surface of the water table.

4.5.5 When the nonuniform density of the test pit medium and the formation of the perched water table was discovered, all the subsurface shots of the wet-sand series were rerun. The subsurface shots designated by the letter "A," except W7.5A, were detonated in a homogeneous wet sand environment. The craters produced in wet sand are shown in Figure 14. Measurements from the craters produced by these subsequent shots are shown on Figures 6 through 11 and listed in Table 4.

4.5.6 A comparison of crater dimensions for all craters formed as a result of surface detonations on both wet- and dry-sand media are shown on Figure 15. Measurements of crater depth, crater radius, and crater volume are plotted against the percentage of moisture contained in the near-surface portion of the sand medium.

4.5.7 All three of these crater parameters displayed a uniform increase in crater size as the moisture content of the sand medium was increased from 5.8 to 11.9 percent; however, smaller craters were produced when the moisture content of the sand medium was increased 12 percent to saturation. When saturated the sand matrix contained approximately 22 percent water by weight.

4.5.8 All craters produced in the wet-sand medium, except shot W2D, had smaller crater radii than the craters produced by surface detonations in dry sand. On the other

VIEW A

W1.5A (DOB -2 IN.)

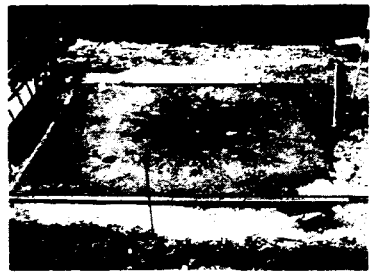

VIEW B

W2.5A (DOB 2 IN.)

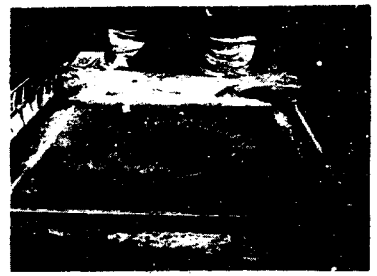

VIEW C

W4.5B (DOB 9 IN.)

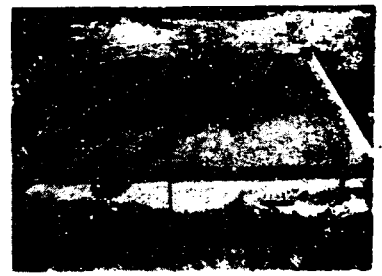

VIEW D

W6.4A (DOB 20 IN.)

VIEW E

W2A (DOB 0 IN.)

VIEW F

W3.5A (DOB 5 IN.)

VIEW G

W5.5A (DOB 15 IN.)

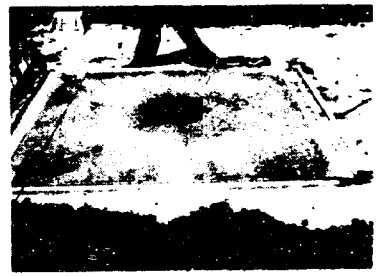

VIEW H

W6.5A (DOB 2 IN.)

VIEW I

W2F (DOB 0 IN.)

VIEW J

W3.5B (DOB 5 IN.)

VIEW K

W5.5B (DOB 15 IN.)

VIEW L

W7.5A (DOB 27 IN.)

Figure 14 Craters [illegible] at Various Depths of Burial

Table 4. Crater Measurements for Wet-Sand Series

Shot Number	Depth of Burial (mm)	Average X-Y Lip Height (mm)	Average X-Y Lip-to-Lip Diameter (mm)	Maximum Crater Depth (mm)	Average Crater Radius (mm)	Maximum Crater Radius (mm)	Crater Volume X 10^6 (mm^3)	Moisture Percent	Density	Photography	
										Motion	Still
W1.5A	-50.8	8	1,050	26	384	700	31.4	10.7	1.87		X
W2A	0	40	1,200	122	441	500	31.2	5.8	1.85		X
W2B	0	36	1,250	130	459	479	37.6	8.12	1.90		X
W2C	0	37	1,300	166	534	589	68.8	13.7	2.00		X
W2D	0	27	1,200	226	461	536	42.2	11.9	1.99		X
W2E	0	34	850	146	354	394	21.7	22	[b]		X
W2F	0	35	1,000	175	379	389	30.8	22	[c]		X
W2.5A[a]	50.8						62.7	8.7	1.94	X	X
W2.5B	50.8	51	1,400	194	561	592	92.1	8.7	1.94		X
W3.5A	102	45	1,700	247	660	690	119.2	9.5	1.99	X	X
W3.5B	102	40	1,850	371	580	590	145.1	7.5			X
W4.5A	228	56	1,900	350	736	823	180.6	13.0	2.02	X	X
W4.5B	228	91	2,050	555	723	804	361.0	11.3	1.98		X
W5.5A	381	56	2,000	467	737	706	284.7	11.0	2.00	X	X
W5.5B	381	115	2,050	565	762	803	416.3	11.9	1.96		X
W6.4A	508	90	1,800	482	734	746	298.5	15	[d]	X	X
W6.5B	533	120	2,100	501	828	863	438.1	10.2	1.89		X
W7.5A	686	122	975	203	600	754	136.6	16.2	2.02	X	X

[a] Only one-half crater was surveyed.
[b] Saturated
[c] Saturated; standing water
[d] 15 percent at surface; saturated at shot point

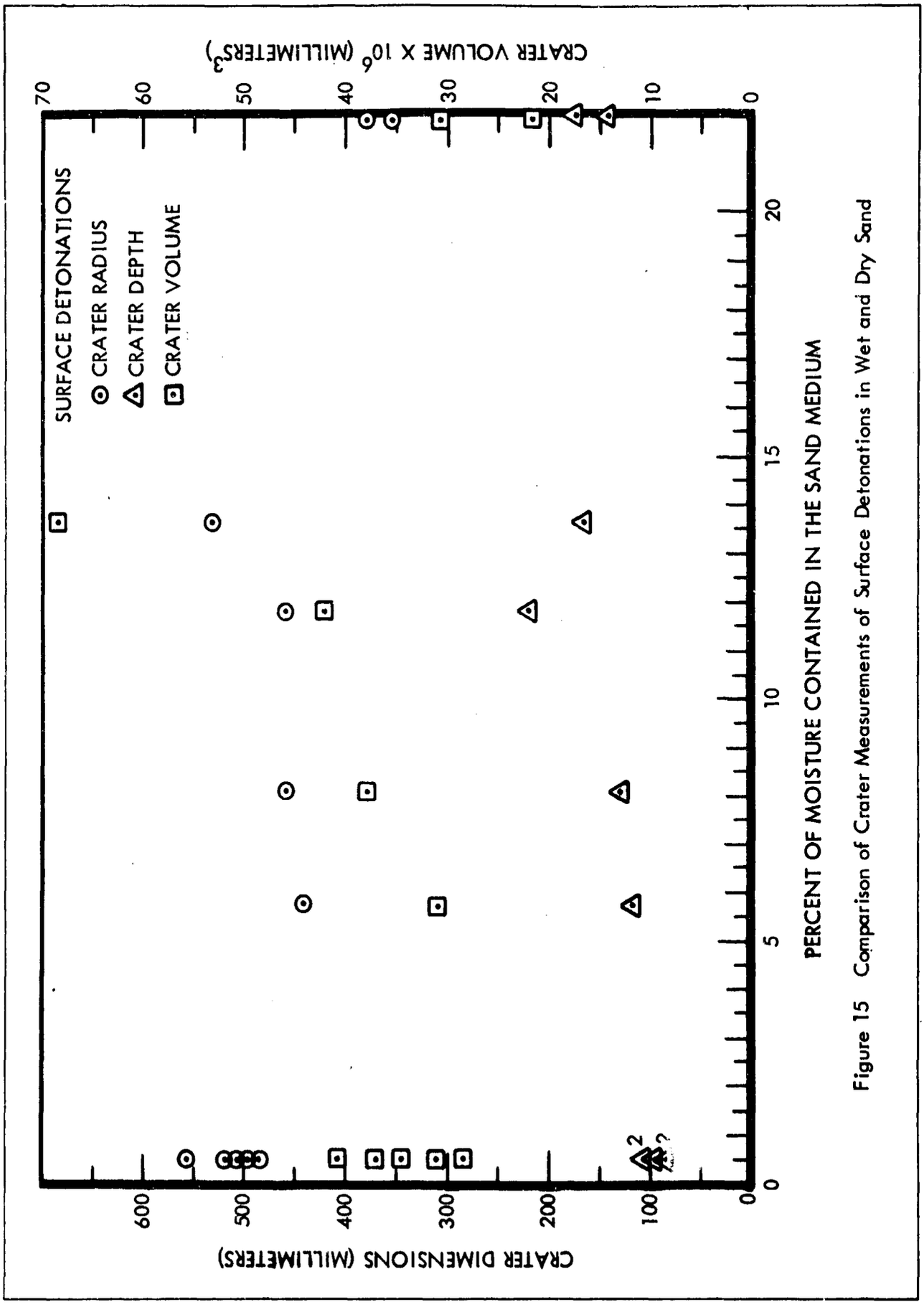

Figure 15 Comparison of Crater Measurements of Surface Detonations in Wet and Dry Sand

hand, all craters produced in wet sand were conspicuously deeper than those produced by surface detonations on dry sand. Also the crater volume increased as the percentage of soil moisture was increased to approximately 12 percent. The volume of the craters produced in wet sand having a moisture content between 12 percent and saturation is approximately equal to the craters produced in dry sand. The volume of crater W2F produced in saturated sand with standing surface water was considerably smaller than that of craters formed by surface detonations in wet sand.

4.6 EFFECT OF WATER TABLE

4.6.1 The effect of the hard, dense, impermeable horizon and water table on crater size is shown on Figure 16. The general effect of this dense, impermeable horizon is to reduce the crater size, particularly with respect to crater depth. The crater radius was not greatly affected by presence of the water table, but average lip crest height was consistently less for craters produced above the perched water table.

4.6.2 The lip-to-lip diameter and volume of the craters produced in wet sand overlying the hard impermeable horizon and water table are considerably less than the corresponding measurements of the craters developed in the homogeneous wet sand medium. The lip-to-lip diameter and the crater volume measurements for all shots of the wet series are shown on Figure 17.

4.6.3 Reduction of crater depth because of the water table and associated more dense material underlying the crater is also indicated by the slightly greater diameter to crater depth ratios. These ratios are shown on Figure 18. They vary from 29.5 for above-surface shots to values of less than 3 for subsurface detonations at optimum burial depth. The crater diameter to crater depth ratio increases greatly if the position of the detonation is moved from the surface to a few inches above the surface. The diameter-to-depth ratio, however, decreases gradually as the burial depth is increased to optimum and slowly increases for greater burial depths.

4.7 COMPARISON OF CRATERING RESULTS

4.7.1 Craters resulting from surface bursts are larger than craters produced by air bursts over a wet- or dry-sand medium; however, the size difference of the two is increased greatly by a wet-sand medium. Table 5 shows the percent of change that occurs in the crater size with a surface detonation and an air burst 50.8 mm above the surface.

4.7.2 The crater volume resulting from a surface detonation on wet sand is approximately 12.5 times larger than the crater volume produced by a similar charge detonated 50.8 mm above the surface of the test pad. On the other hand, crater volume resulting from a surface burst on dry sand is only 1.6 times larger than that resulting from a similar charge detonated above the test pad.

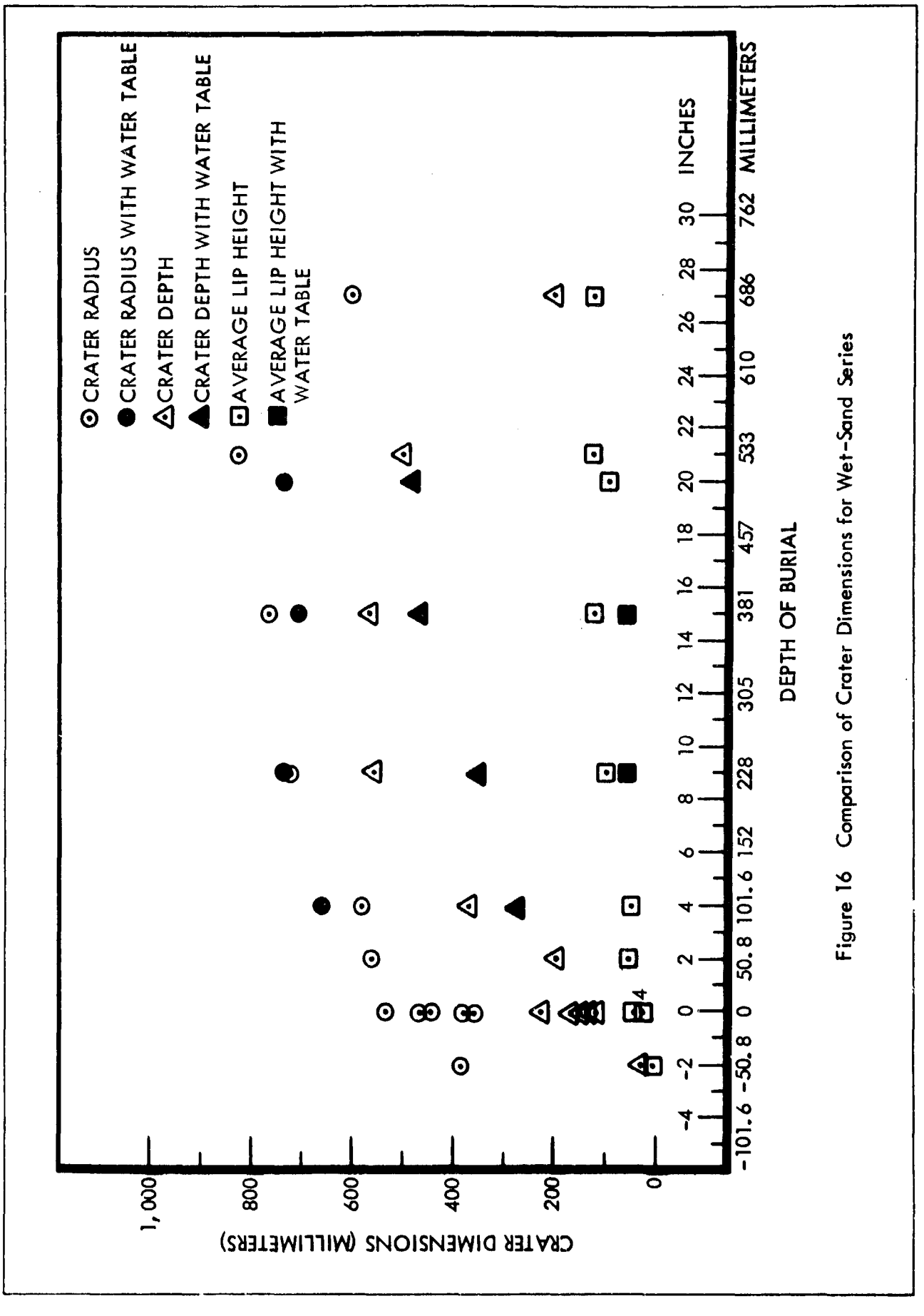

Figure 16 Comparison of Crater Dimensions for Wet-Sand Series

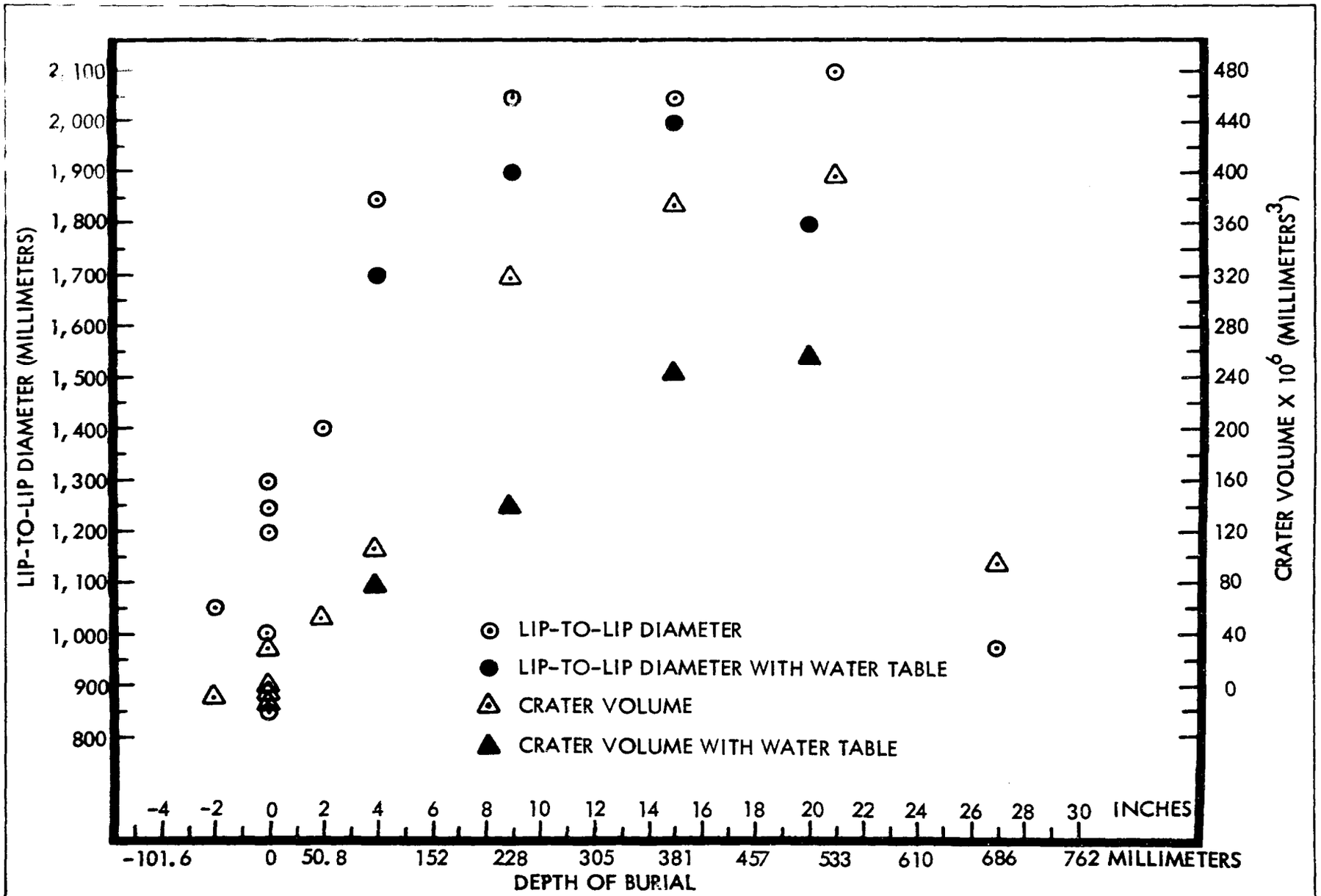

Figure 17 Lip-to-Lip Diameter and Crater Volume Versus Depth of Burial for Wet-Sand Series

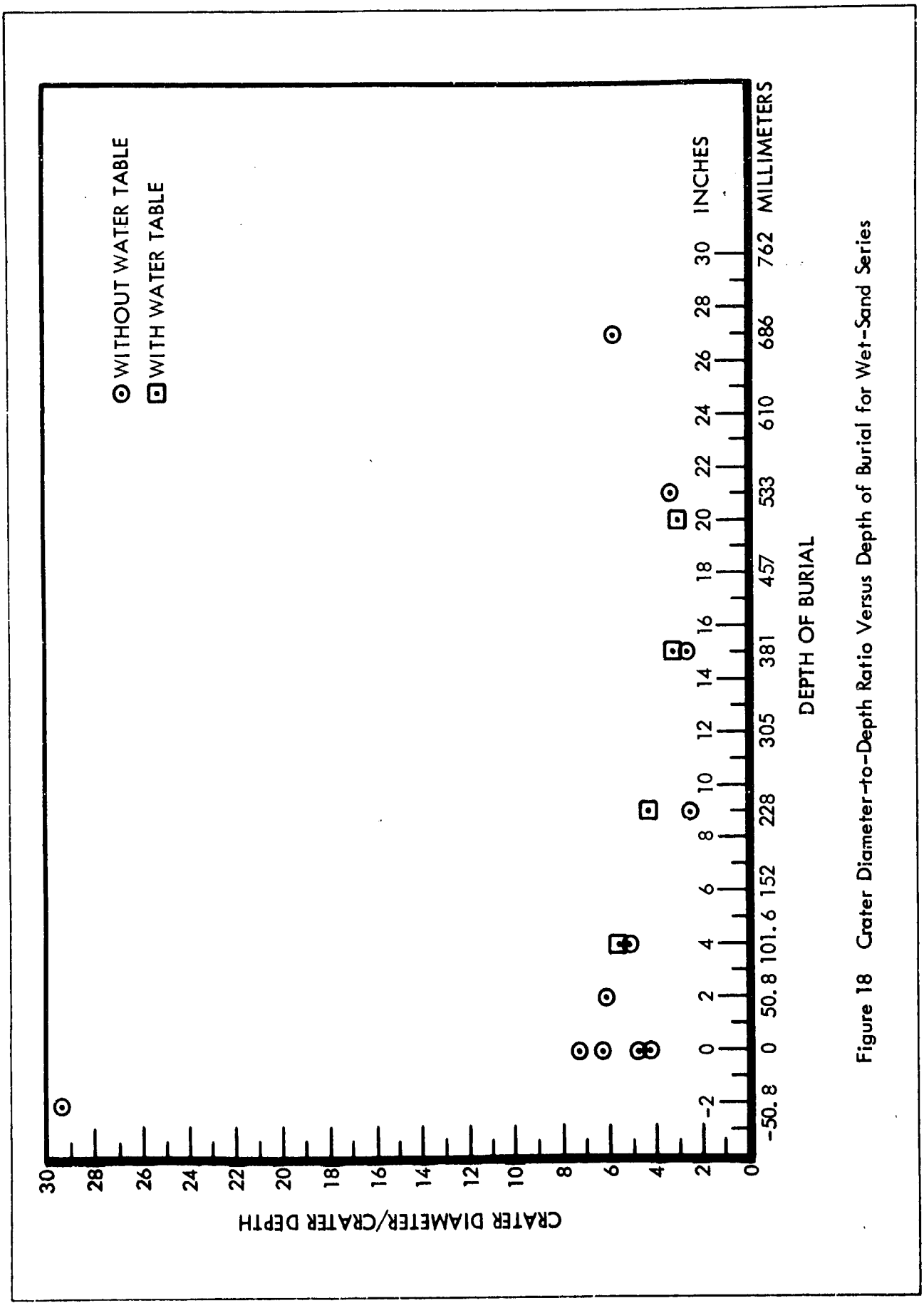

Figure 18 Crater Diameter-to-Depth Ratio Versus Depth of Burial for Wet-Sand Series

Table 5. Changes in Crater Dimensions for Surface and Air-Burst Shots

Depth of Burial (mm)	Average Crater Radius (mm)		Maximum Crater Depth (mm)		Crater Volume X 10^6 (mm^3)	
	Dry	Wet	Dry	Wet	Dry	Wet
-50.8	459[a]	385[a]	71[a]	26[a]	22.5[a]	3.1[a]
0	513[b]	438[c]	98[b]	160[c]	36.4[b]	38.7[c]
Percent of Change	-10.5	-12.3	-27.6	-83.8	38.2	-92
Surface / Air Burst	1.12	1.13	1.38	6.15	1.61	12.48

4.7.3 Upon examining the tables and charts from which the curves relating the various crater parameters are derived, one cannot fail to be impressed by the scatter of points. This scatter is real and has been observed at all controlled tests of explosive craters when test duplication has been attempted. The Tulalip experiment included a series of five shots that were detonated under nearly identical surface conditions in a dry-sand medium. The crater measurements obtained through these detonations provided data on the range of variation one might expect in crater measurements of a single detonation in a similar environment. Crater measurements of the five surface shots in dry sand were found to have the following variation:

Crater Measurement	Variation (percent)
Average lip crest height	±14
Average crater radius	±2.7
Crater depth	±8
Crater volume	±15

4.7.4 The above figures are somewhat less than the figure of ±25 percent variation for crater dimensions cited by Baldwin (Reference 6, p. 116) for craters that result when several identical charges of a given explosive are detonated in a supposedly identical environment. Accurate information concerning the expected variation in measurements of craters produced by subsurface detonations in dry or wet sand is not known at the

present time. Despite the lack of information concerning the standard deviation likely to be encountered in crater measurements, certain generalities can be stated concerning the relative size relationships of craters formed in a wet- and dry-sand medium. Table 6 contains comparative values of the average radius, maximum depth, and volume for craters produced in wet- and dry-sand media and craters resulting from detonations above a hard, dense, impervious horizon and water table.

4.7.5 Craters produced in the wet- and dry-sand medium during the course of these experiments can be summarized as follows:

1. Craters resulting from detonations in dry sand at burial depths less than optimum have larger average crater radii than craters resulting from the same burial depth in wet sand.

2. If the burial depth is greater than optimum, the average radius of craters produced in dry sand is 6 to 10 percent smaller than for craters formed in wet sand at the same charge burial depth.

3. The maximum depth, volume, and average lip crest height of all craters produced in wet sand, except those resulting from air burst, are greater than for craters resulting from detonations in dry sand at the same burial depth. The depth of craters resulting from surface and subsurface detonations in the homogeneous wet-sand medium were 27 to 71 percent greater than craters produced by detonations at identical depths of burst in the dry-sand medium. Wet-sand crater volumes varied from 6 to 168 percent larger than for craters produced in dry sand when the same burial depth was used. The average lip crest height of craters resulting from surface and subsurface detonations in wet sand were 20 to 100 percent greater than their counterpart produced in dry sand.

4. Craters produced by detonations above the hard, dense, impermeable horizon and water table are characterized by a greater degree of variability. The average crater radius produced by detonation at burial depths above optimum are slightly larger than those produced by comparable detonations in a dry-sand medium. Crater radius for detonations produced at or below the optimum burial depth are 6 to 13 percent smaller than for craters resulting from detonations at the same burial depth in dry sand. The maximum depth of the craters resulting from subsurface shots in wet sand above the water table is considerably less than for craters produced in wet homogeneous sand without any water table.

4.7.6 All craters produced above the water table, except W4.5A, had a maximum depth exceeding the craters produced in dry sand at identical burial depths. Crater volume resulting from subsurface detonations above the water table was found to be both larger and smaller than for craters from identically placed charges detonated in dry sand.

Table 6. Changes in Crater Dimensions Resulting From Detonations in Wet and Dry Sand

Depth of Burial (mm)	Average Crater Radius (mm)					Maximum Crater Depth (mm)					Crater Volume X 10^6 (mm^3)				
	Dry	Wet	Percent Change	Wet with Water Table	Percent Change	Dry	Wet	Percent Change	Wet with Water Table	Percent Change	Dry	Wet	Percent Change	Wet with Water Table	Percent Change
-50.8	459	384	-16.3			71	26	-63.3			22.5	3.1	-86.2		
0	513[a]	438[b]	-14.6			98[a]	160[b]	+63.3			36.4[a]	38.7[b]	+6.3		
50.8	587	561	-4.4			139	194	+39.6			55.2	92.1	+66.8		
101.6	633	580	-8.3	660	+4.3	202	371	+83.7	247	+22.3	97.5	145.1	+48.8	119.2	+22.2
228	729	723	-0.8	736	+0.9	374	555	+48.4	350	-6.4	227	361	+59.0	180.6	-20.2
381	846	762	-9.9	736	-13.0	445	565	+26.9	467	+4.9	380	416	+9.5	285	-25.0
533	779	828	+6.3	734	-5.8	339	501	+47.8	482	+42.2	253	438	+73.1	299	+18.2
686	543	600	+10.5			119	203	+70.6			51	137	+168.3		

[a] Average of five shots
[b] Average of six shots

5 CONCLUSIONS

The following conclusions were derived by analyzing the experimental data:

1. Average radius of craters produced in wet sand is 11 to 16 percent smaller than comparable craters produced in dry sand for air, surface, and subsurface detonations to and including the optimum burial depth. Below this depth, wet-sand craters are 4 to 11 percent larger.

2. Maximum depth for craters produced in wet sand is 27 to 71 percent larger than for comparable craters in dry sand for surface and subsurface detonations. Craters produced as the result of air bursts over wet sand are considerably smaller (63 percent) than comparable craters in dry sand.

3. Crater volumes as produced in dry sand are 10 to 169 percent smaller than for comparable craters produced in wet sand, except for craters resulting from air bursts.

4. Explosions on wet and dry sand surfaces yield significantly greater crater dimensions than do air bursts of the same charge over the same medium.

5. The deepest crater produced by surface detonation in wet sand was obtained when the moisture content of the sand medium was approximately 12 percent.

6. The maximum crater dimensions produced by detonation of 1-pound TNT spheres was obtained at a burst depth of 381 millimeters (15 inches) in both wet- and dry-sand medium.

7. Detonations of high-explosive charges in sand result in both an increase and a decrease in size classes composing the sand matrix.

8. The bulk of the grain size reduction takes place in the midrange size class near the mean diameter of the sand medium.

9. Shock-agglutinated missiles represent increases in grain-size of the sand medium and are capable of forming low-velocity impact craters.

10. Shock-agglutinated missiles are formed by the breakup and ejection of the greatly shocked material from the bottom and sides of the crater.

11. Intercone structures are best developed and preserved when the detonation takes place at or above the surface of the test pad.

12. Intercone structures are not produced by detonations in a wet-sand medium.

13. Apical angles of the intercone structures vary from 135 to 160 degrees.

14. The size of craters produced above a hard, dense, impermeable horizon and water table are smaller than for craters formed in a homogeneous wet-sand medium.

APPENDIX A

INTRACONE AND CRATER CHARACTERISTICS

The intercone and crater are features confined to the central portion of the larger craters. These features are always located directly beneath the burst position and are most likely to be developed when the explosion takes place above the test pad surface. However, similar structures may have developed at all charge burial depths, but such features would have been destroyed or modified by debris that fell back into the crater. The intercone is generally composed of finely divided sand flour with a less disturbed sand matrix agglutinated by shock compression. The agglutinated material is harder and more compact than the surrounding sand medium. There is no evidence that fusion has taken place, and the compressed material is easily friable when rubbed lightly. The composition and the character of the intercone material is very similar, if not identical, to the shock-agglutinated missiles discussed under paragraph 4.4. The similarity between shocked material composing the intracone and the material in ejected missiles suggests a relationship in time and mode of origin. If this surmise is correct, these missiles would represent broken and ejected fragments of shock-produced cone material. The presence of shock-agglutinated missiles resulting from all detonations in dry sand suggests that intracone or similar structures may have formed at all burial depths in the dry-sand environment. Both the intracone and ejected missiles must have formed early in the explosion sequence to have been ejected by the expanding gas pressure from the crater area.

Baldwin (Reference 6, p. 118) suggests a different mode and origin for the intracone structure based on the unpublished work (1944) of Lieutenant Fred Olsen. Olsen and Baldwin suggest elastic rebound as the origin for the intracone structure. If intracones are formed by elastic rebound, they must originate relatively late in the explosion sequence and after the shock and gas pressure have been greatly reduced.

Lieutenant Olsen's experiment employed a 100-pound block of TNT detonated on the surface of the natural silty loam soil. The center of gravity of the charge was above the surface of the ground; therefore, this shot would be classified as a near-surface air burst. The apparent crater produced by this charge was 7 feet in diameter and approximately 10 inches deep. A relatively hard, compressed, shocked intercone measuring 5 by 5 by 10 inches high was produced by this detonation.

The cone in the crater is not made by pieces of earth falling back into the crater. There is a displacement of ground roughly equivalent to the final apparent crater dimenaions. However, the dry nature of the soil as well as the packing of the loam, coupled with the intermittent layers of lava makes the ground comparatively resilient. On restoration after compression the dense compressed material from the bottom of the crater is broken up and piled up in a cone. (Reference 6, p. 118)

Ejected debris and pressure-agglutinated missiles were not reported by Olsen.

The intracone produced by the detonation of 100 pounds of TNT differs markedly from the intracone (shown on Figure A. 1) that was produced by the detonation of a 1-pound sphere of TNT during the Tulalip experiment. The cone described by Olsen differs from its Tulalip counterpart because there is an intracrater superimposed upon the cone. The intracone is somewhat larger than the diameter of the TNT charge and located directly beneath the burst position.

Small intracone structures, some with intracraters, were produced during experiments conducted by U. S. Army Engineers at Waterways Experiment Station (Reference 7) during a study on the effects of soil-rock interface on cratering. These experiments employed an overburden of varying thickness composed of air-dried, "pit run" river sand placed initially to a maximum depth of 12. 55 feet over a massive concrete slab. Three different charge types and sizes were employed in these experiments and all dimensions were scaled by dividing the distance or thickness by the cube root of the charge weight.

Small intracone structures produced by surface detonations of the 256-pound charges of TNT were confined to a narrow range of overburden thickness. Surface detonations of these charges produced intracone structures when the overburden thickness was 6. 35 (λ_o = 1) and 3. 13 (λ_o = 0. 5) feet. However, these structures were not formed when the thickness of sand overburden was increased to 12. 55 (λ_o = 2) feet or decreased to 1.56 (λ_o = 0. 25) feet. The intracones resulting from surface detonation of 54-pound charges of dynamite and 27-pound charges of C-4 explosive were further restricted: these were formed only at an overburden thickness of 3. 13 (λ = 0. 5).

Shots 14 and 15 of the Waterways experiment are especially pertinent to intracone formation. These shots were surface detonations of 256 pounds of TNT on a sand mantle 3. 13 (λ = 0. 5) feet in thickness. Both true and apparent crater dimensions were reported as identical. The crater did not penetrate the underlying concrete slab; however, the slab was swept clean of sand for an approximate distance of 2 feet around the intracone base. The intracone structure formed by these detonations appeared to be a residual mass, unrelated to elastic rebound or reflected seismic-shock effects. The scouring ability of the expanding sphere of gas appears to be an important factor in the formation of intracone structures of this type.

The apical angle of the intracone structures developed during experiments conducted by Lieutenant Olsen, by Waterways, and by the author at Tulalip show considerable similarity despite dissimilar test conditions. The apical angles for the intracones produced during these experiments are shown on Table A. 1.

During the course of the Waterways and Tulalip high-explosive detonations, intracones did not form in a wet-sand medium. Wet sand may be less compressible but more easily removed from the crater floor by the expanding gas.

Similar intracrater cone structures were produced by surface shots III-3A and III-3B (W = 6, 000 pounds) and by an air burst, shot II-1 (W = 256 pounds, λ = -0. 14), of the Air Vent series. Carlson and Jones (Reference 8, p. 43) report that the conical formation may

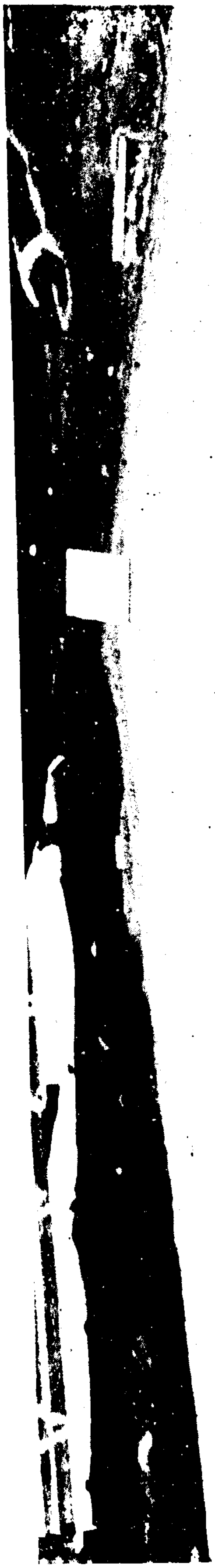

Figure A-1 [illegible] Produced by Detonation of 1-Pound Sphere of TNT During the [illegible] Experiment

be the result of fallback, peculiar only to the interaction of expanding gases associated with surface and near-surface bursts.

Table A. 1. Intracone Apical Angles

Detonation Event		Apical Angle of Intracone
Waterways Experiment Station:	Shot 8	135
	Shot 9	165
	Shot 14	155
	Shot 15	165
	Shot 18	150
	Shot 19	165
	Shot 21	155
Lieutenant Olsen's Experiment		145
Tulalip Experiment		150 to 160

APPENDIX B

DISTRIBUTION OF EJECTA

The ejected debris produced as a result of detonation at various depths in dry sand were studied to gain experience and knowledge that would help in analyzing and predicting the character of ejected debris obtained from much larger chemical and nuclear detonations. Such information is important in the prediction of damage resulting from high-explosive and nuclear detonation, the design of protective structures, and engineering application to earth excavation.

In an attempt to gain as much information as possible from each shot, small catch-trays were placed in a pattern on the surface of the test area to collect samples to be used in ejecta distribution studies. These trays were placed along radial rays 180, 222, 320, 570, and 1,070 centimeters from ground zero. The same pattern of catch-trays was maintained for each shot; the location of the sample stations are shown on Figures 4 and 5. Each concentric ring of catch-trays contains 12 trays in which samples were collected. Each sample was weighed and, with the known area of the catch-trays, the areal density of the ejected mass was calculated. An average areal density was computed for each distance from ground zero for each shot.

The crater volume, crater mass, ejecta mass, ejecta mass/crater mass ratio, region of ejecta samples, and the average crater measurements used in the calculations of ejecta distribution are listed on Table B. 1. This table also shows that important information from the near-crater region (1 to 2 crater radii) was not sampled. Previous cratering experiments have shown that most of the ejected mass is distributed in this region. Catch-trays placed in this locale are badly disturbed and sometimes removed entirely by the forces of detonation. The ejecta deposited in the near crater region can be estimated from the topographic map; however, for the Tulalip experiments the amount of uplift and compression that has taken place in the near-crater region is unknown.

AREAL DENSITY

The ejected materials recovered from the catch-trays were weighed and converted to areal density (gm/cm^2). The ejecta areal density as a function of distance from ground zero has been plotted for each shot and fitted by one or more power law functions as indicated by the actual data points. The power law relationships represent the best fit to the data by the method of least squares. Data plots and their corresponding power law fits are shown on Figures B. 1 through B. 10.

MASS CALCULATIONS

The total ejecta mass for these craters was calculated by employing a method first used by Carlson and Roberts (Reference 9). The ejecta mass is calculated by evaluating integrals in the form of

$$M_p = 2\pi \int_{D1}^{D2} \delta(D)\ DdD$$

Where: M_p = that portion of the total ejecta mass falling within the radial distance D1 to D2

$\delta(D)$ = the experimentally derived areal density distance function of the least squares fit of the areal density data

The total ejecta mass, Me, is sum of the incremental masses, M_p, or

$$Me = \int_{P=1}^{n} M_p$$

and

$$Me = 2\pi K \int_{1.2}^{a} \delta(D)\ DdD$$

The distribution of the ejecta mass relative to the craters is shown on Figures B. 11 through B. 18. In these figures, the ratio Mi/Me is plotted as the ordinate versus the ratio D/R as the abscissa, where Mi is the cumulative ejecta mass between the crater edge and any distance of interest, Me is the total ejecta mass, D is distance, and R is the radius of the apparent crater. These mass distribution curves were derived by integrating (using the above equation) in successive increments the areal density versus distance curves shown in Figures B. 1 through B. 10.

The ejected mass of craters D6. 5A, D7. 5A, and D8. A each exceeds their respective apparent crater mass. These craters are the result of the deepest detonations of this experiment. A similar situation was found to exist for the deeper-buried detonation of the Air Vent series. This condition according to Carlson and Jones (Reference 8, p. 58) is due to the bulking effect that is attained for craters resulting from deeply buried charges. Sufficient data are not available to resolve this question here.

Table B. 1 Ejecta Distribution

Shot Number	Depth of Burial (mm)	Average Crater Depth (mm)	Average Crater Radius (mm)	Crater Volume (cm^3) X 10^3	Crater Mass (gm/cm^3) X $10^{(\ )}$	Ejecta Mass (gm/cm^3) X $10^{(\ )}$	Ejecta Mass Crater Mass Ratio	Region of Ejecta Samples (Crater Radii)
D1. 5A	-50. 8	71	459	22. 25	3. 56(4)	3. 0175(3)	0. 0847	4 to 10+
D2B	0	91	506	32. 15	5. 144(4)	3. 20235(4)	0. 6225	3. 6 to 10+
D2. 5A	50. 8	139	587	55. 26	8. 842(4)	4. 238(4)	0. 479	3 to 10+
D3. 5A	102	202	633	102. 6	1. 6416(5)	7. 828(4)	0. 4768	3 to 10+
D4. 5A	228	374	729	225. 8	3. 6128(5)	3. 2864(5)	0. 909	2. 5 to 10+
D5. 5A	381	445	846	372. 3	5. 9568(5)	5. 66476(5)	0. 951	2. 2 to 10+
D6. 5A	533	339	779	249. 3	3. 9888(5)	7. 421(5)	>1. 0	2. 3 to 7
D7A	610	222	740	177. 4	2. 8384(5)	2. 51554(5)	0. 886	2. 3 to 8
D7. 5A	686	119	543	50. 0	8. 0(4)	10. 087(5)	>1	3. 5 to 10
D8A	762	80	376	16. 8	2. 688(4)	9. 310(5)	>1	4. 9 to 9

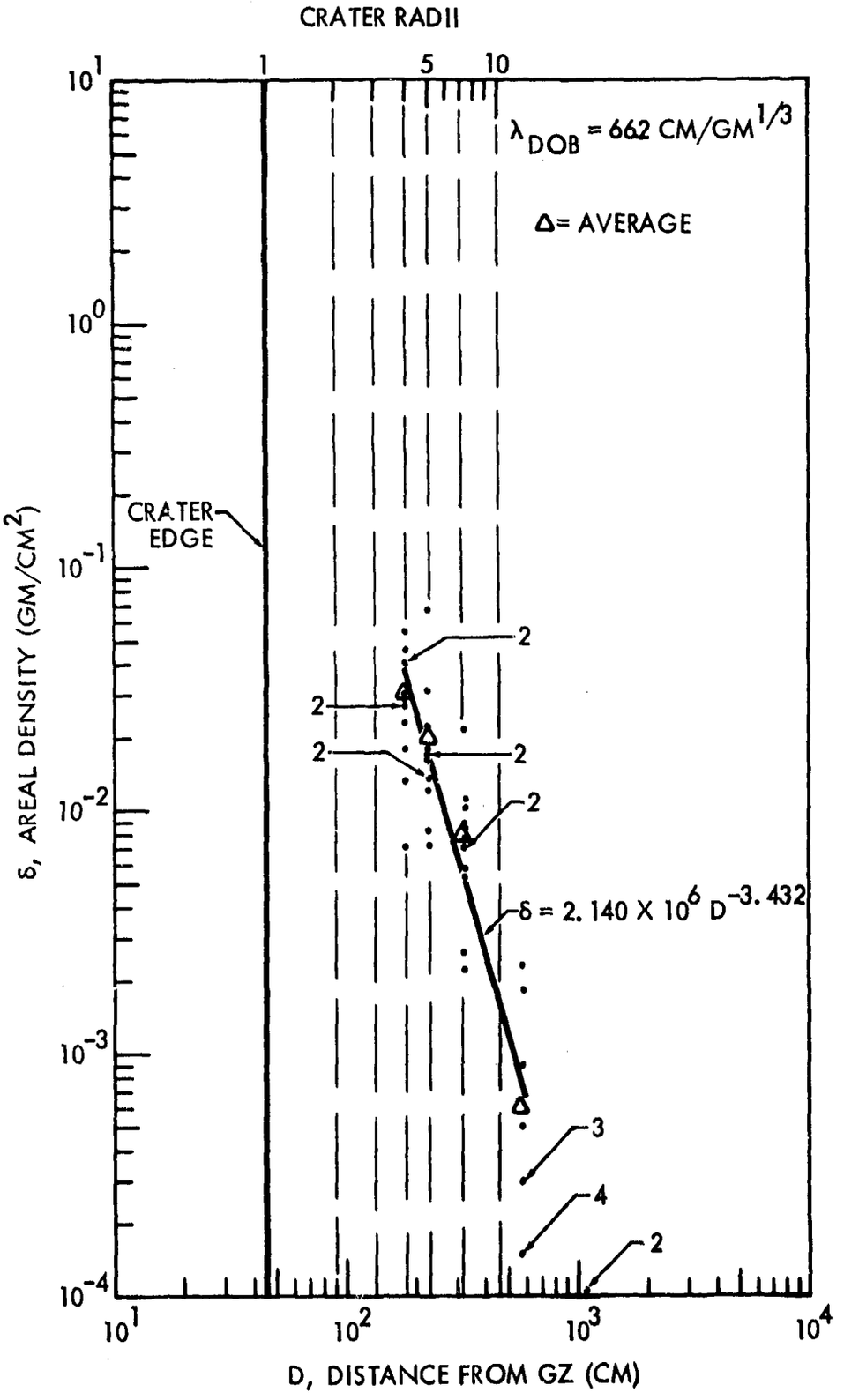

Figure B.1 Areal Density Versus Distance From Ground Zero for Shot D1.5A

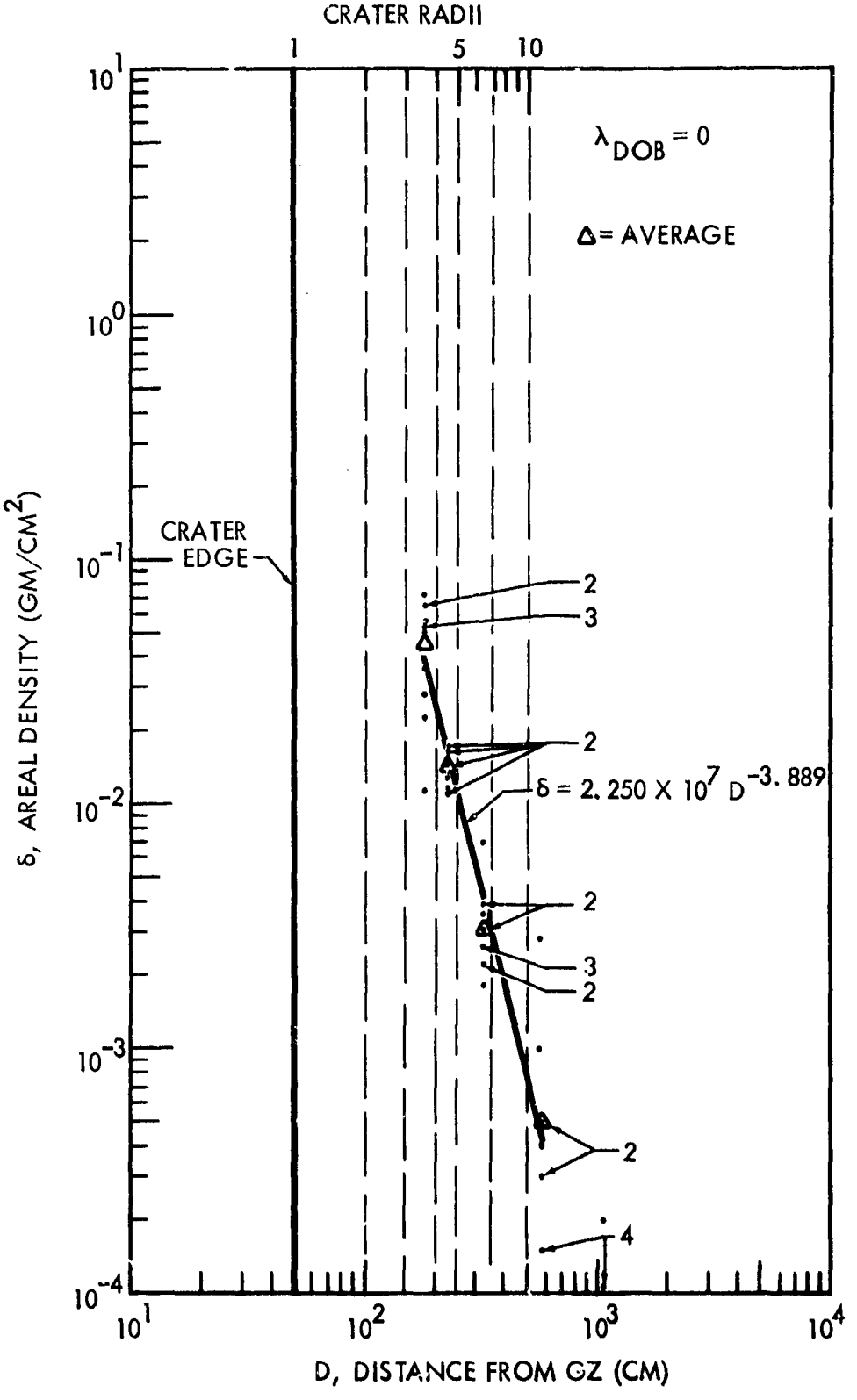

Figure B.2 Areal Density Versus Distance From Ground Zero for Shot D2R

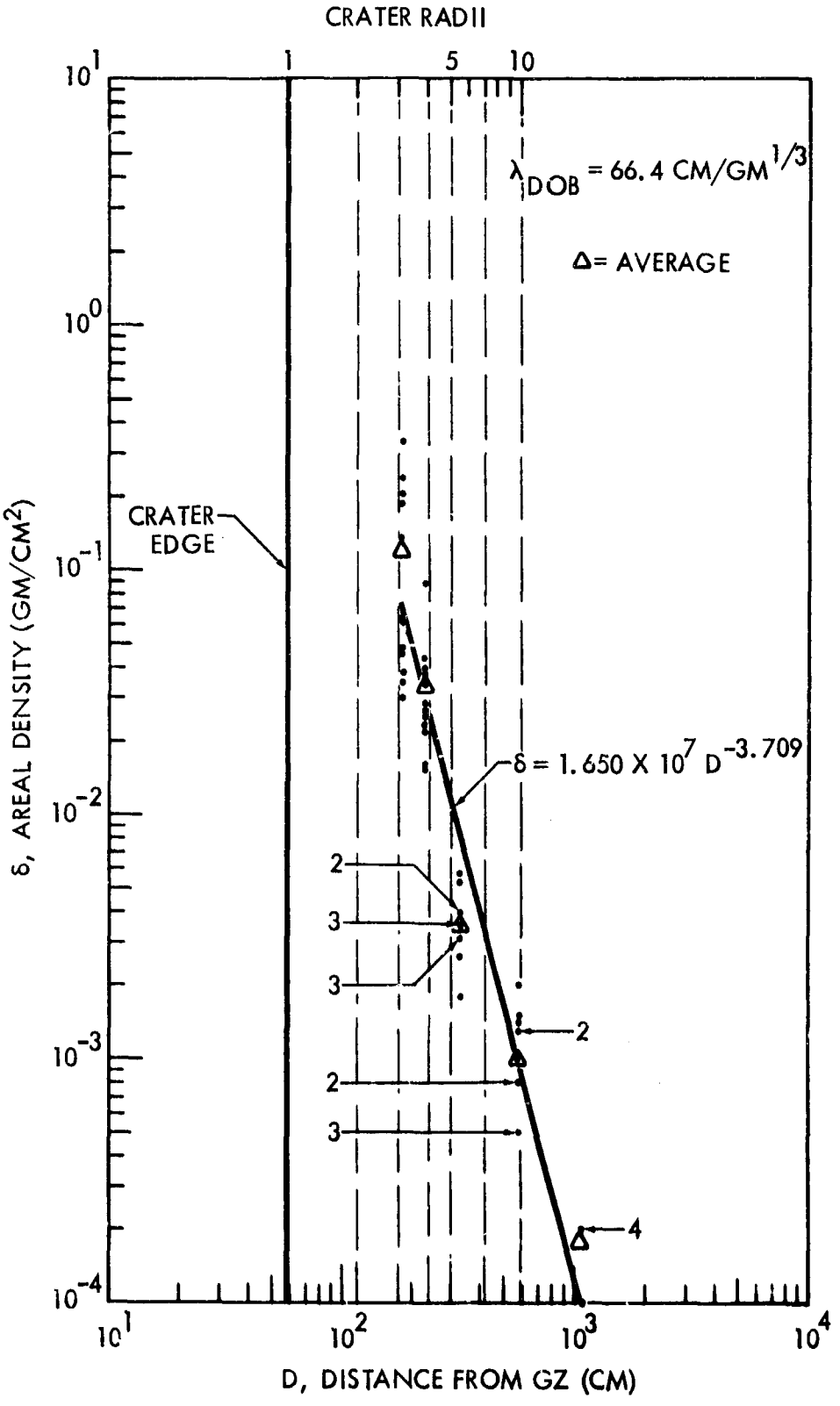

Figure B.3 Areal Density Versus Distance From Ground Zero for Shot D2.5A

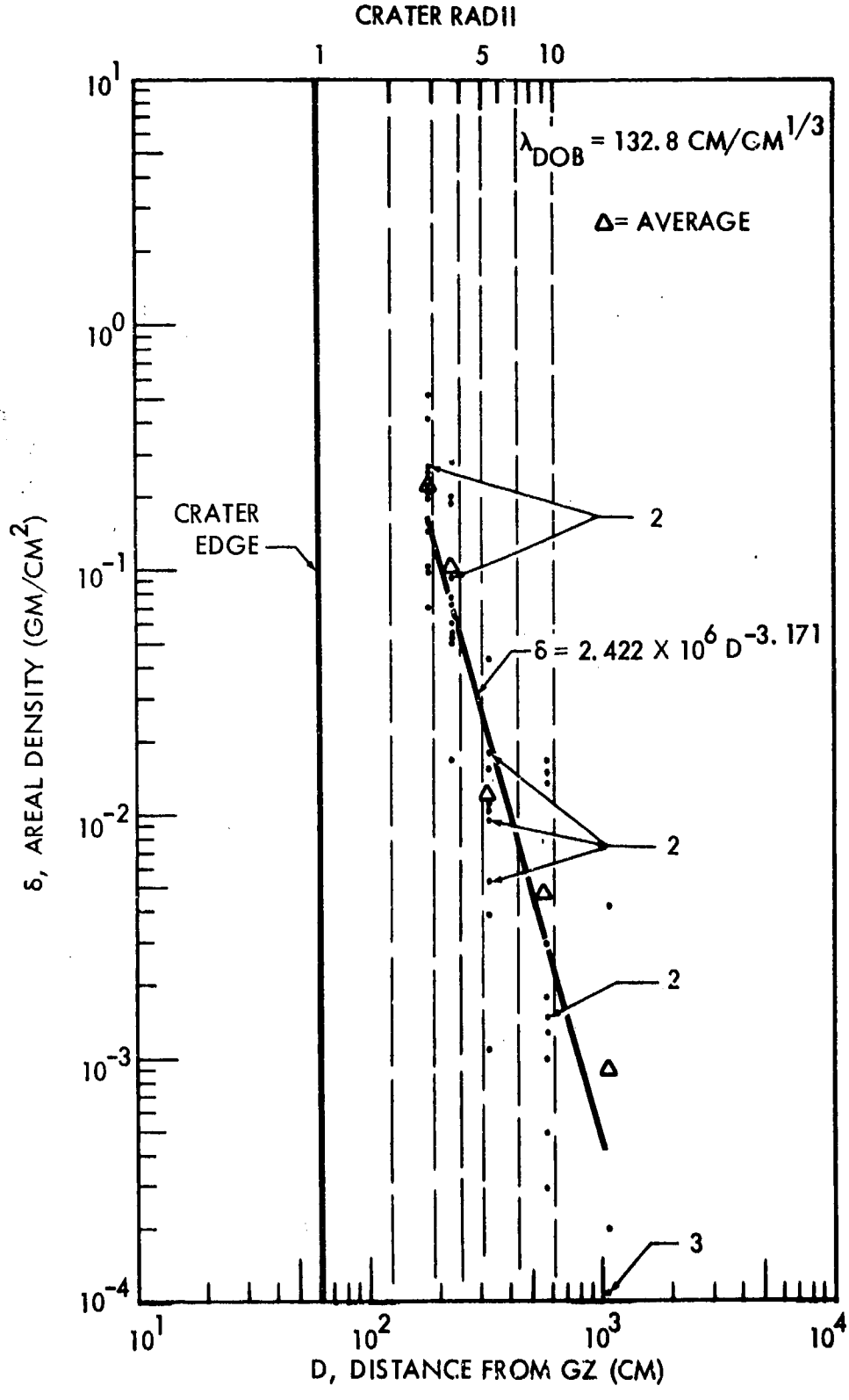

Figure B.4 Areal Density Versus Distance From Ground Zero for Shot D3.5A

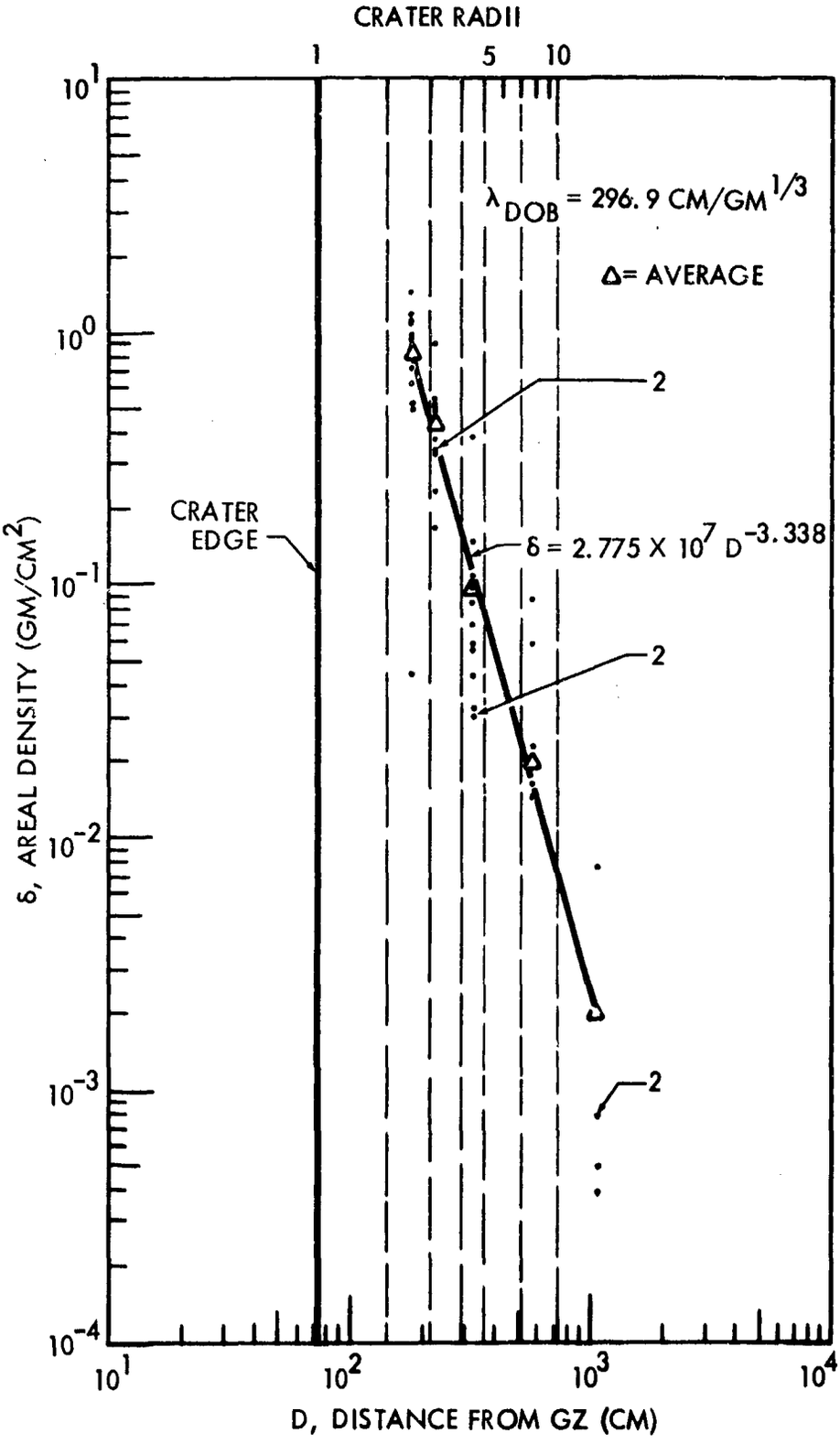

Figure B.5 Areal Density Versus Distance From Ground Zero for Shot D4.5A

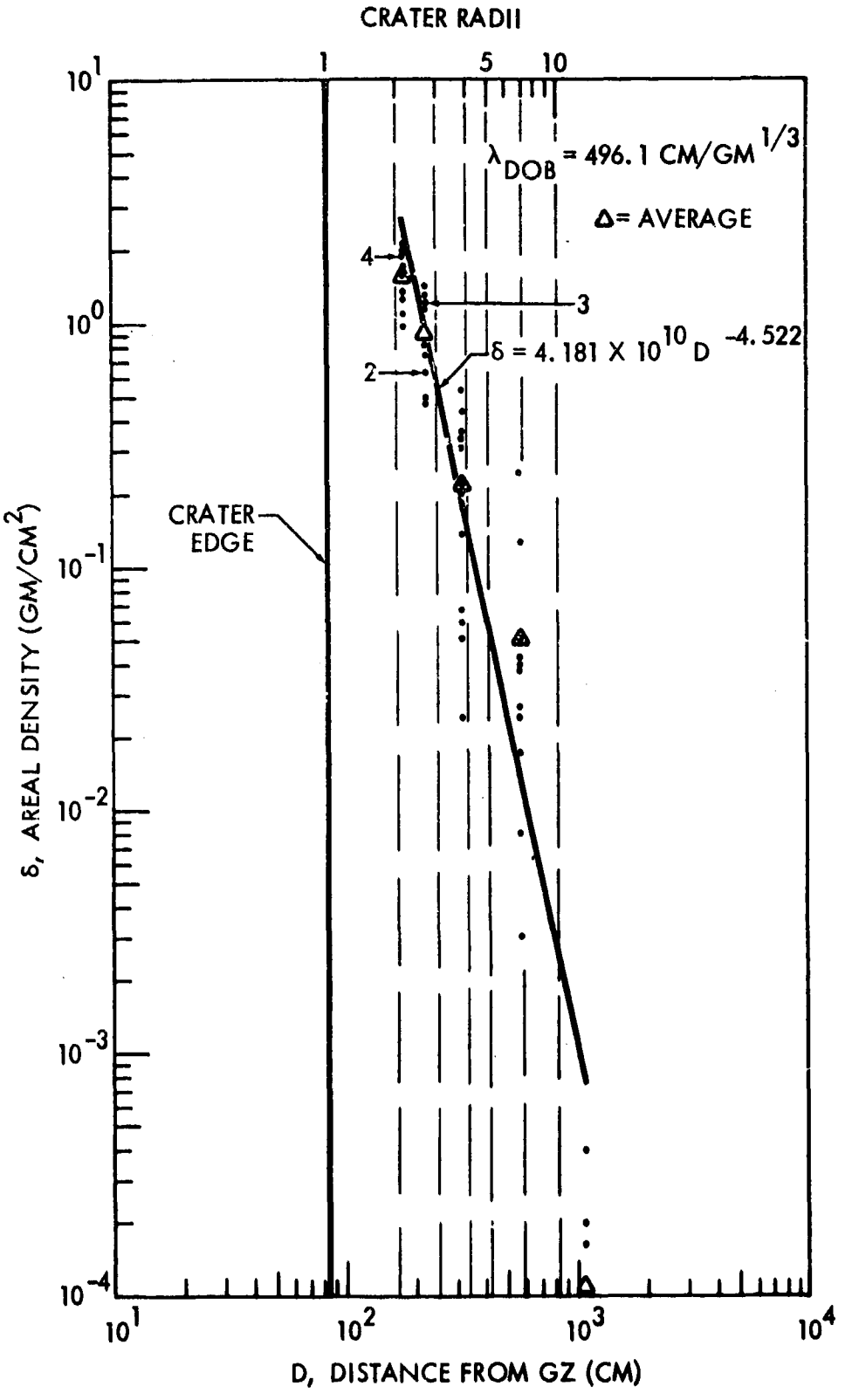

Figure B.6 Areal Density Versus Distance From Ground Zero for Shot D5.5A

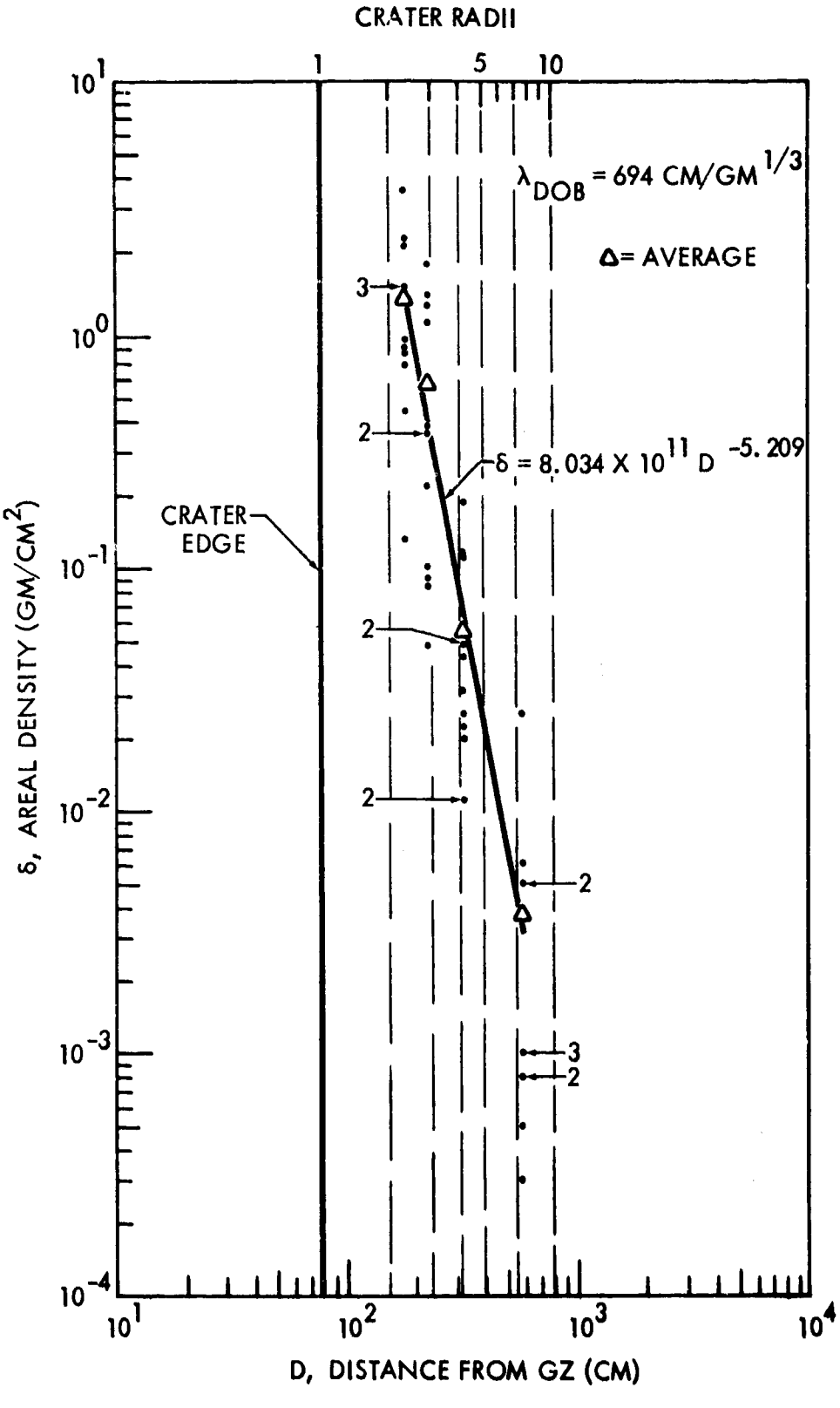

Figure 8.7 Areal Density Versus Distance From Ground Zero for Shot D6.5A

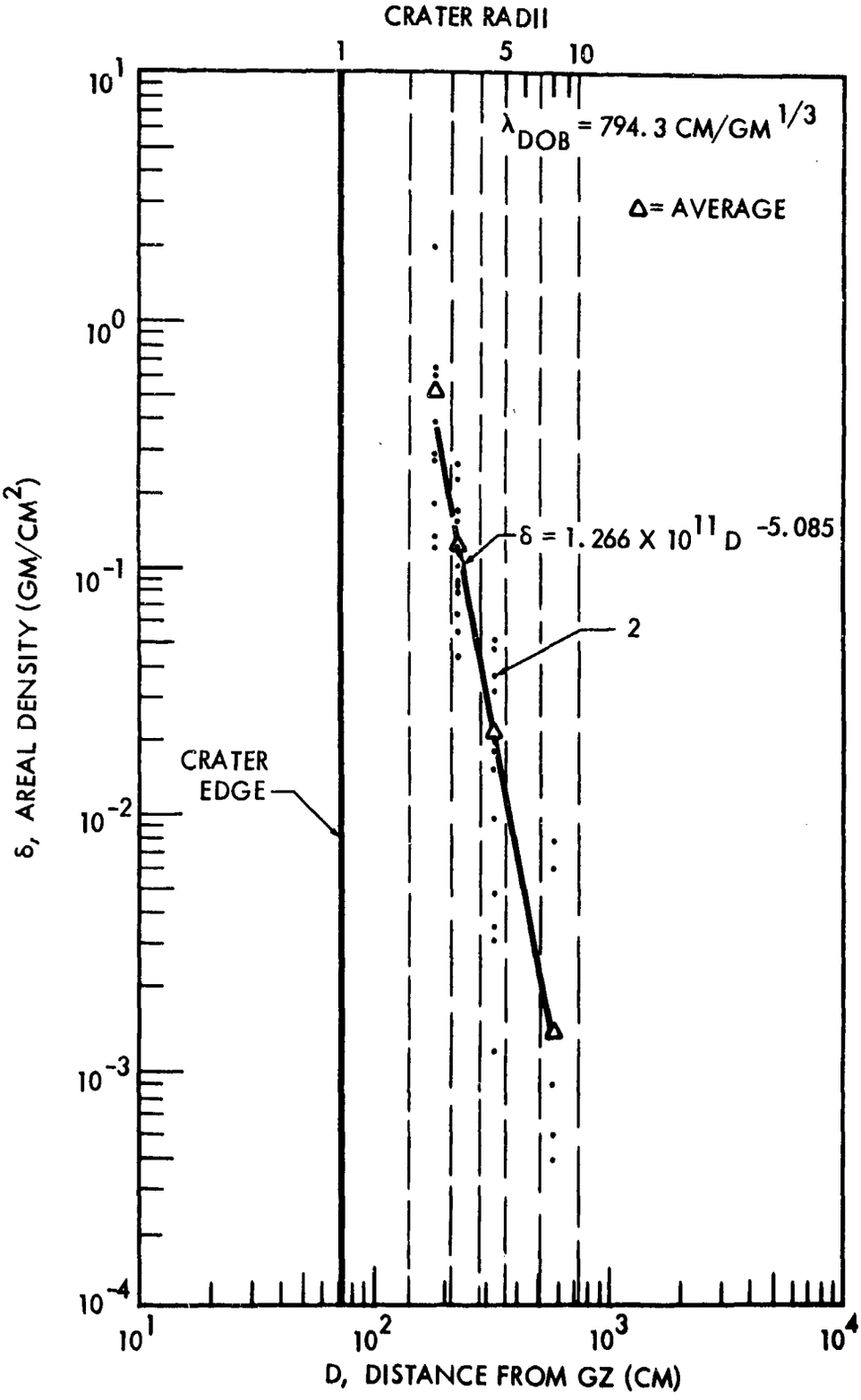

Figure B.8 Areal Density Versus Distance From Ground Zero for Shot D7A

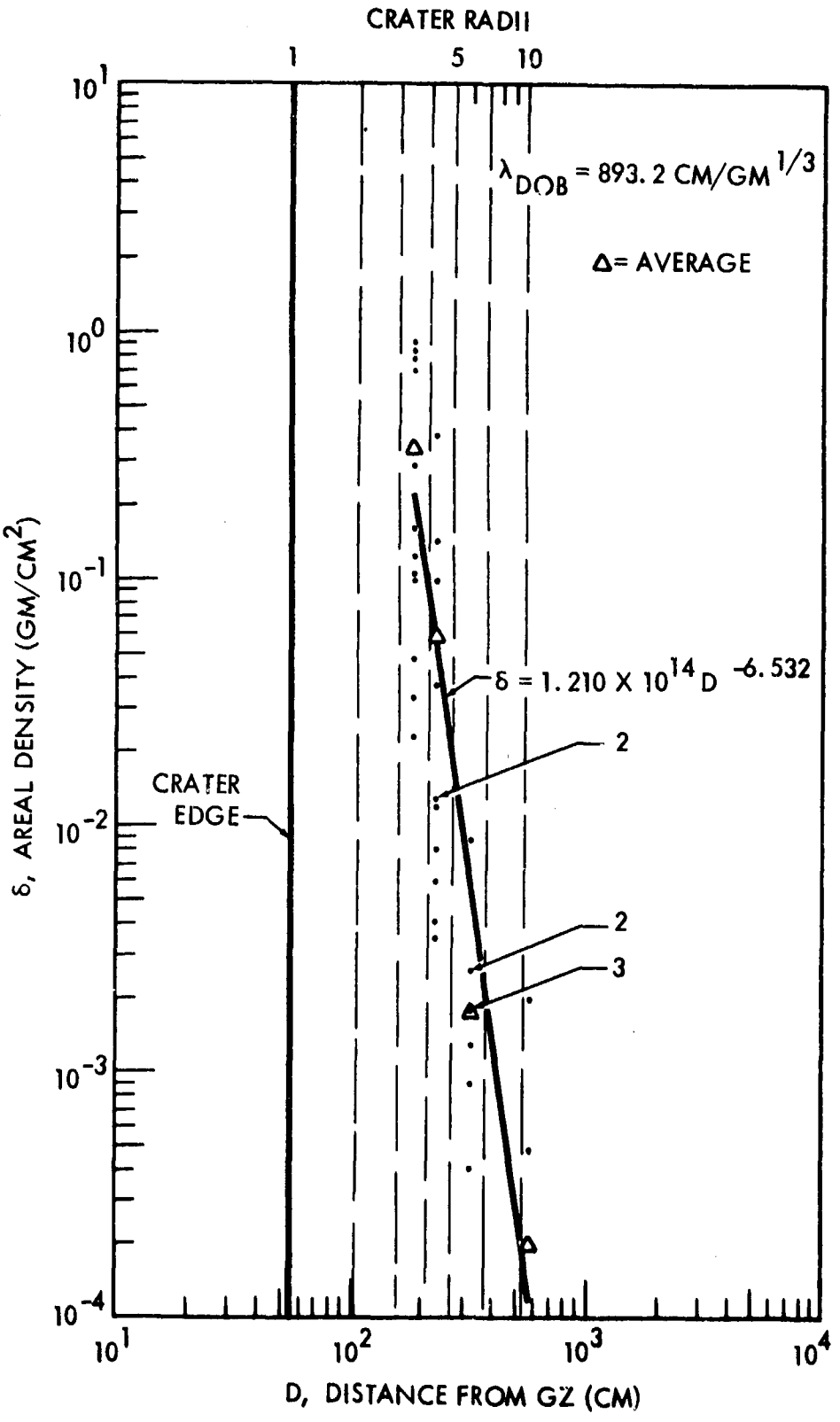

Figure B.9 Areal Density Versus Distance From Ground Zero for Shot D7.5A

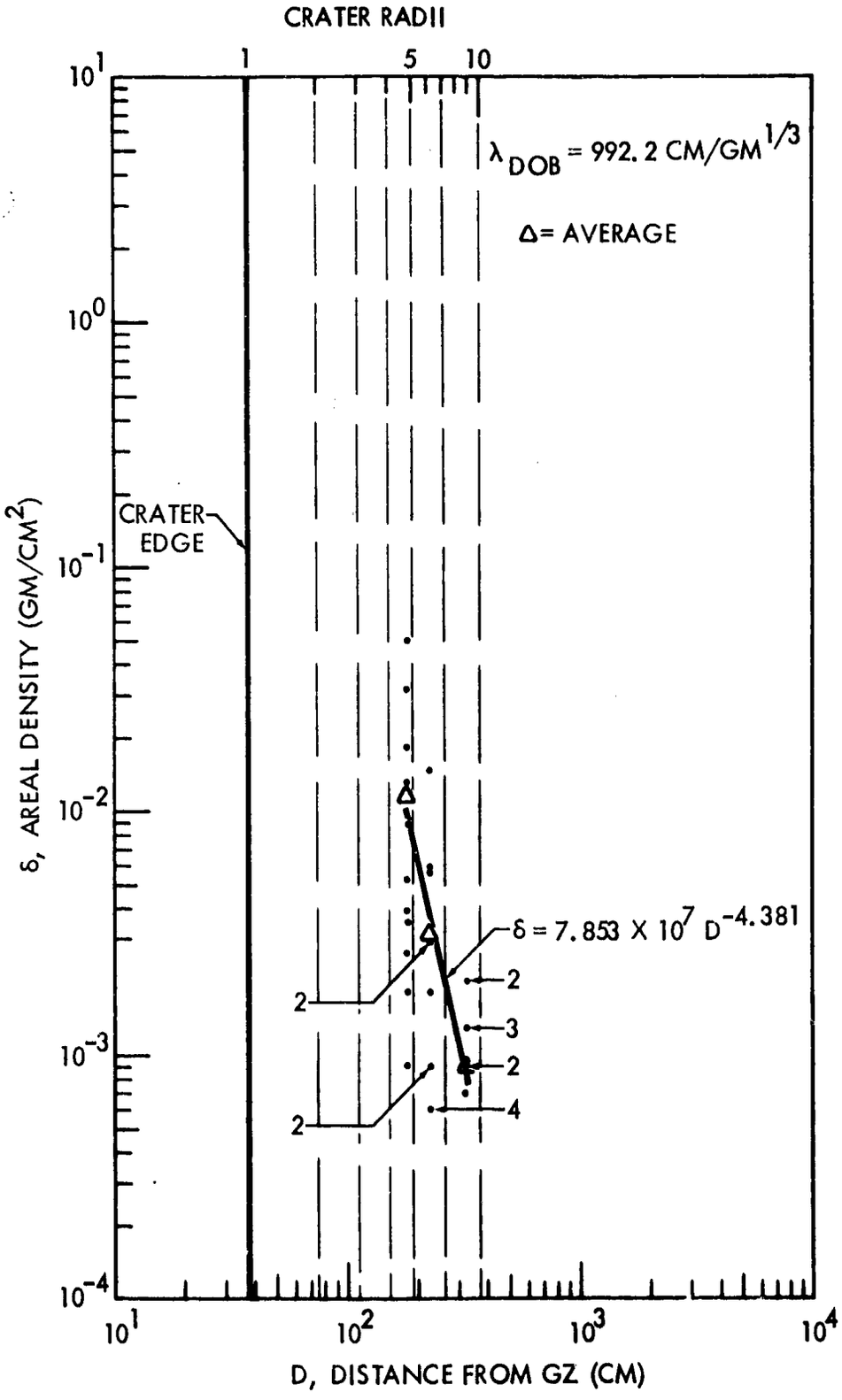

Figure B.10 Areal Density Versus Distance From Ground Zero for Shot D8A

APPENDIX C

CRATER MAPS AND PROFILES

Topographic profiles measured in accordance with the procedure shown in Figure 1, Views C and D, are shown in Figures C. 1 through C. 29.

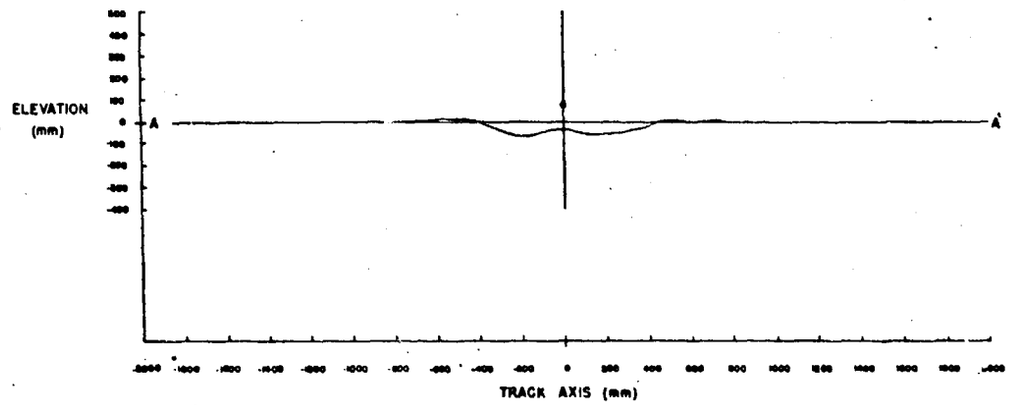
ELEVATION
(mm)
A
A'
TRACK AXIS (mm)

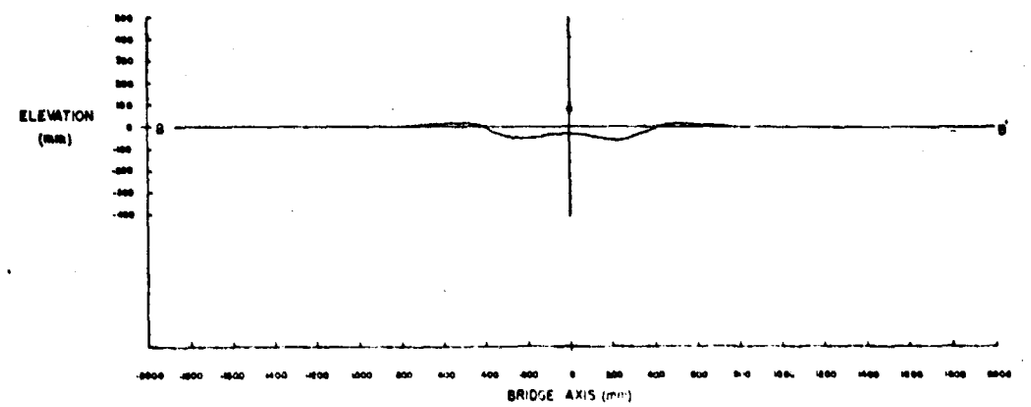
ELEVATION
(mm)
B
B'
BRIDGE AXIS (mm)

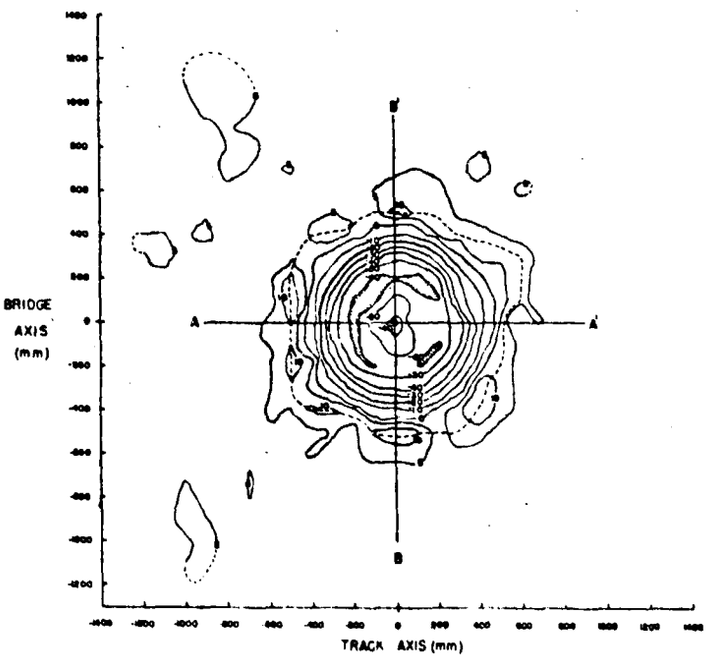

2

BOEING
J D1A

Figure C.1 Crater Map and Profile for Shot D1A

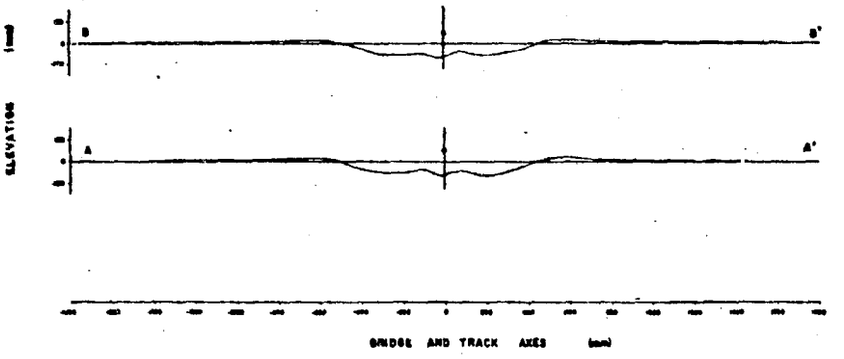
ELEVATION (mm)
B
B'
A
A'
BRIDGE AND TRACK AXES (mm)

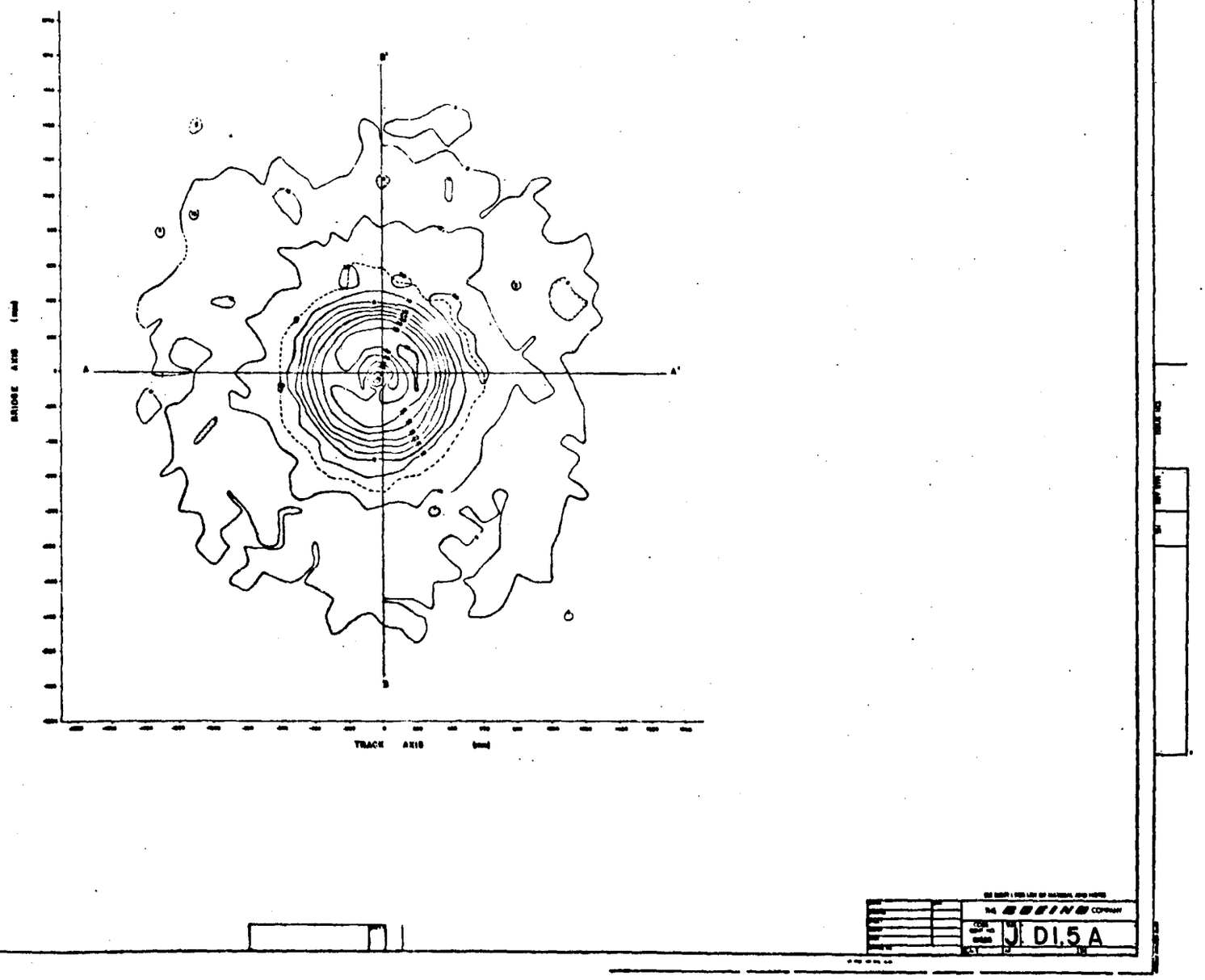

Figure C. 2 Crater Map and Profile for Shot D1. 5A

2

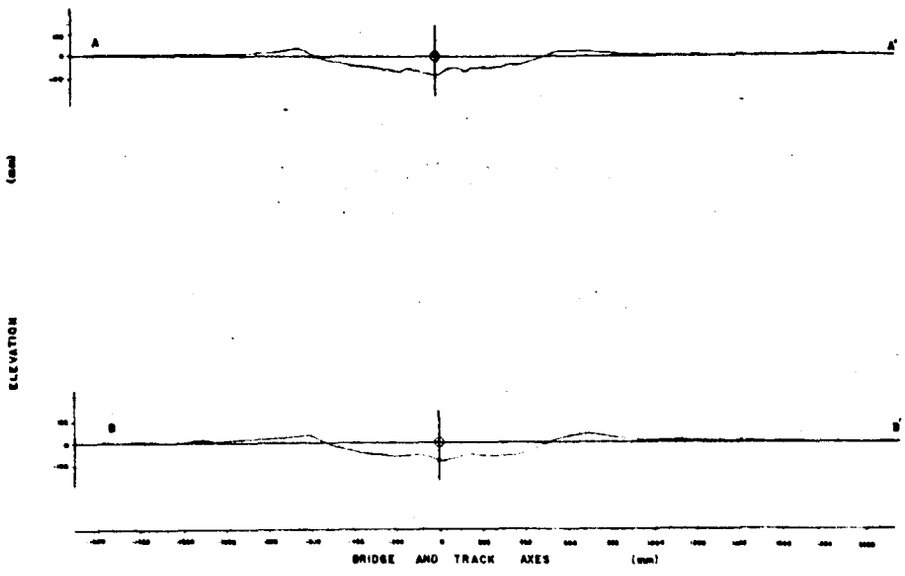
A
A'
B
B'
ELEVATION
BRIDGE AND TRACK AXES
(mm)

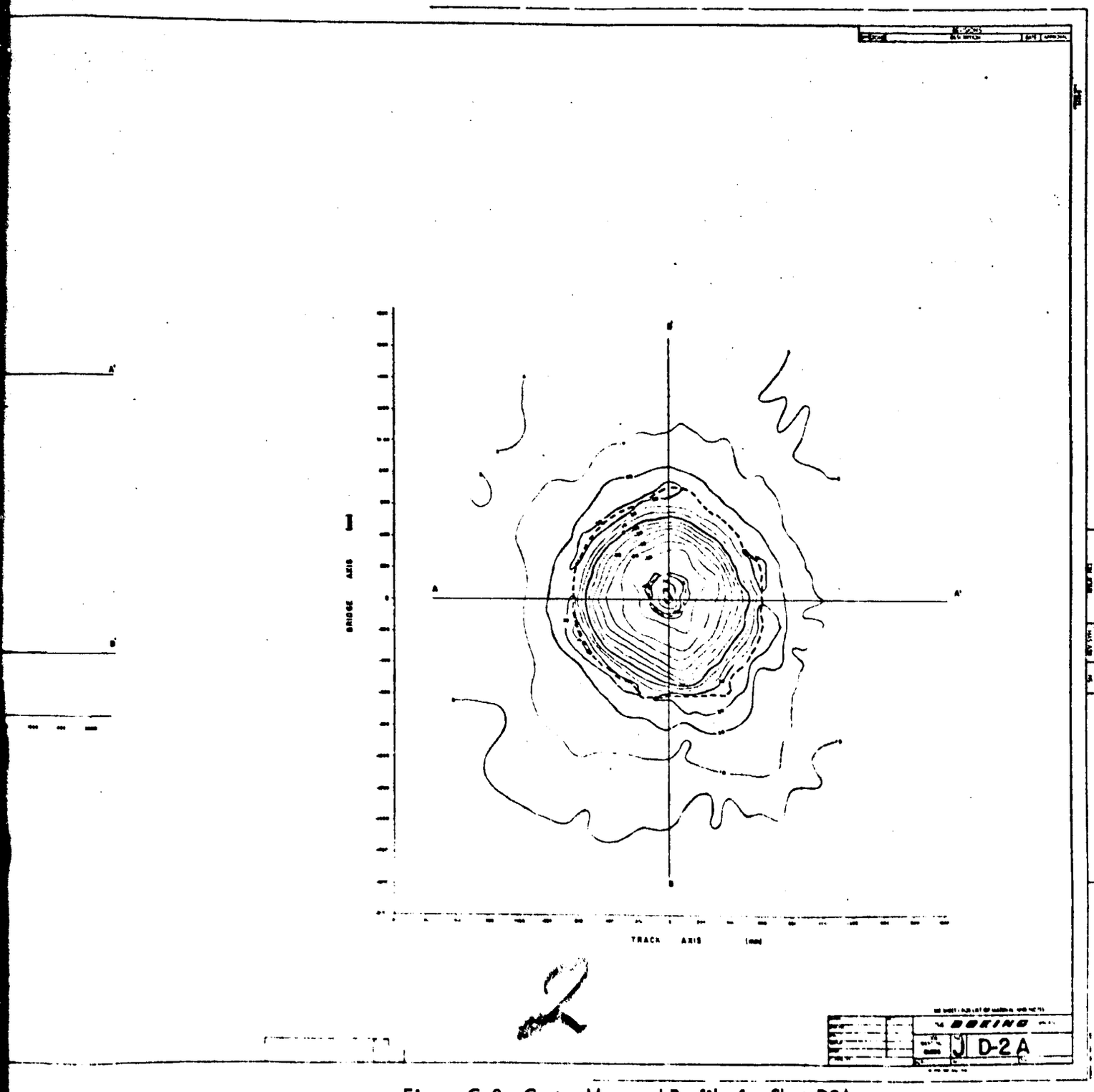

Figure C. 3 Crater Map and Profile for Shot D2A

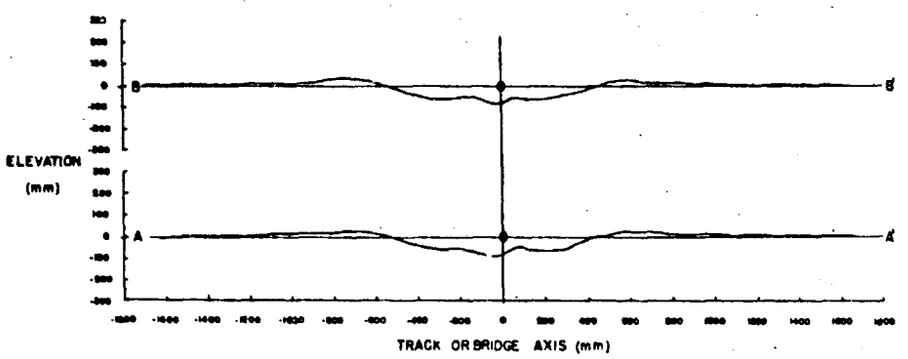

BRIDGE
AXIS
(mm)

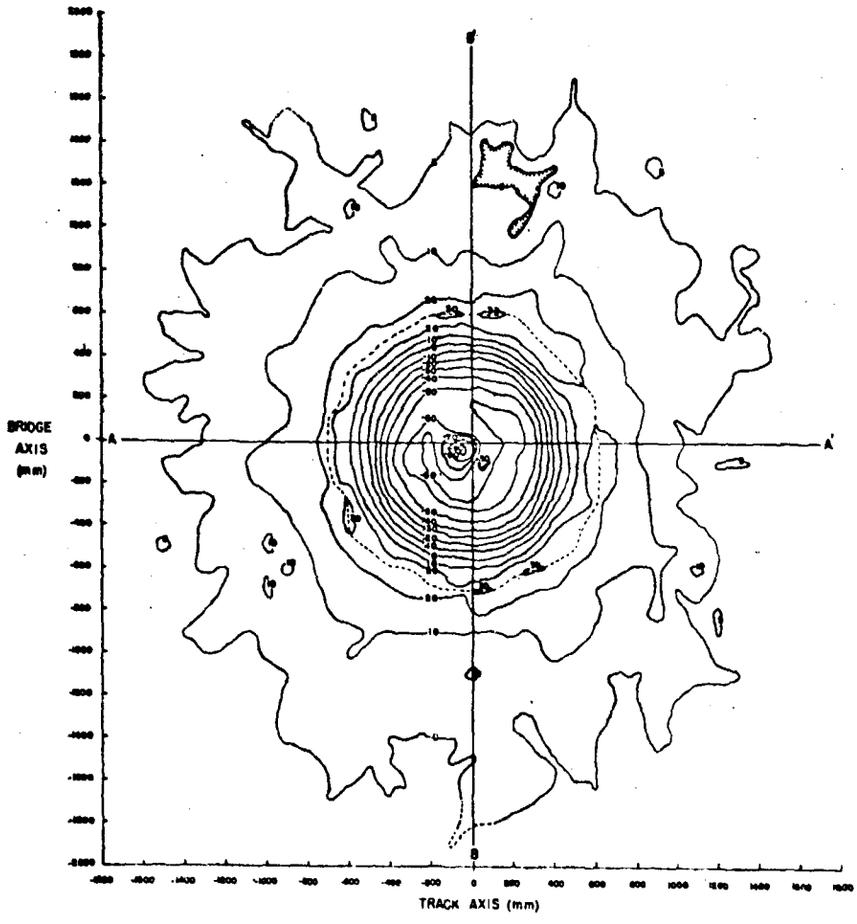

Figure C. 4 Crater Map and Profile for Shot D2B

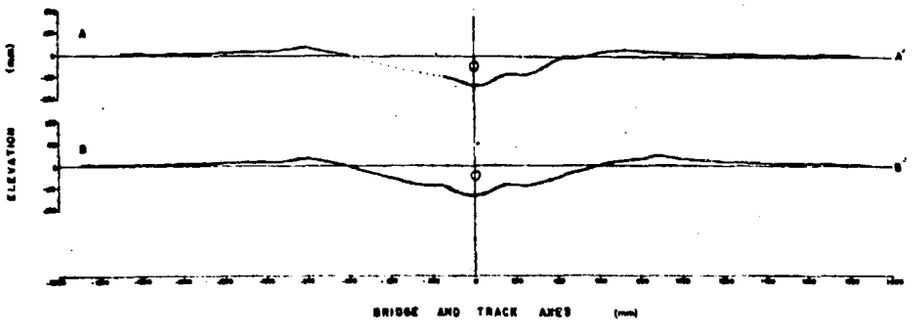
ELEVATION (mm)
A
A'
B
B'
BRIDGE AND TRACK AXES (mm)

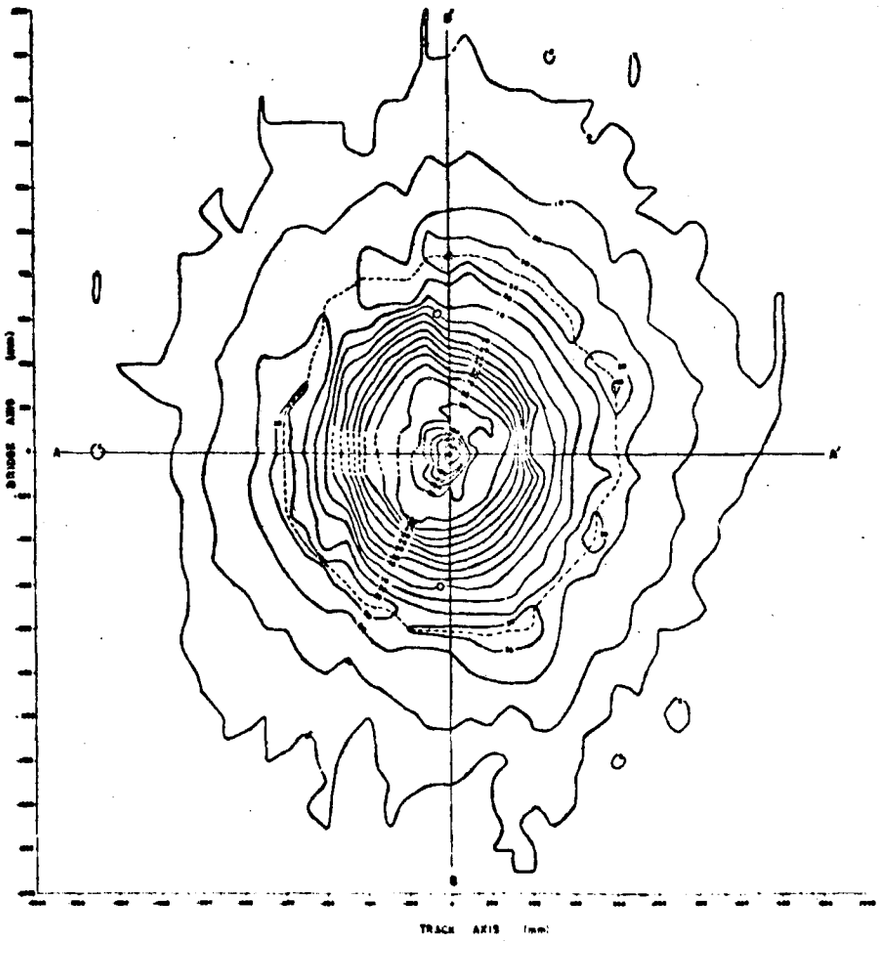

BOEING
D 2.5A

Figure C.5 Crater Map and Profile for Shot D2.5A

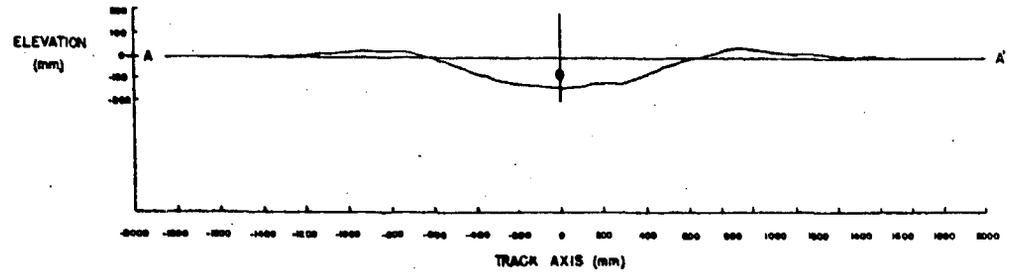
ELEVATION
(mm)
A
A'
TRACK AXIS (mm)

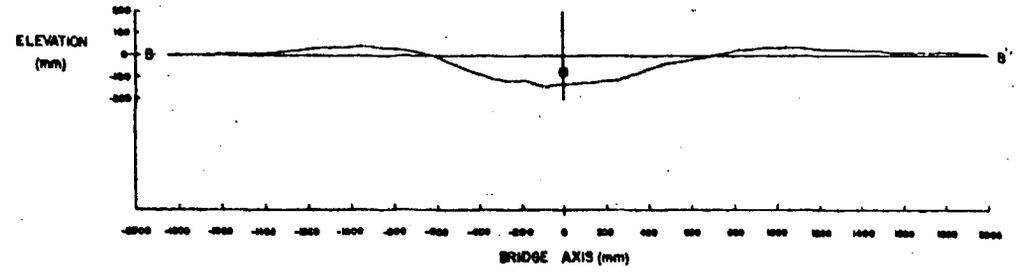
ELEVATION
(mm)
B
B'
BRIDGE AXIS (mm)

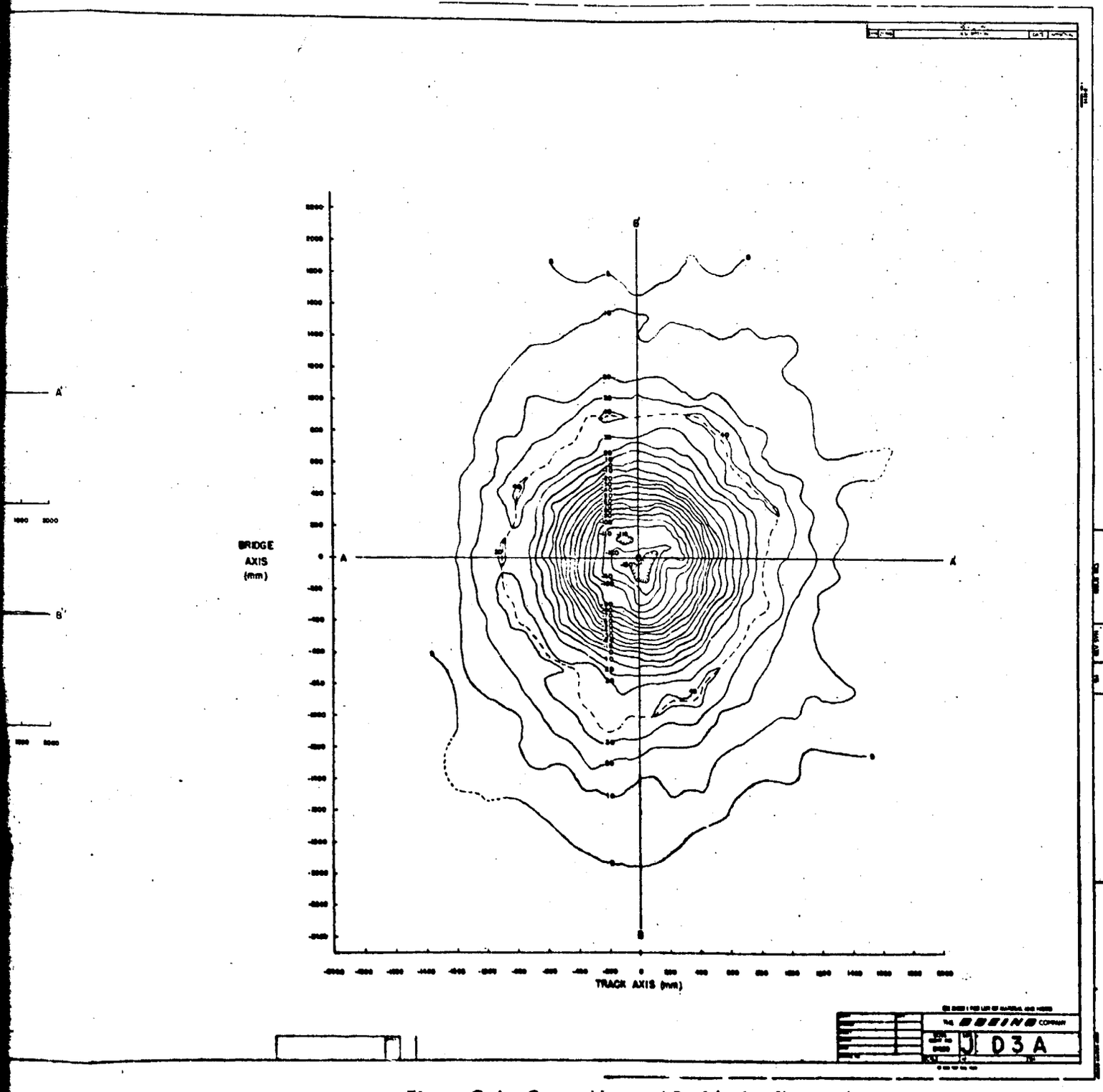

Figure C.6 Crater Map and Profile for Shot D3A

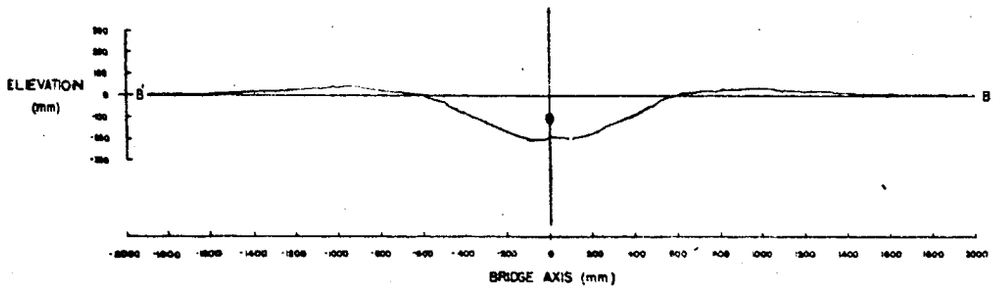
ELEVATION
(mm)
B'
B
BRIDGE AXIS (mm)

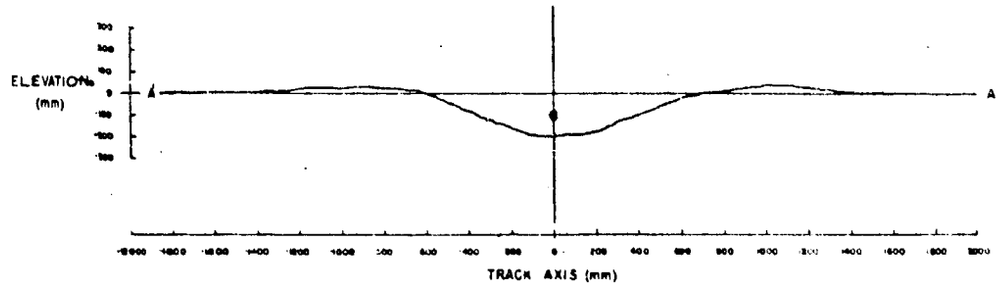
ELEVATION
(mm)
A
A
TRACK AXIS (mm)

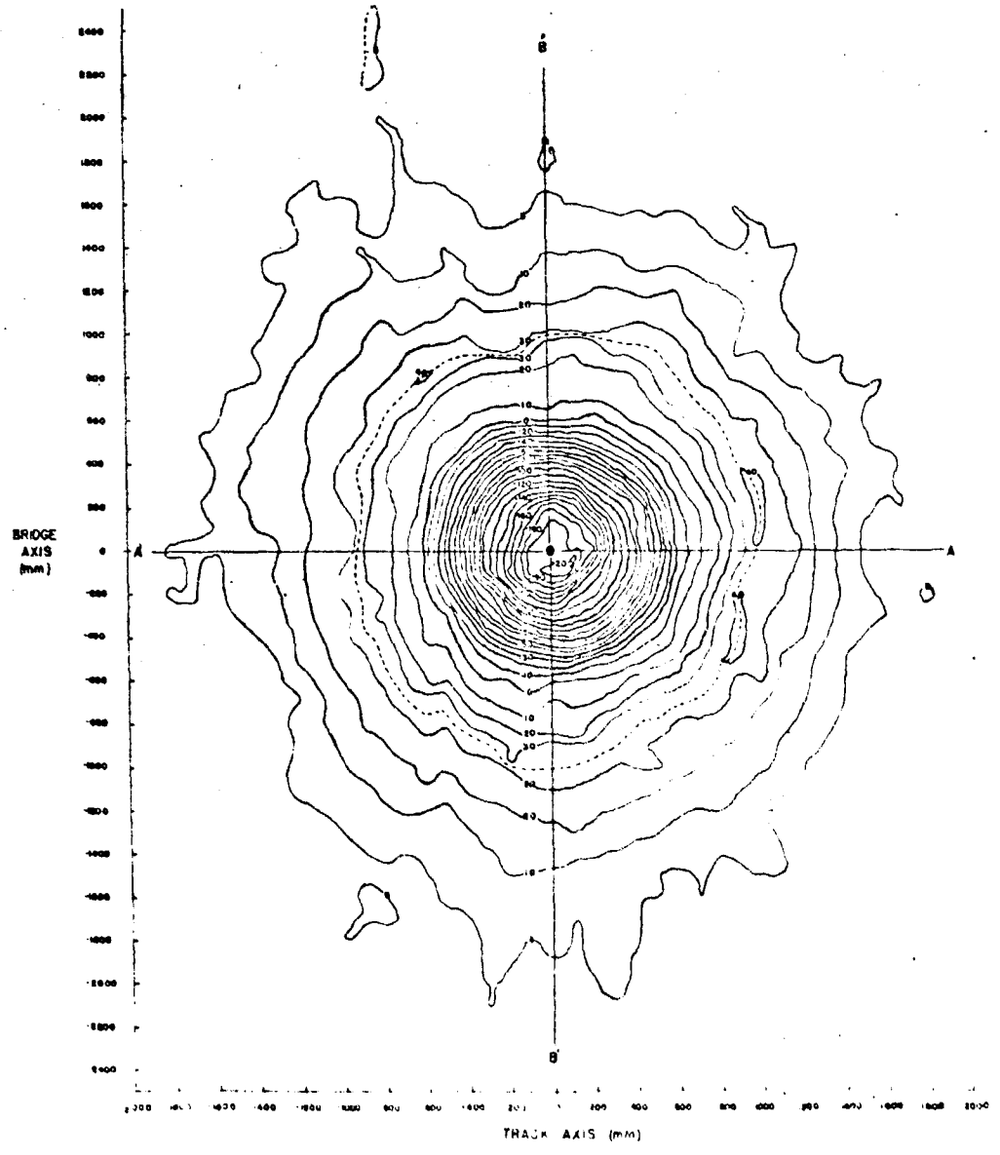

Figure C.7 Crater Map and Profile for Shot D3.5A

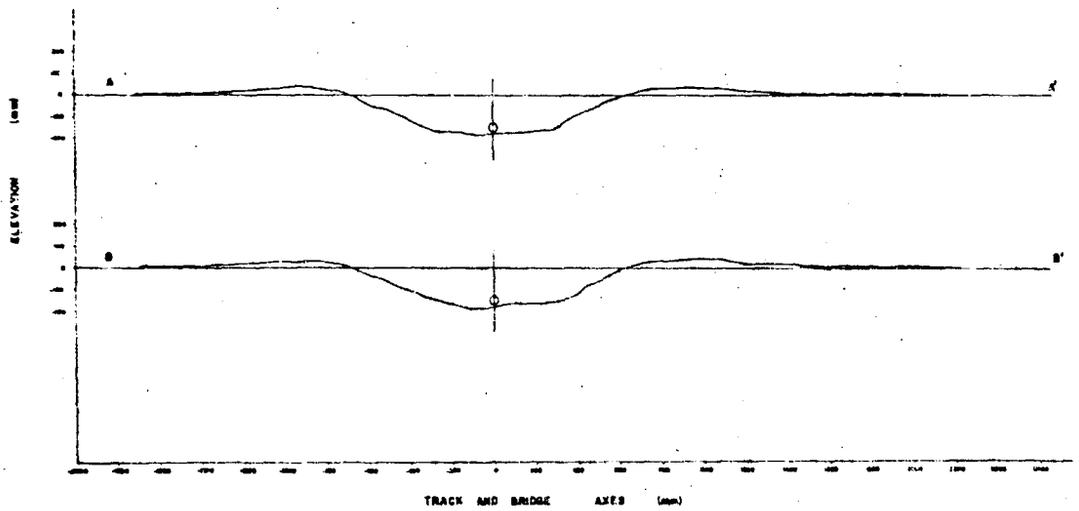
A
A'
B
B'
ELEVATION (mm)
TRACK AND BRIDGE AXES (mm)

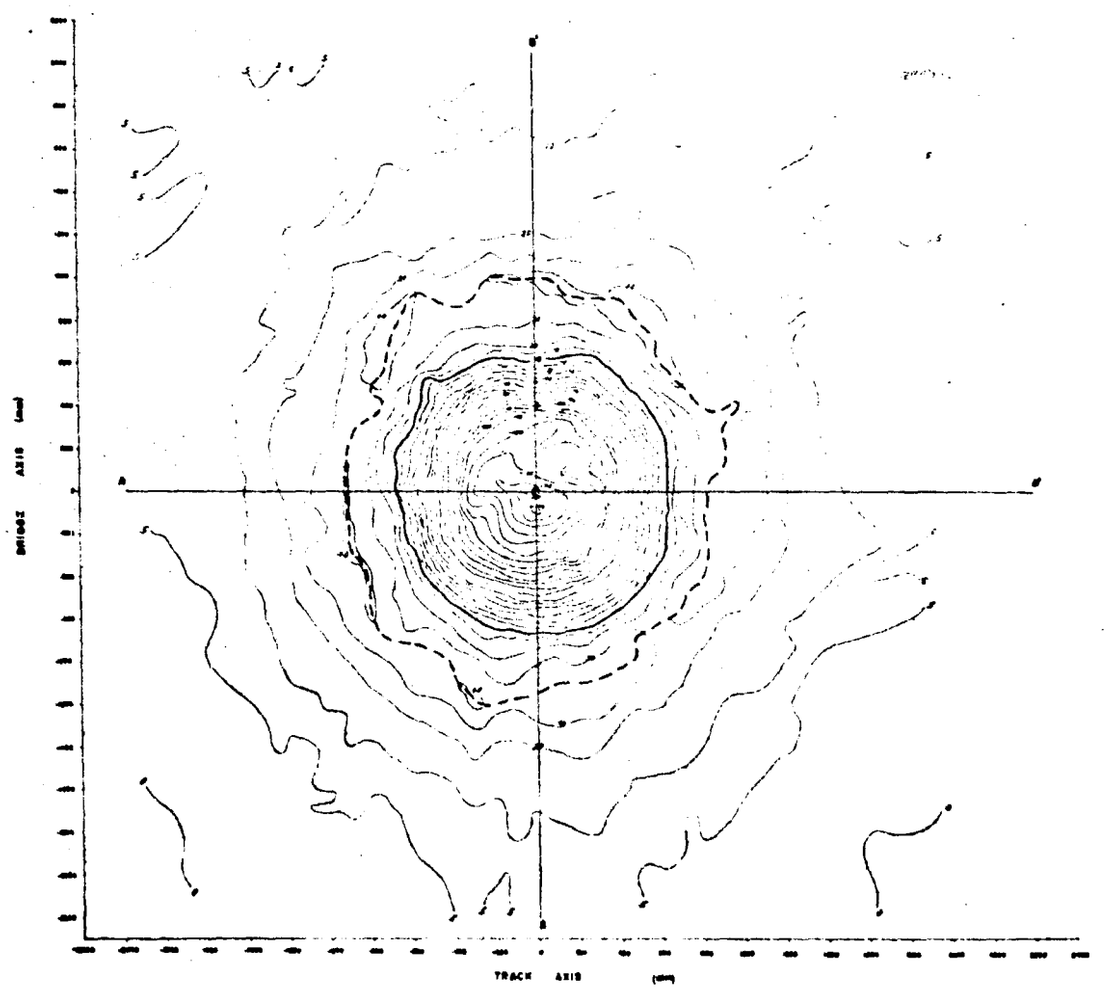

Figure . o . . ap and Profile for Shot D4A

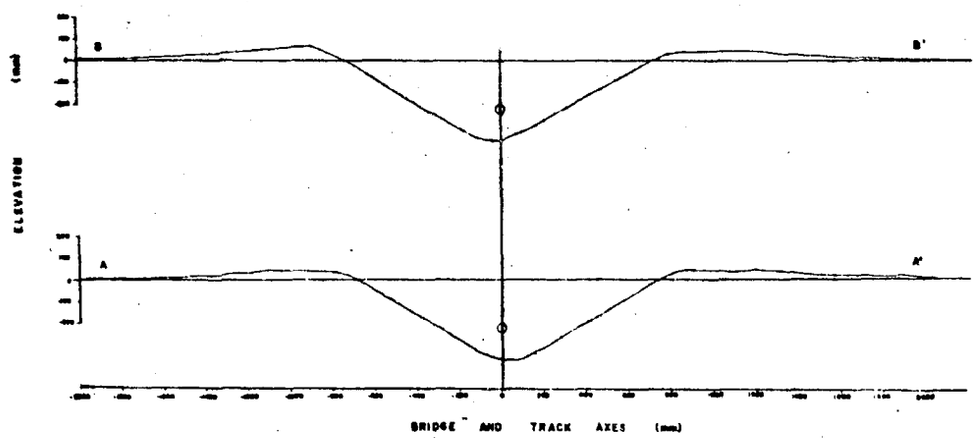
ELEVATION (mm)
B
B'
A
A'
BRIDGE AND TRACK AXES (mm)

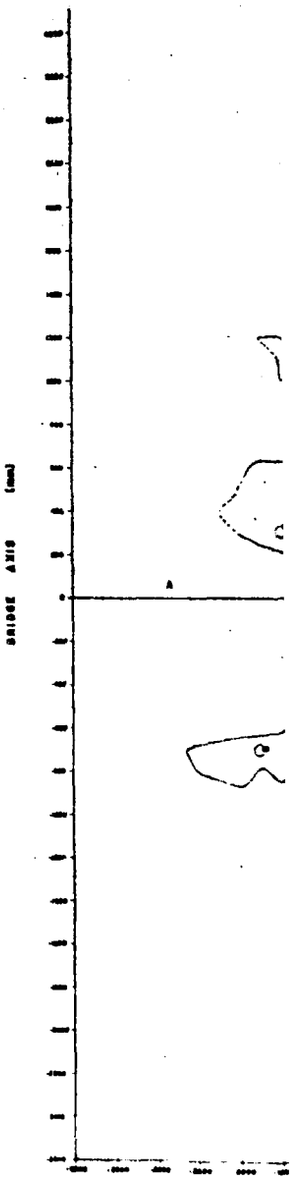
BRIDGE AXIS (mm)
A

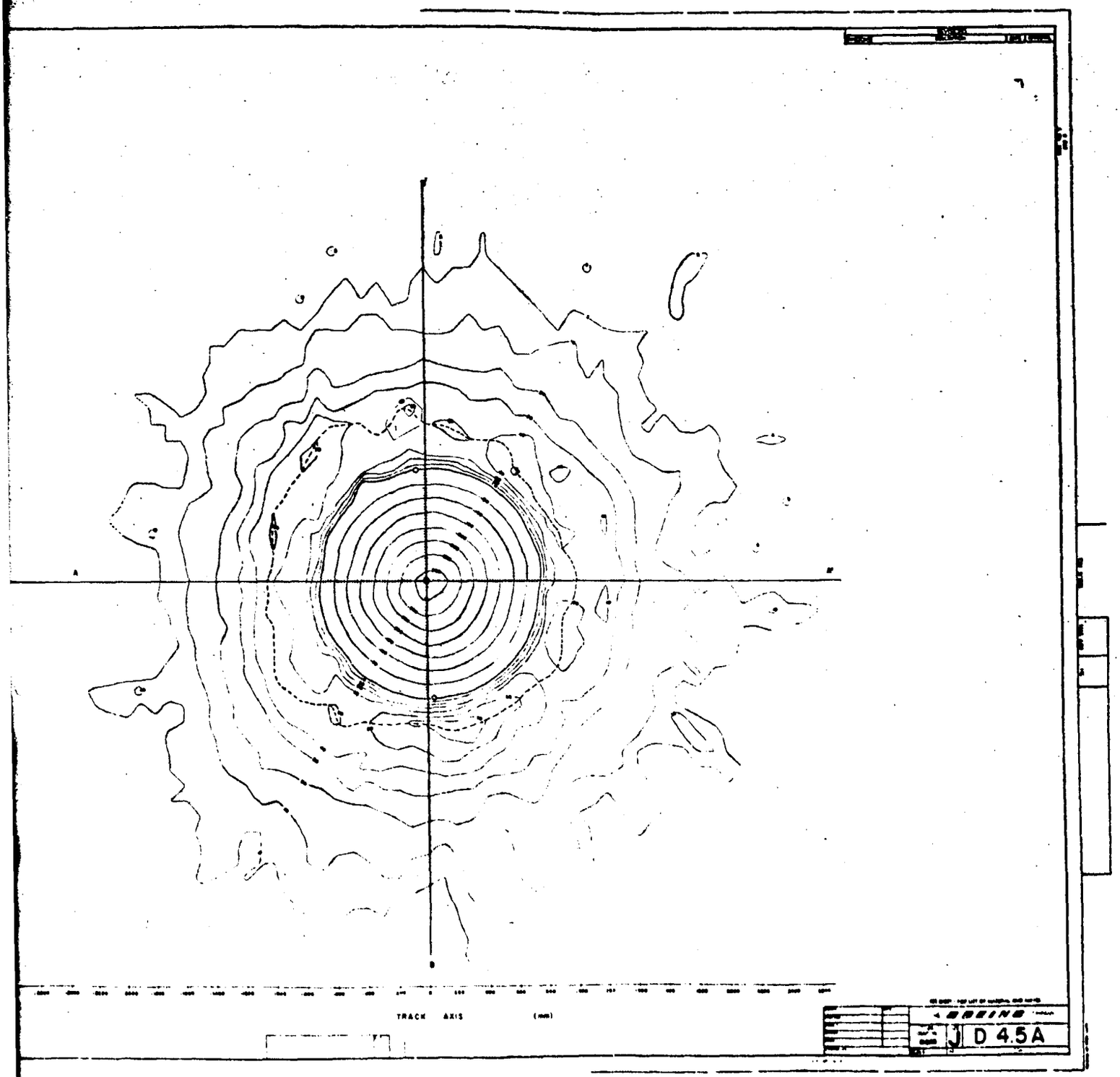

Figure C.9 Crater Map and Profile for Shot D4.5A

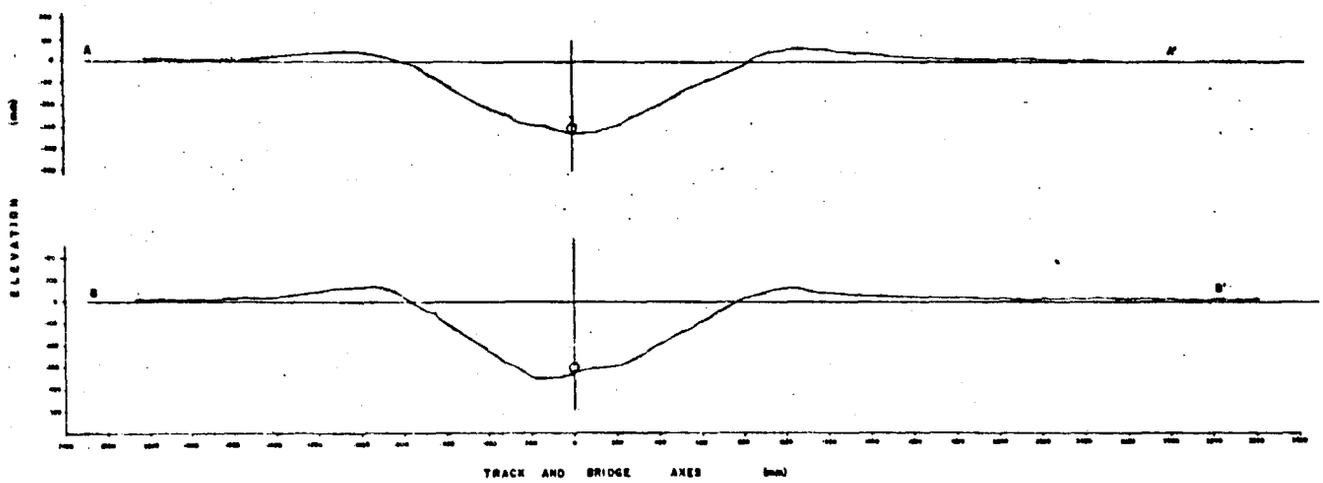
A
A'
B
B'
ELEVATION
TRACK AND BRIDGE AXES

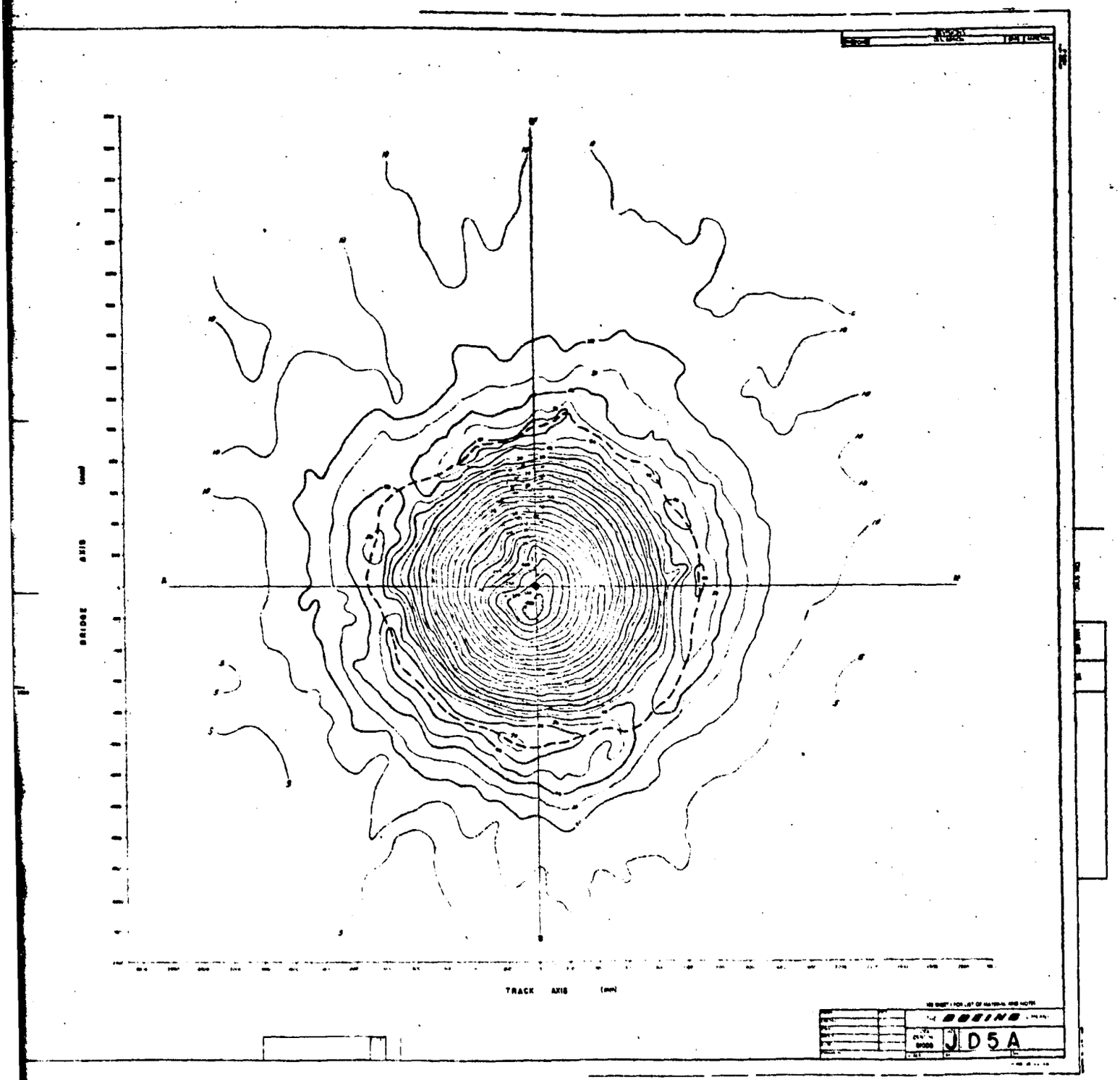

Figure C. 10 Crater Map and Profile for Shot D5A

2

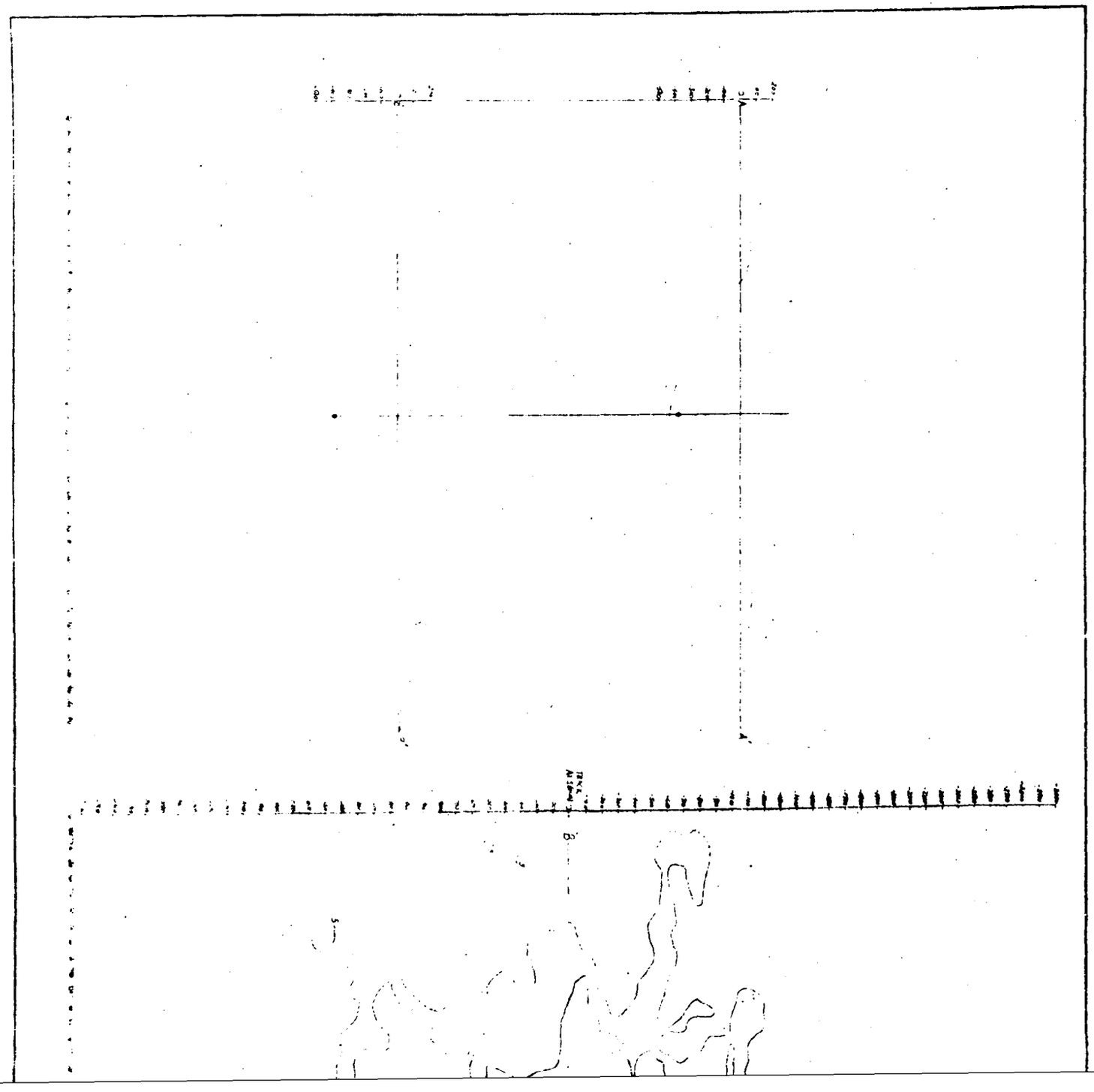

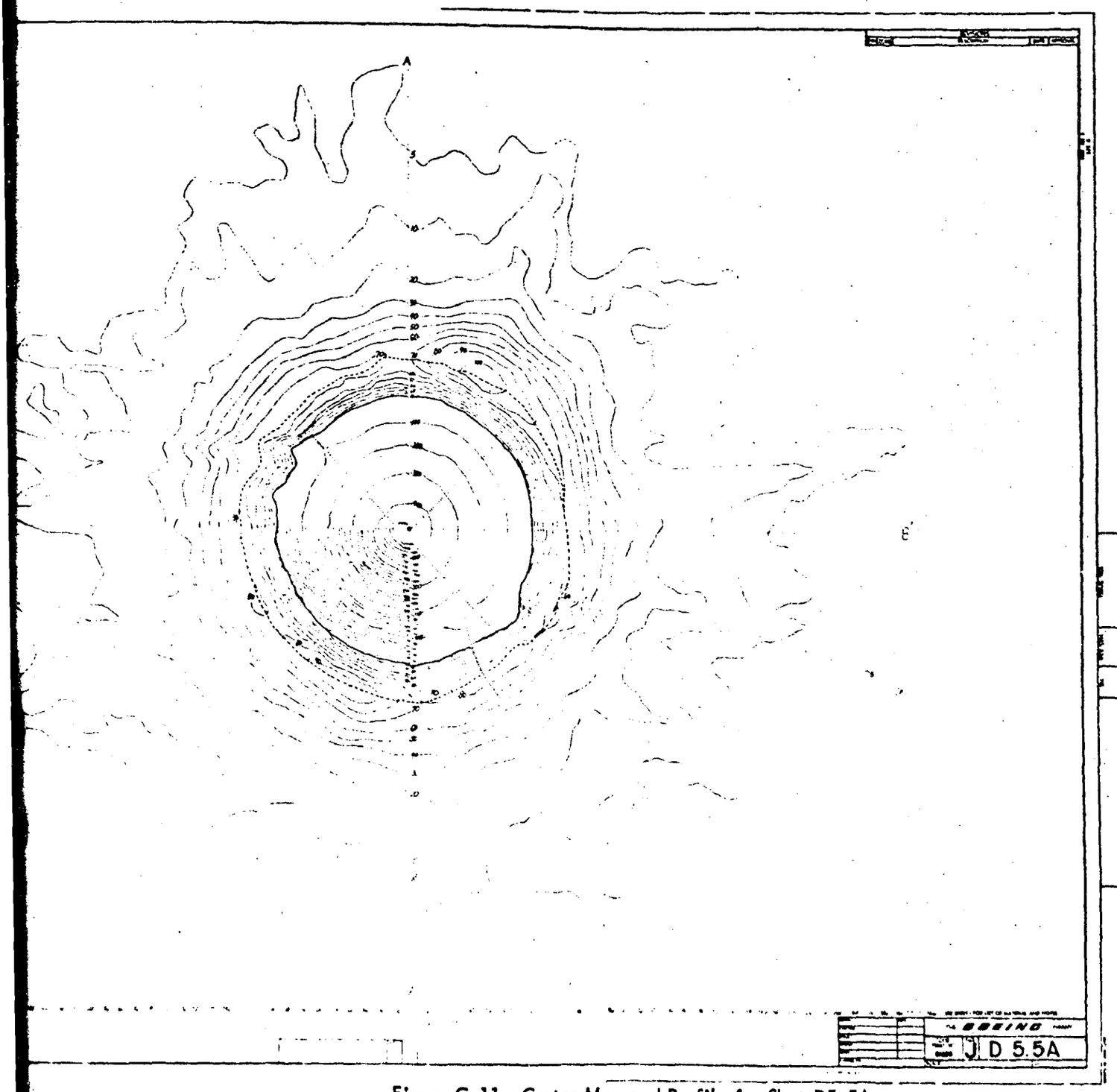

Figure C.11 Crater Map and Profile for Shot D5.5A

2

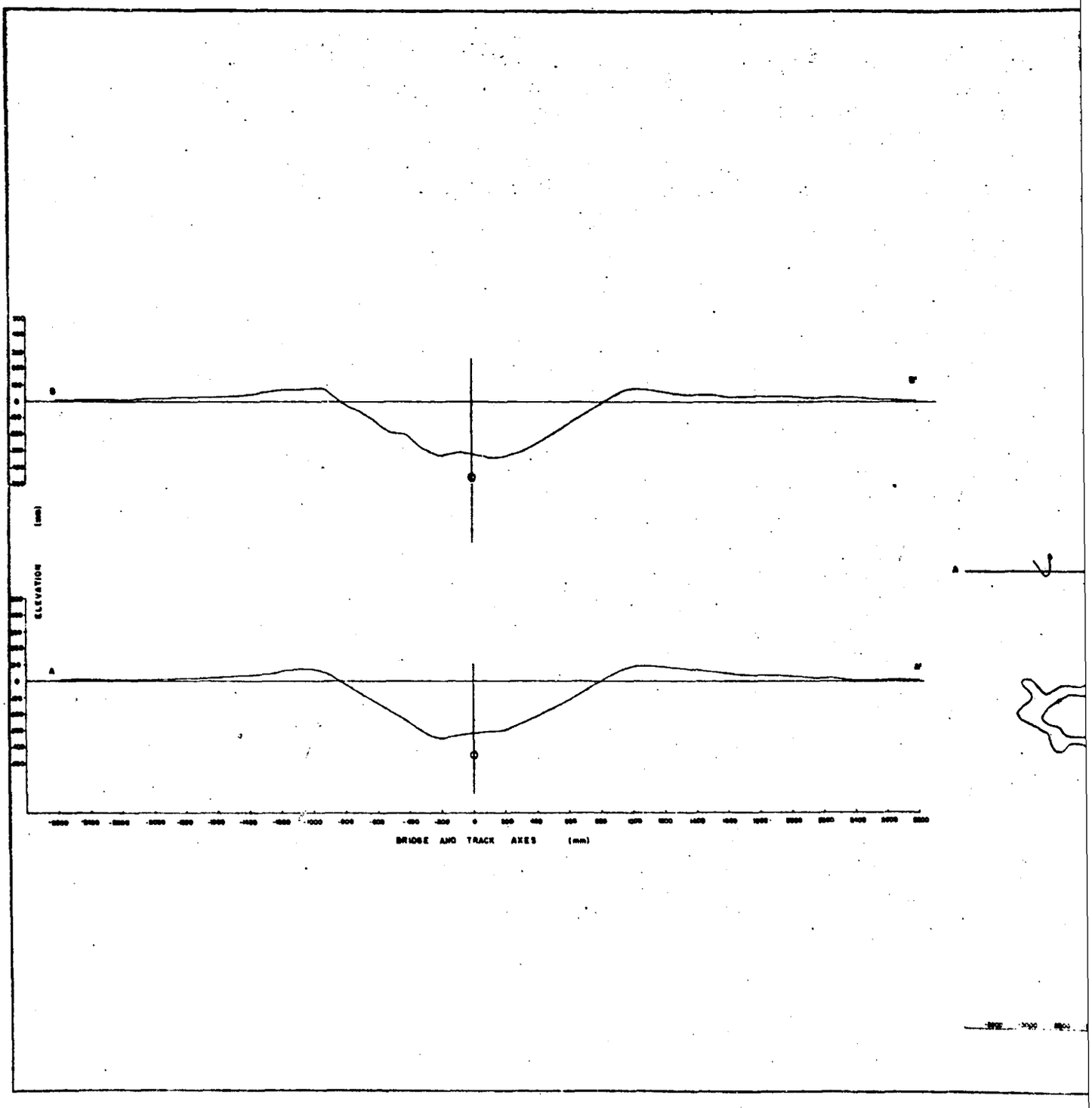
ELEVATION (mm)
B
A
BRIDGE AND TRACK AXES (mm)

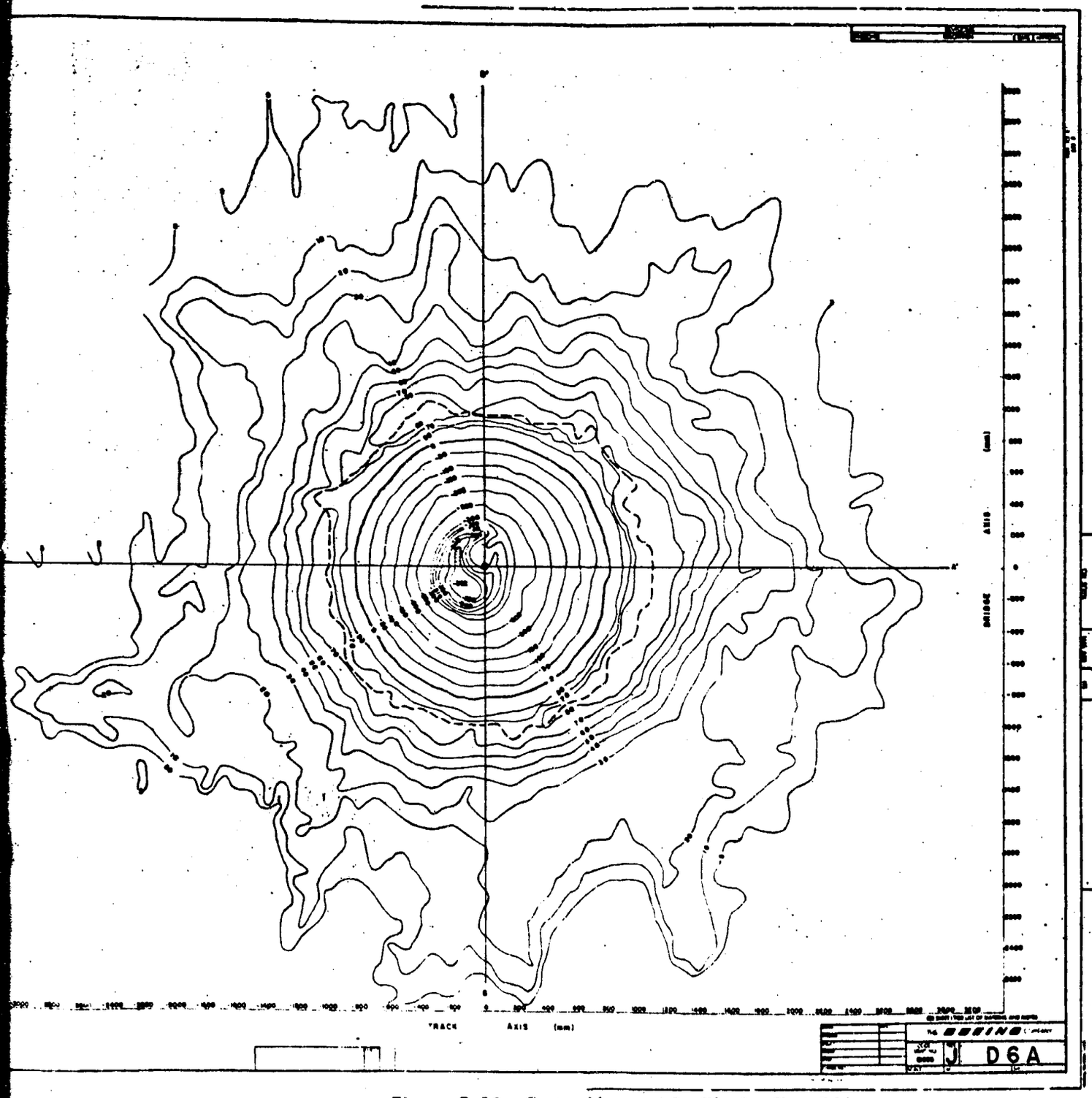

Figure C. 12 Crater Map and Profile for Shot D6A

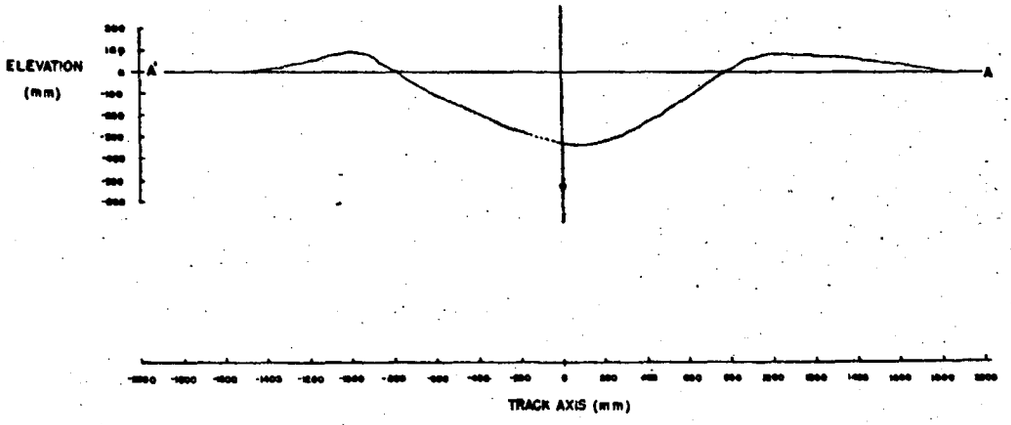
ELEVATION
(mm)
A'
A
TRACK AXIS (mm)

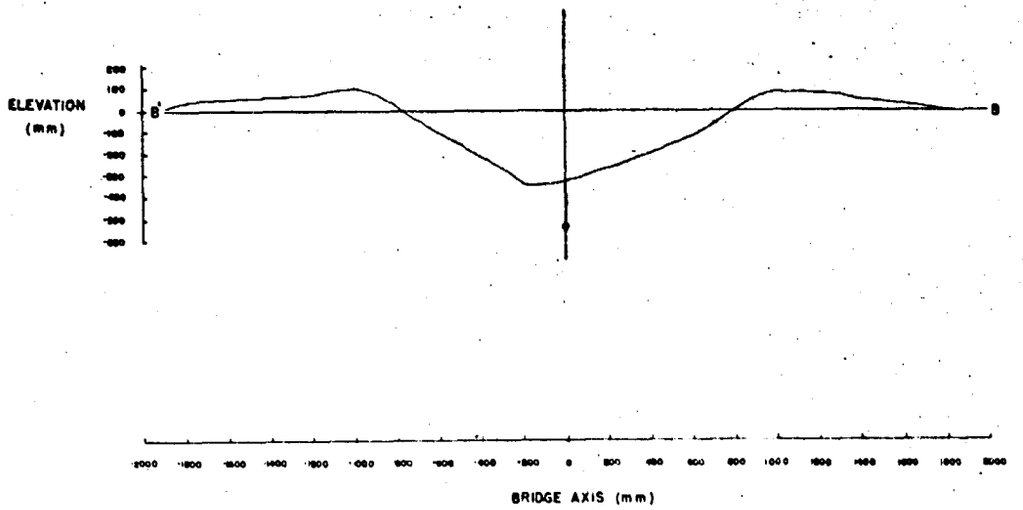
ELEVATION
(mm)
B'
B
BRIDGE AXIS (mm)

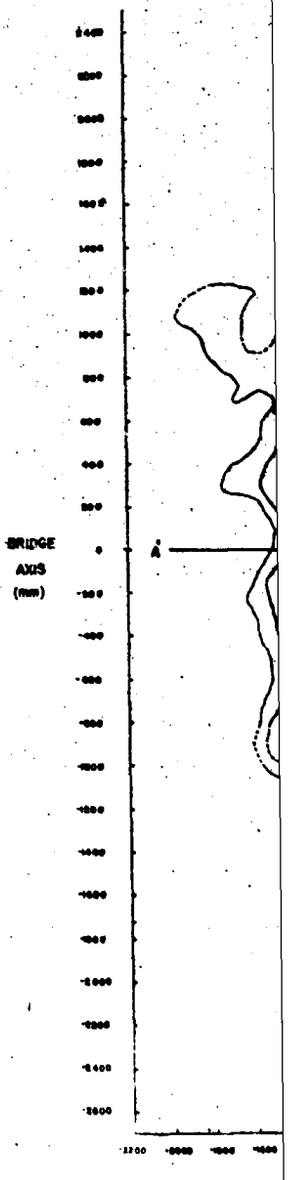
BRIDGE
AXIS
(mm)
A'

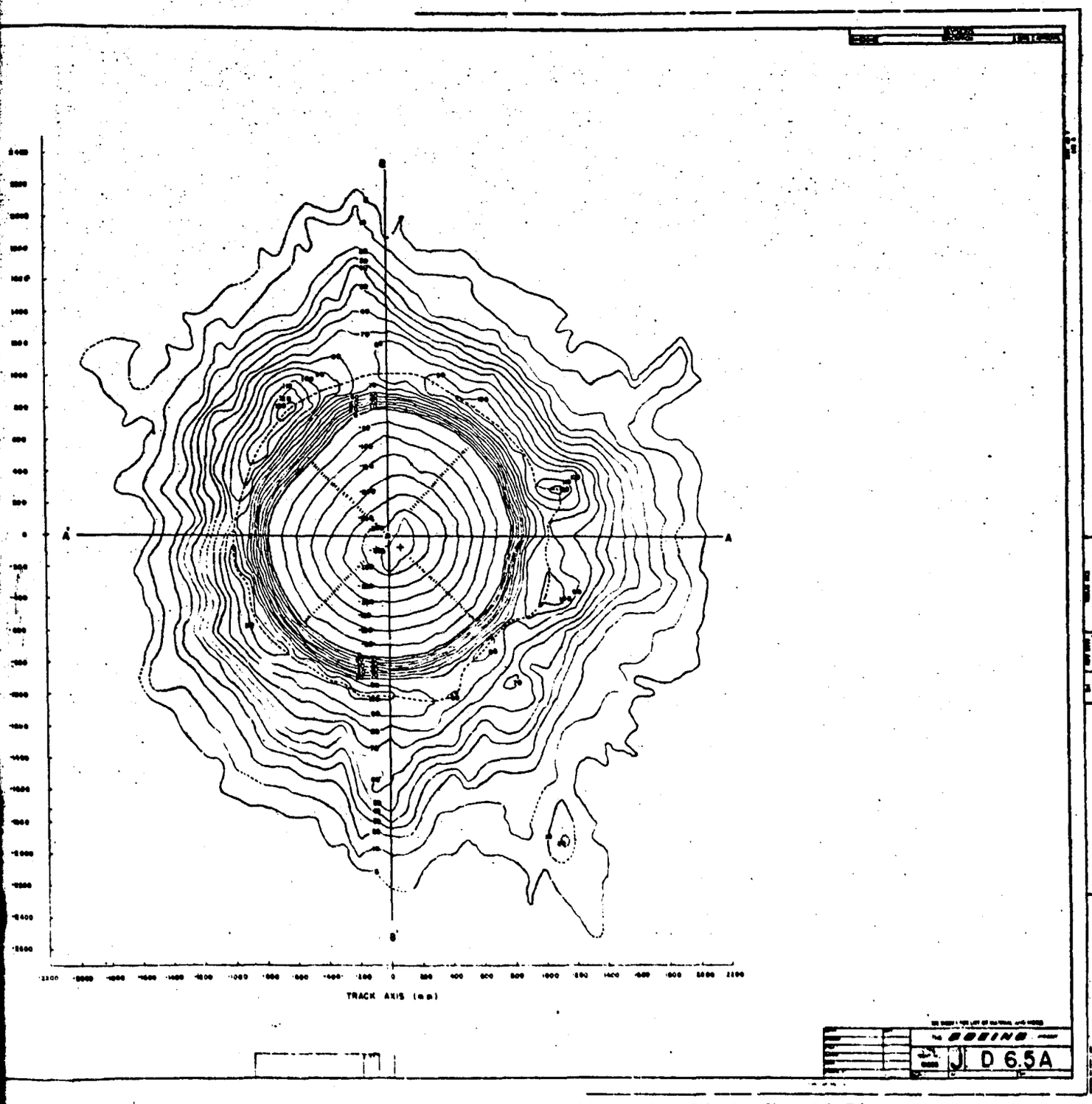

Figure C.13 Crater Map and Profile for Shot D6.5A

2

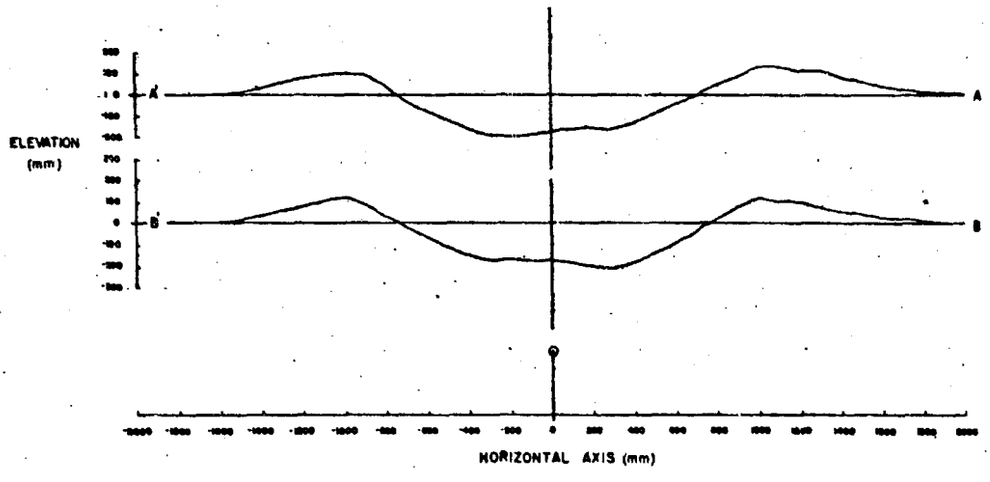
ELEVATION
(mm)
A'
A
B'
B
HORIZONTAL AXIS (mm)

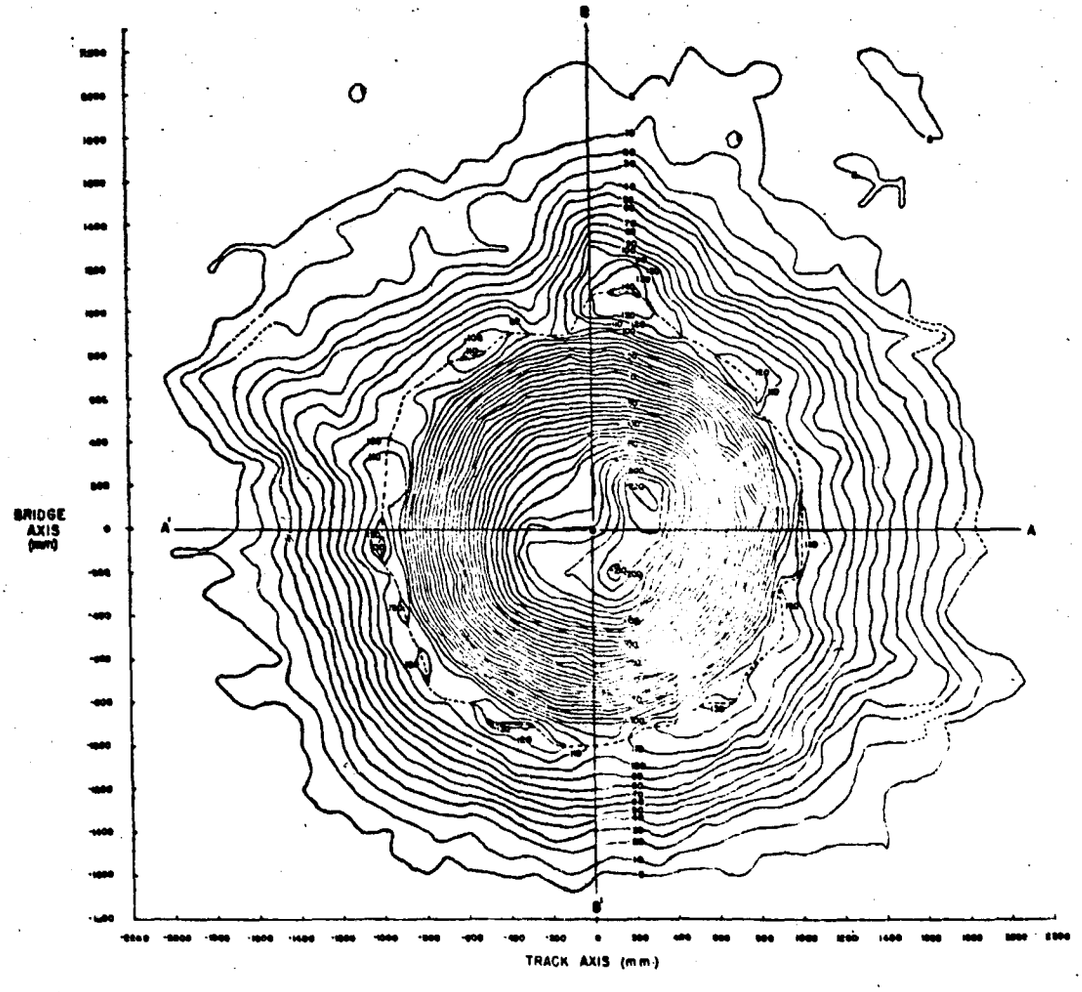

Figure C. 14 Crater Map and Profile for Shot D7A

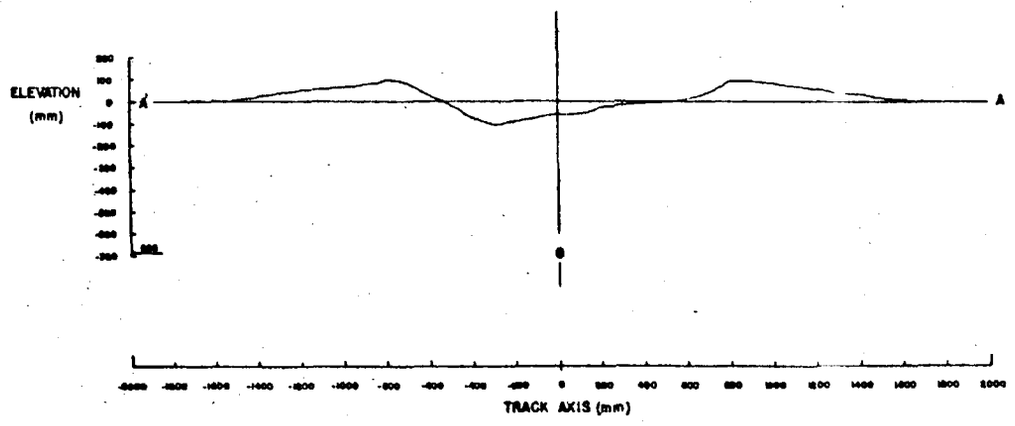
ELEVATION
(mm)
A
A
TRACK AXIS (mm)

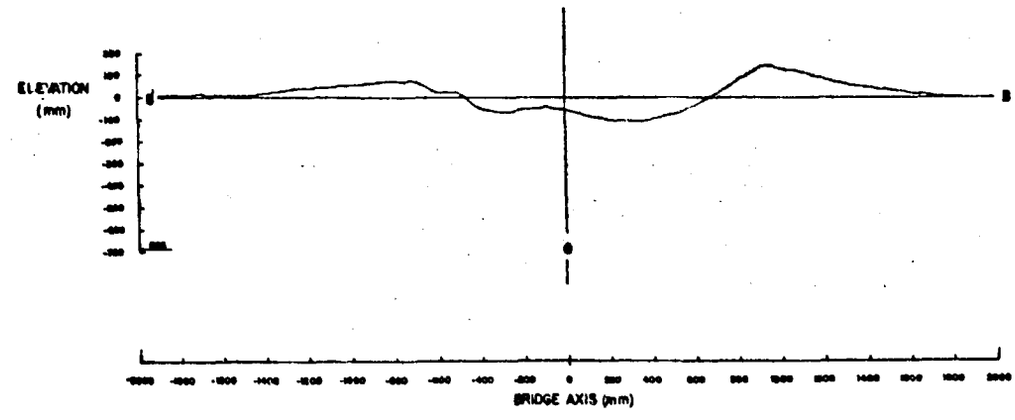
ELEVATION
(mm)
B
B
BRIDGE AXIS (mm)

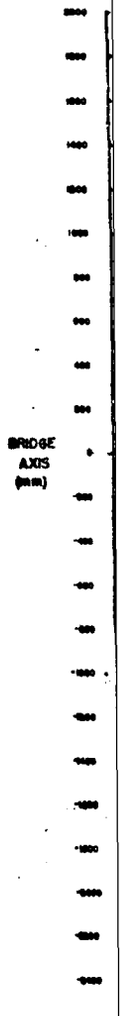
BRIDGE
AXIS
(mm)

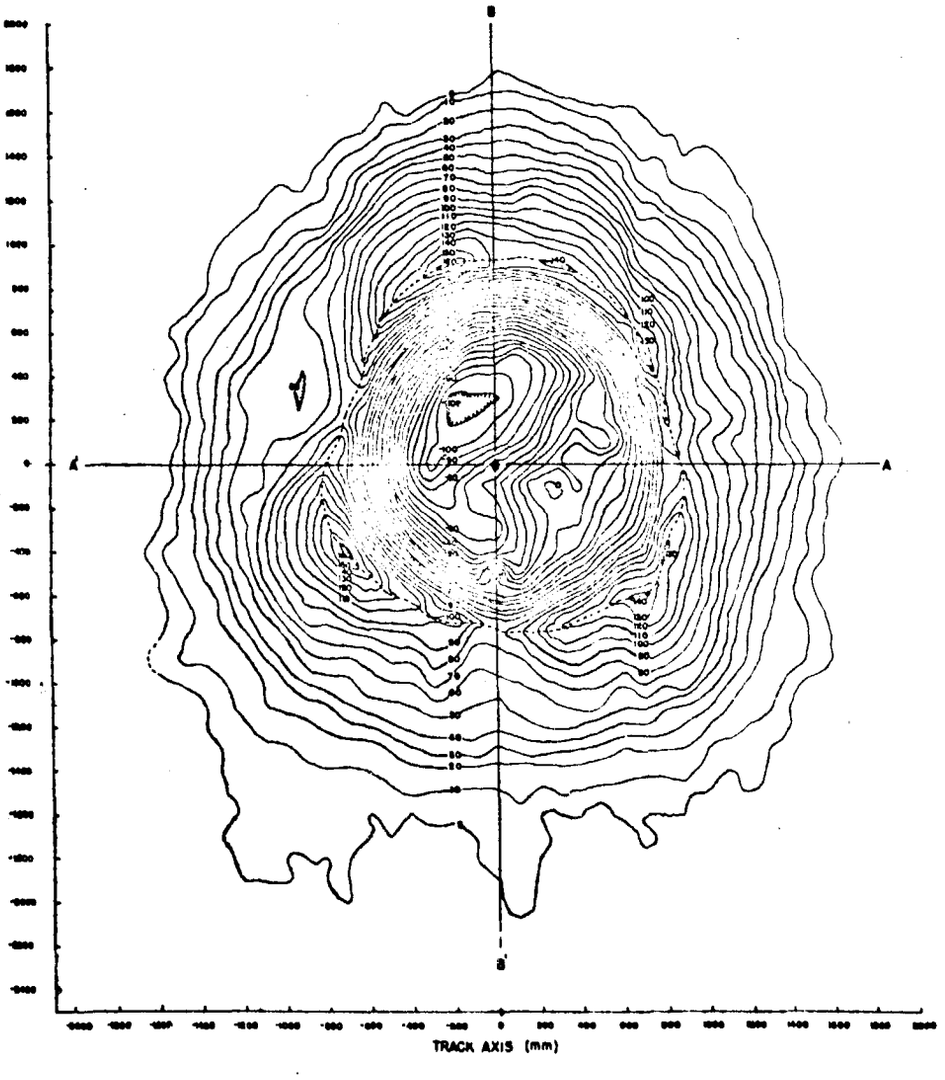

Figure C. 15 Crater Map and Profile for Shot D7.5A

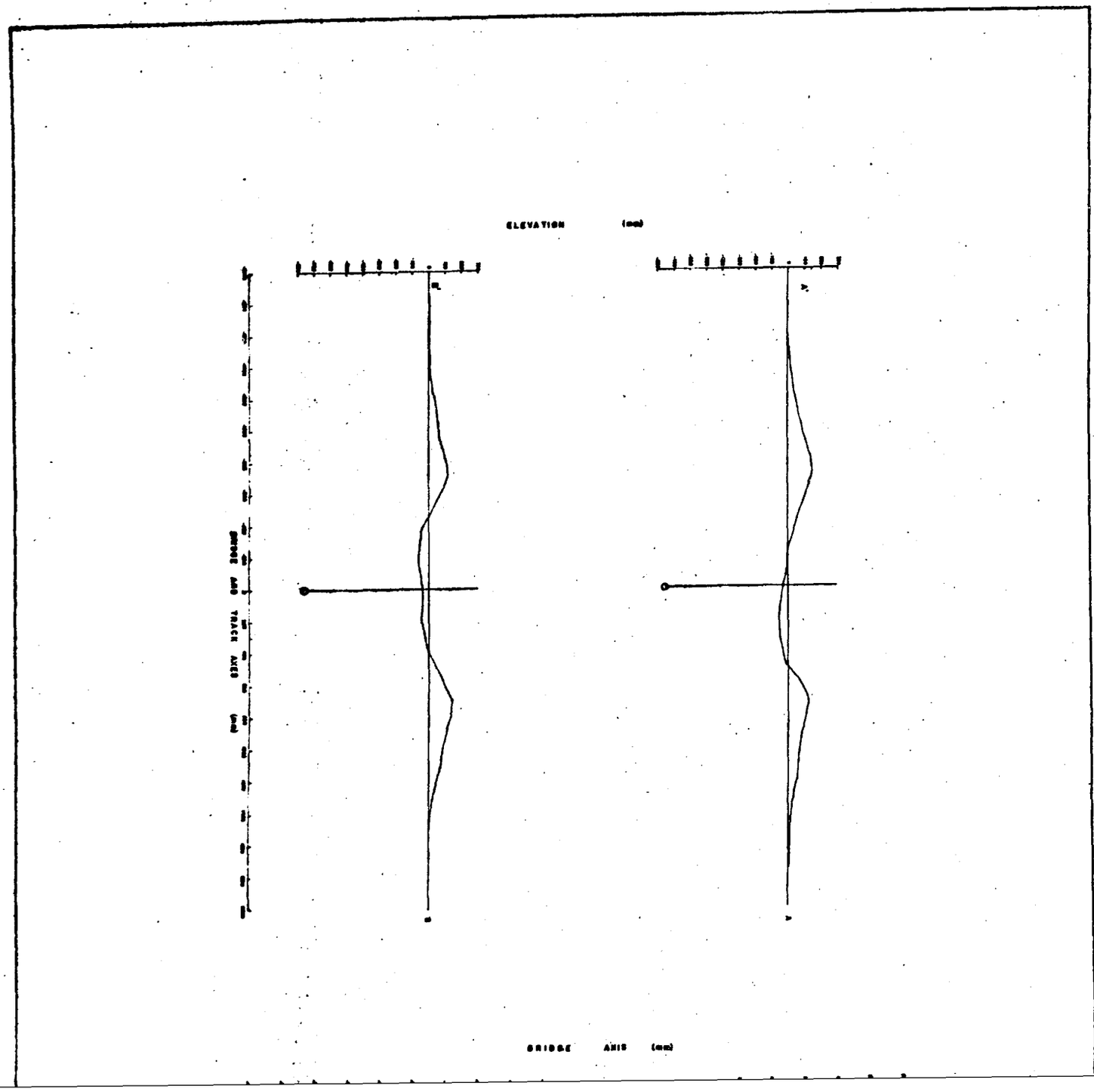
ELEVATION (mm)
BRIDGE AXIS (mm)

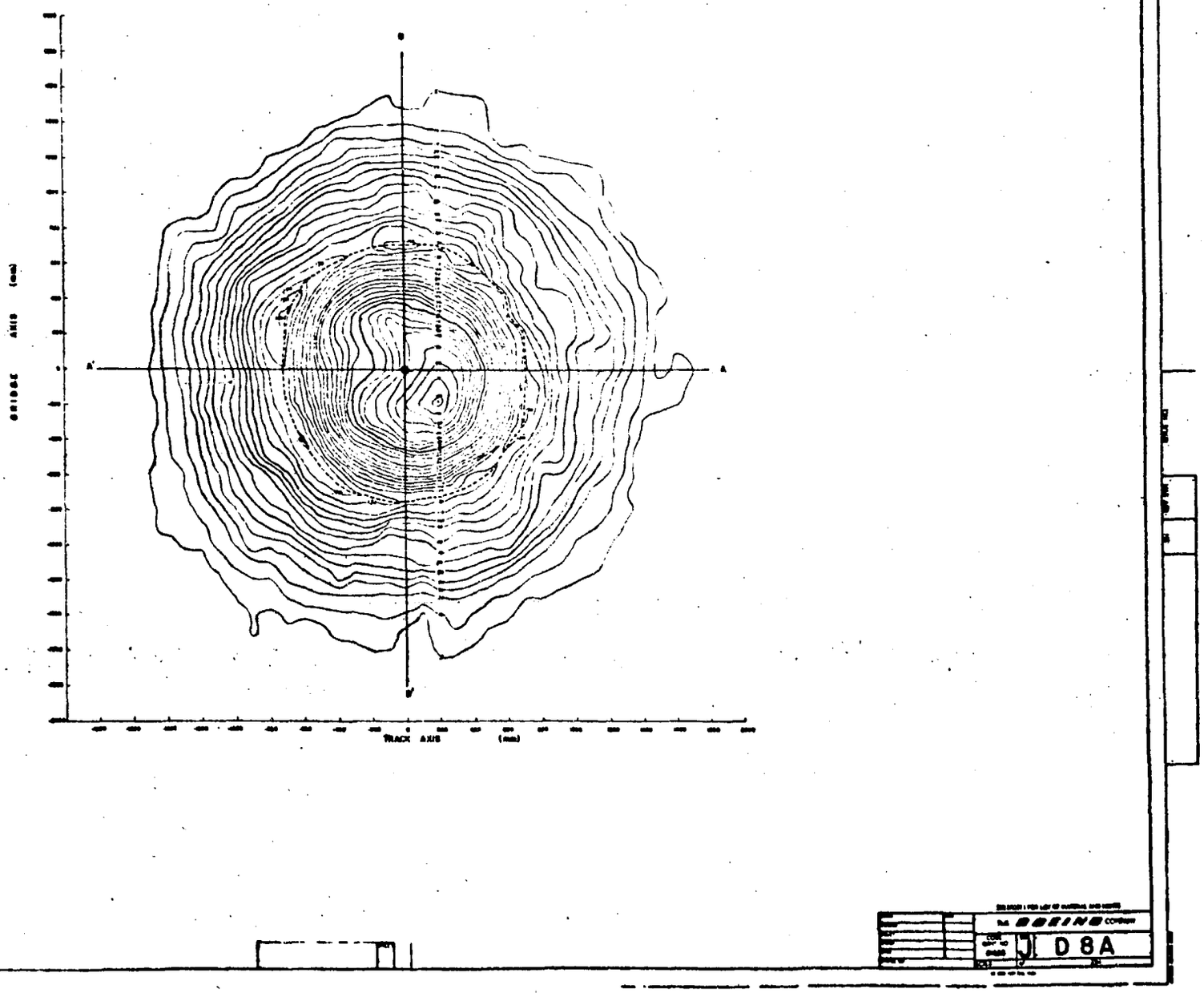

Figure C. 16 Crater Map and Profile for Shot D8A

2

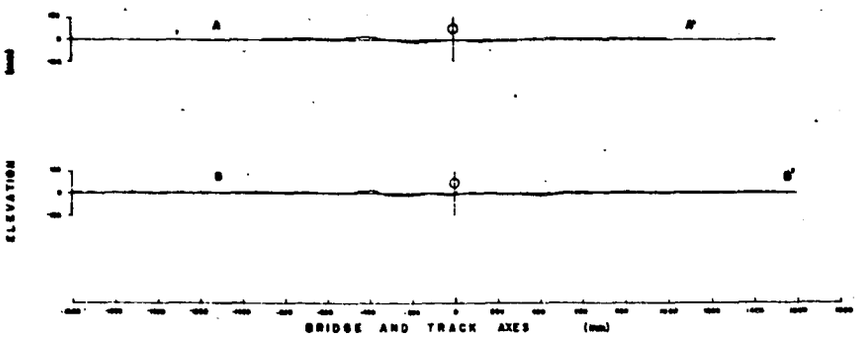
A
A'
B
B'
ELEVATION
BRIDGE AND TRACK AXES (mm)

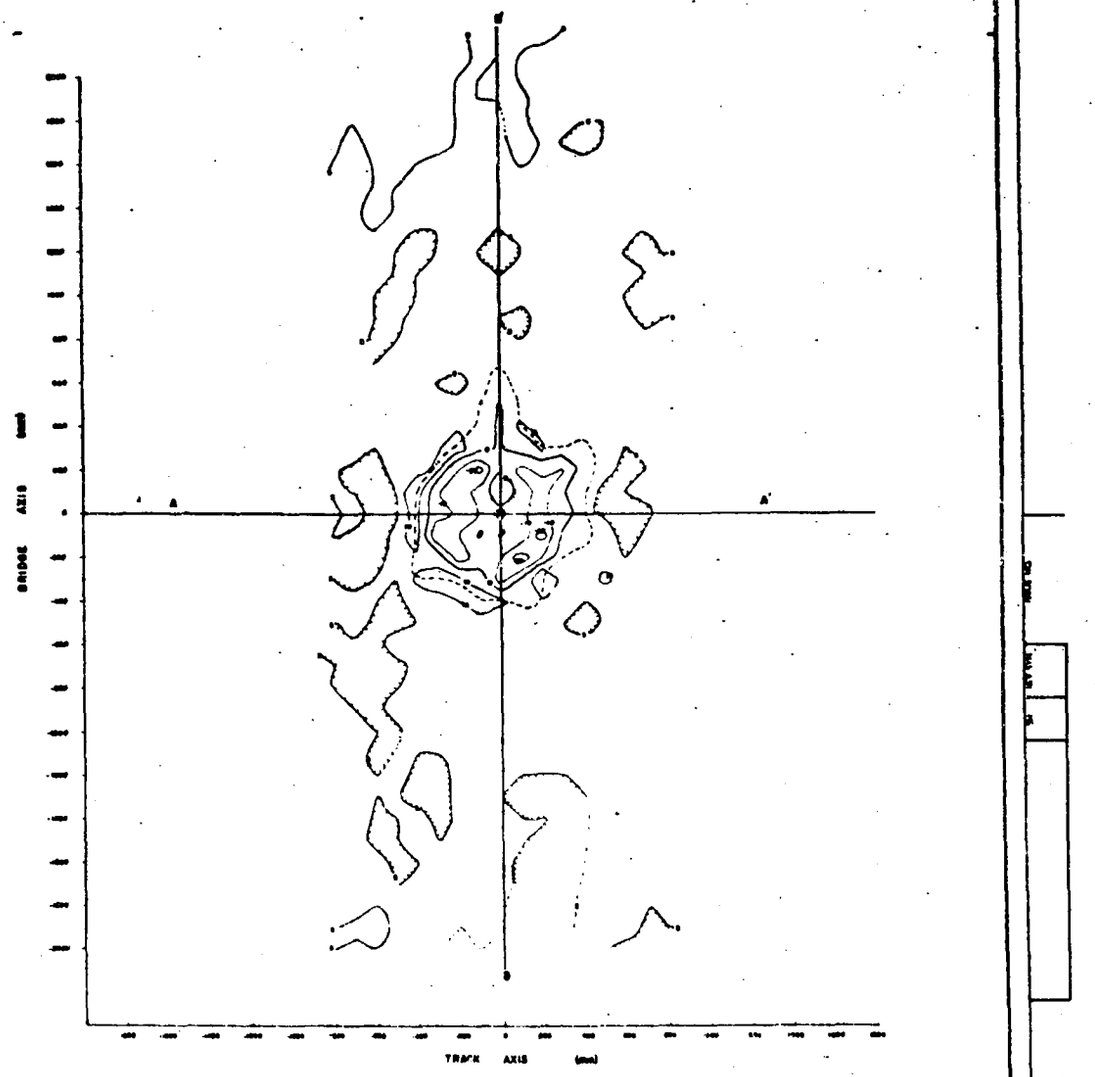

Figure C. 17 Crater Map and Profile for Shot W1.5A

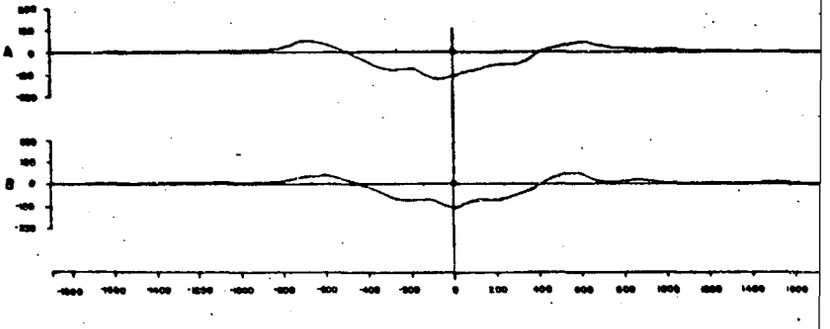

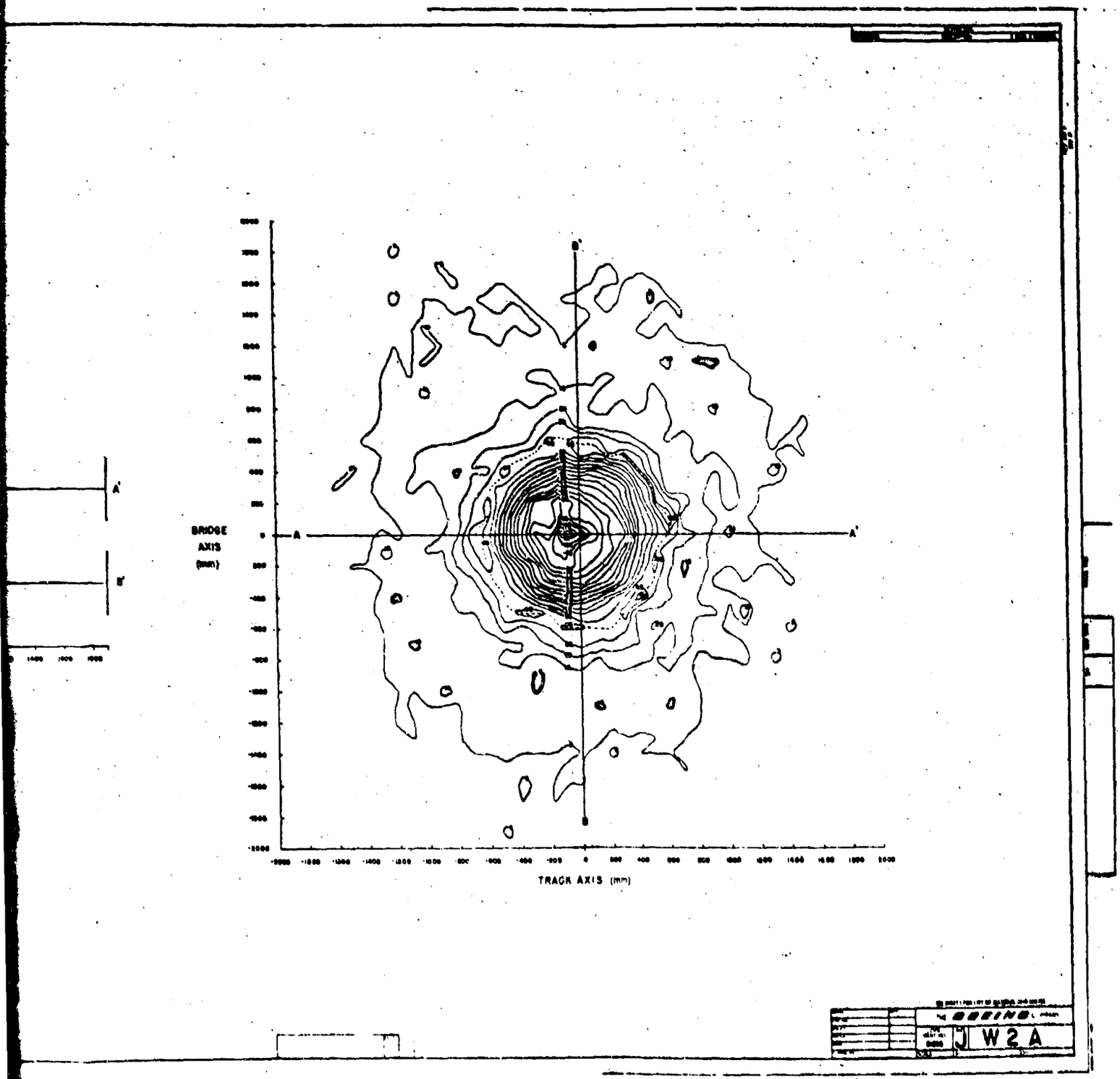

Figure C. 18 Crater Map and Profile for Shot W2A

2

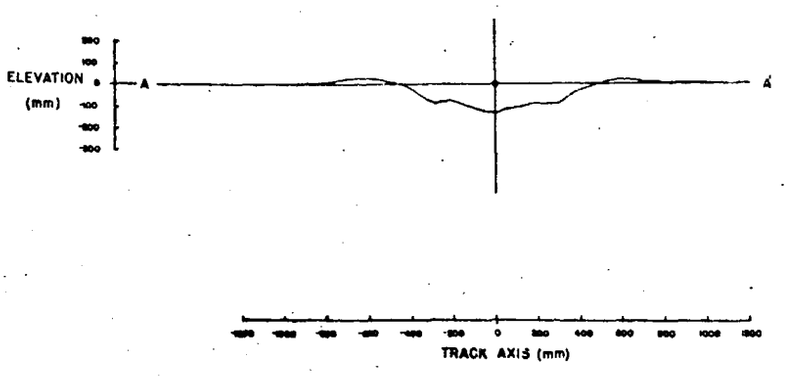
ELEVATION
(mm)
A
A'
TRACK AXIS (mm)

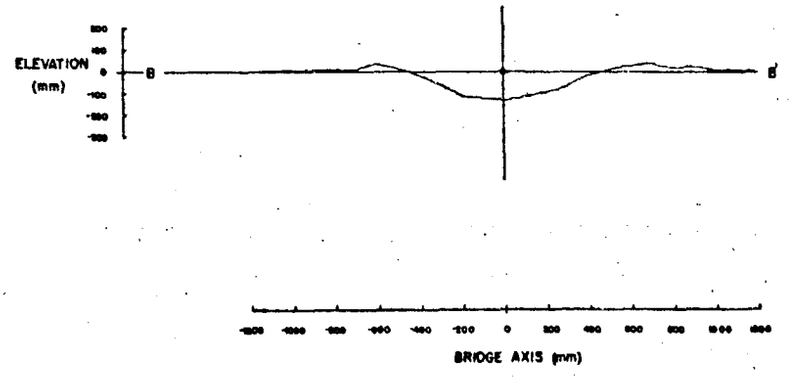
ELEVATION
(mm)
B
B'
BRIDGE AXIS (mm)

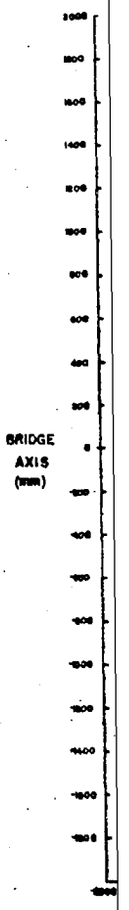
BRIDGE
AXIS

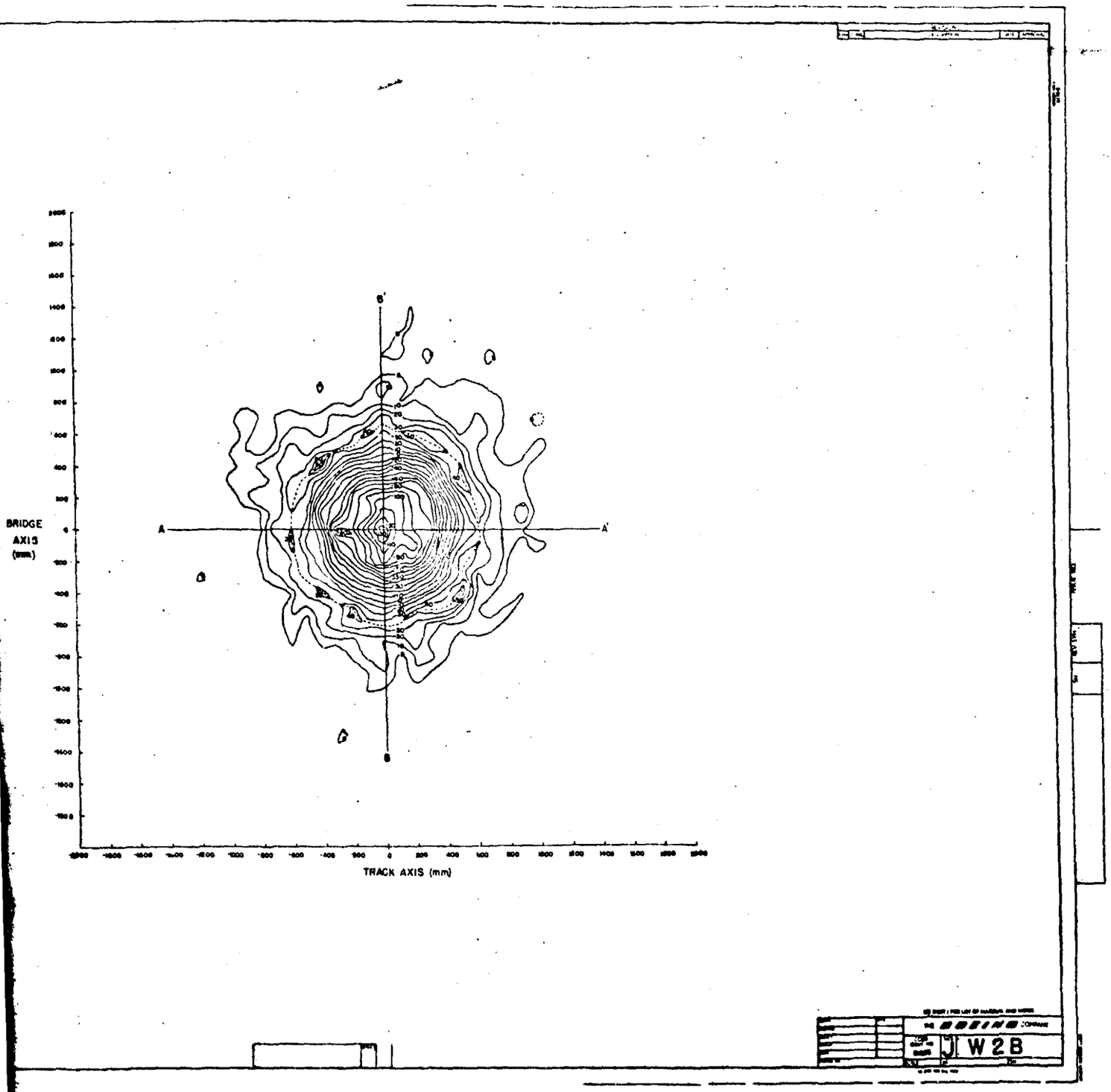

Figure C. 19 Crater Map and Profile for Shot W2B

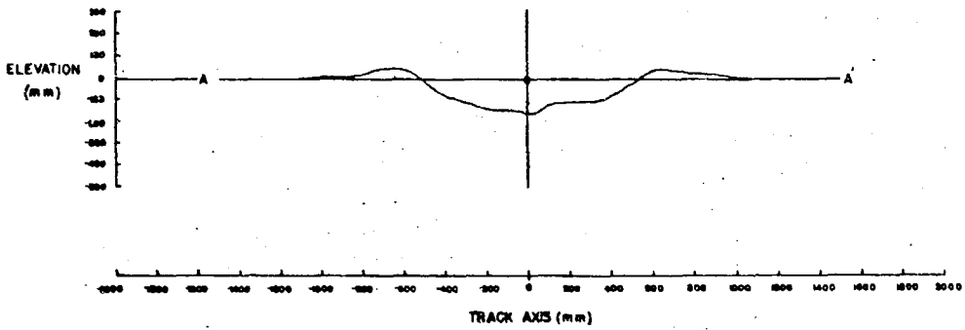
ELEVATION
(mm)
A
A'
TRACK AXIS (mm)

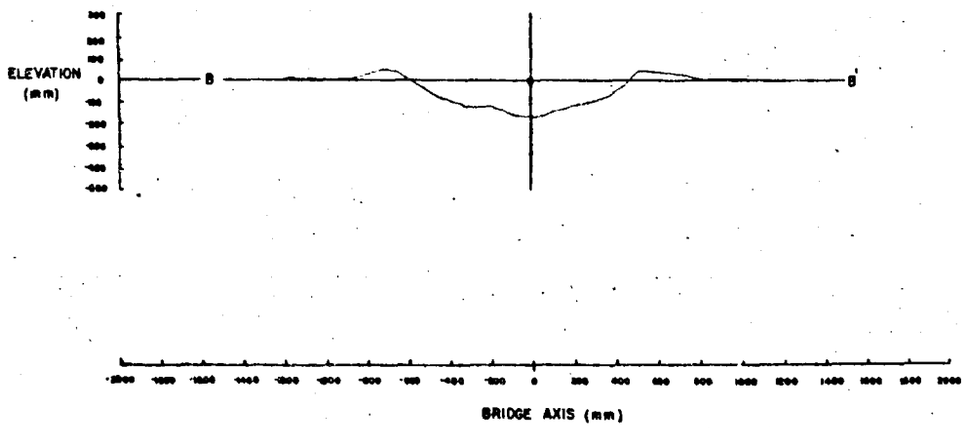
ELEVATION
(mm)
B
B'
BRIDGE AXIS (mm)

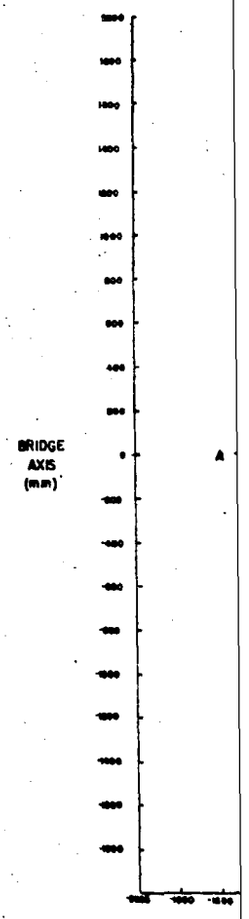
BRIDGE
AXIS
(mm)
A

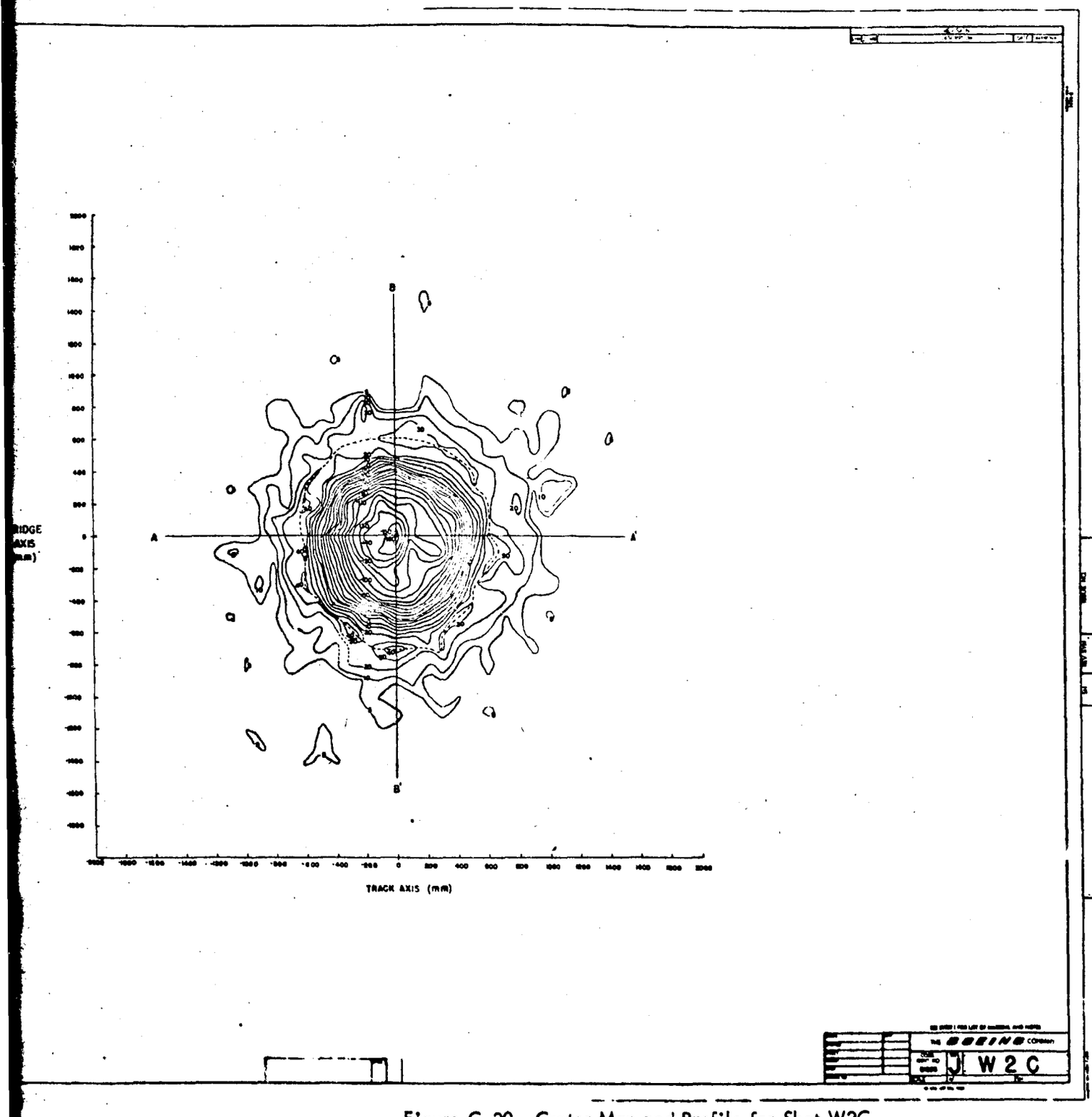

Figure C. 20 Crater Map and Profile for Shot W2C

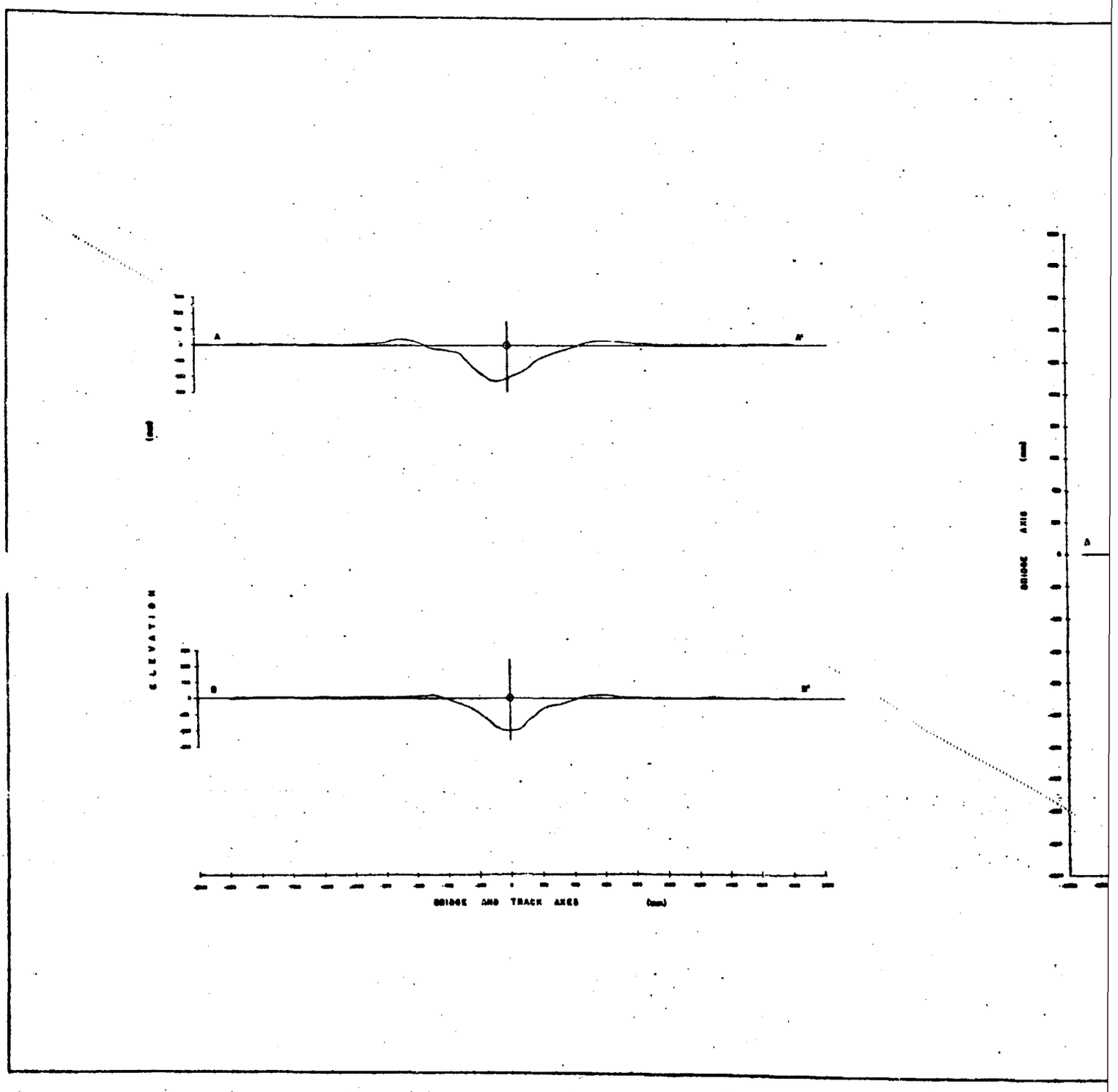
A
A'
B
B'
ELEVATION
BRIDGE AND TRACK AXES
(mm)
BRIDGE AXIS
(mm)
D

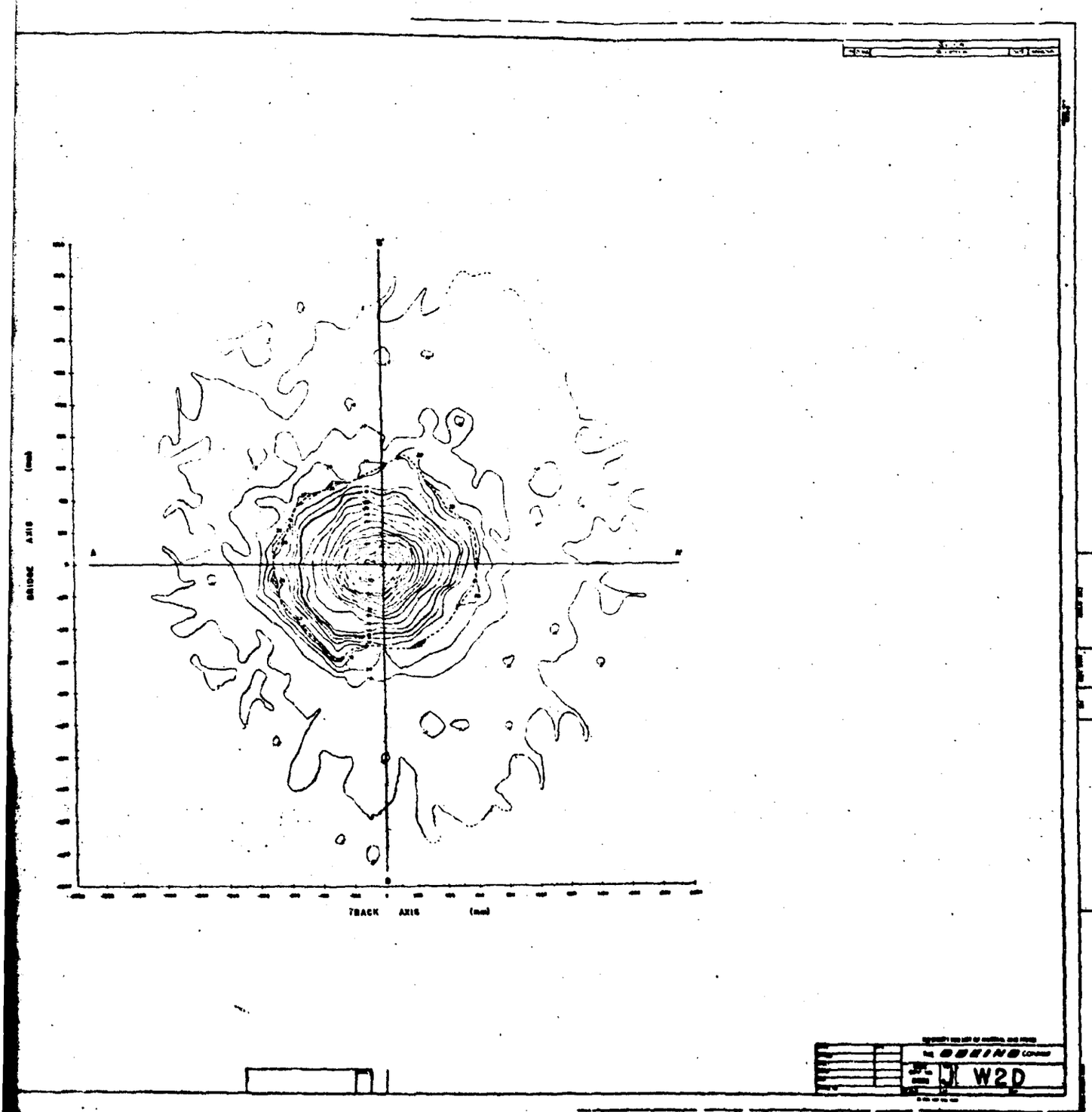

Figure C. 21 Crater Map and Profile for Shot W2D

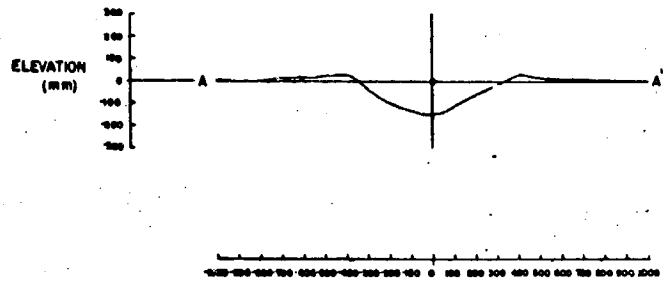

TRACK AXIS (mm)

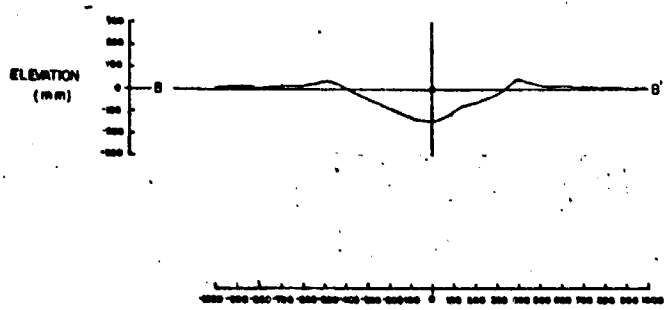

BRIDGE AXIS (mm)

BRIDGE AXIS (mm)

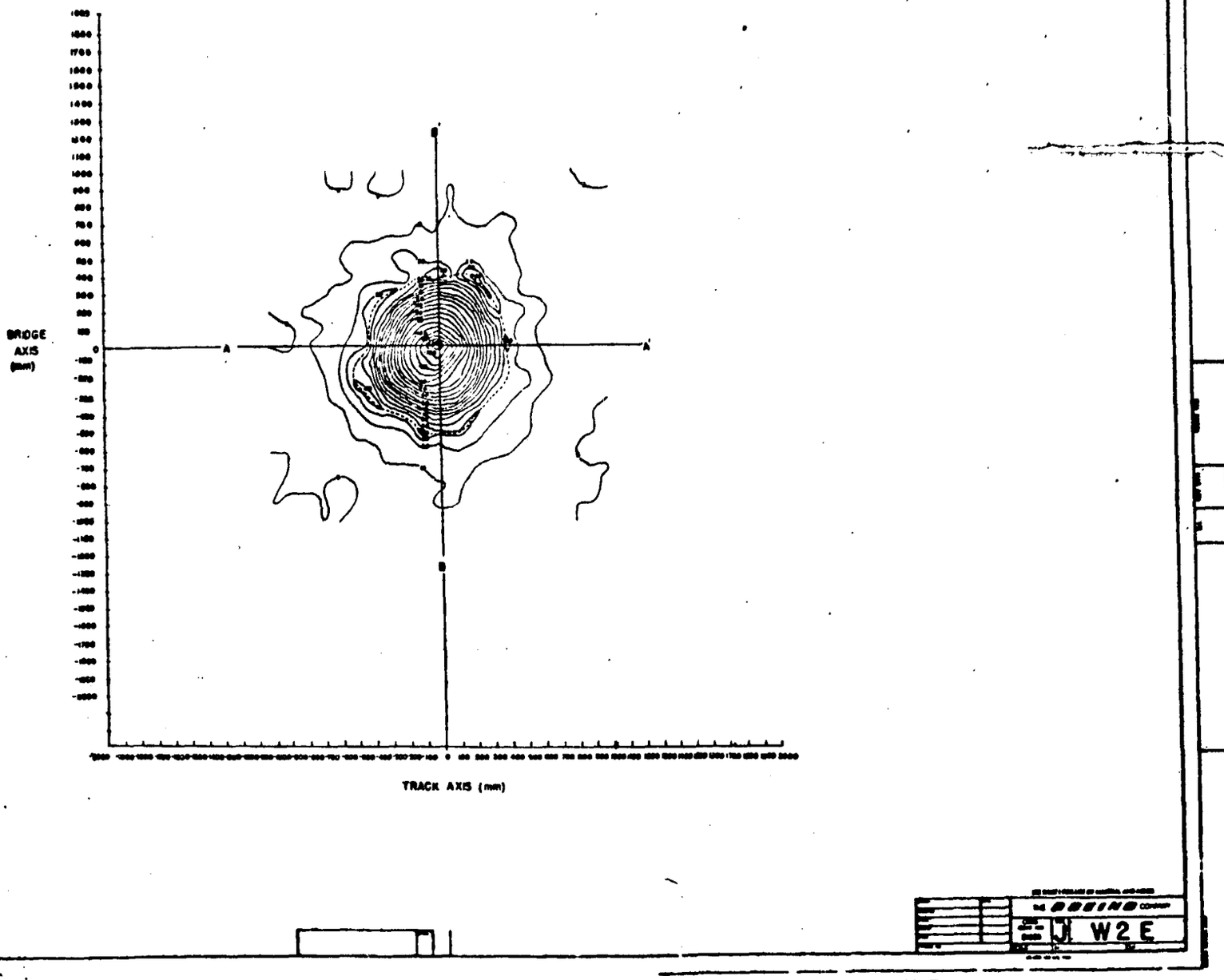

Figure C. 22 Crater Map and Profile for Shot W2E

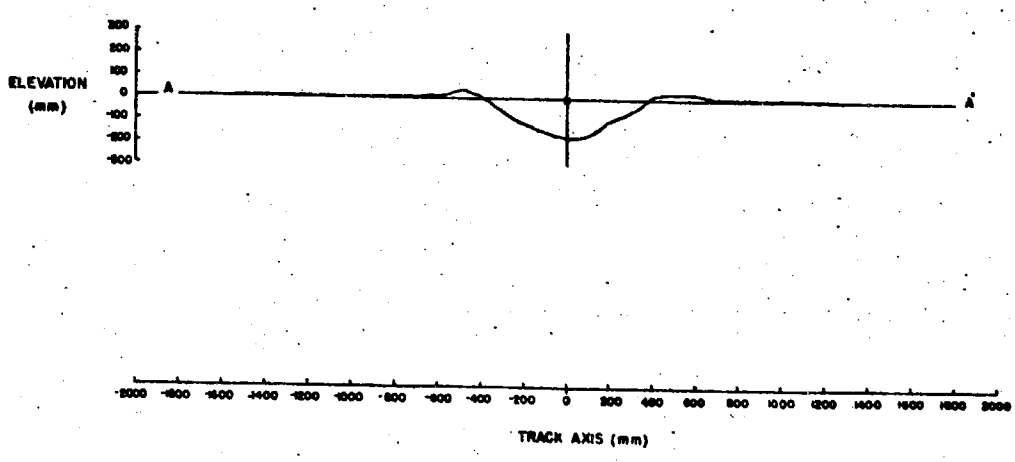
ELEVATION
(mm)
A
A'
TRACK AXIS (mm)

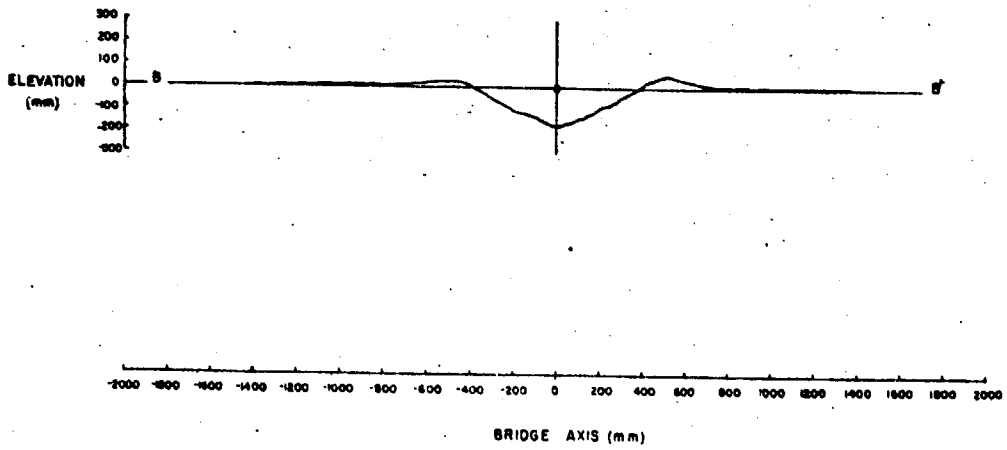
ELEVATION
(mm)
B
B'
BRIDGE AXIS (mm)

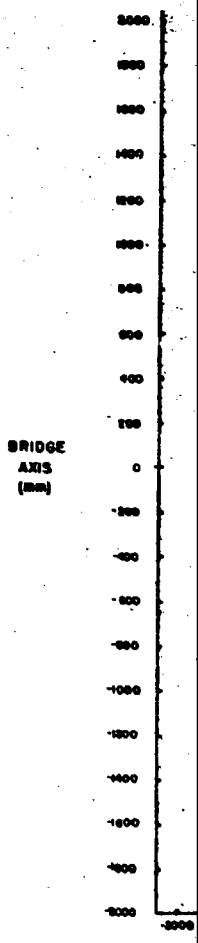
BRIDGE
AXIS
(mm)

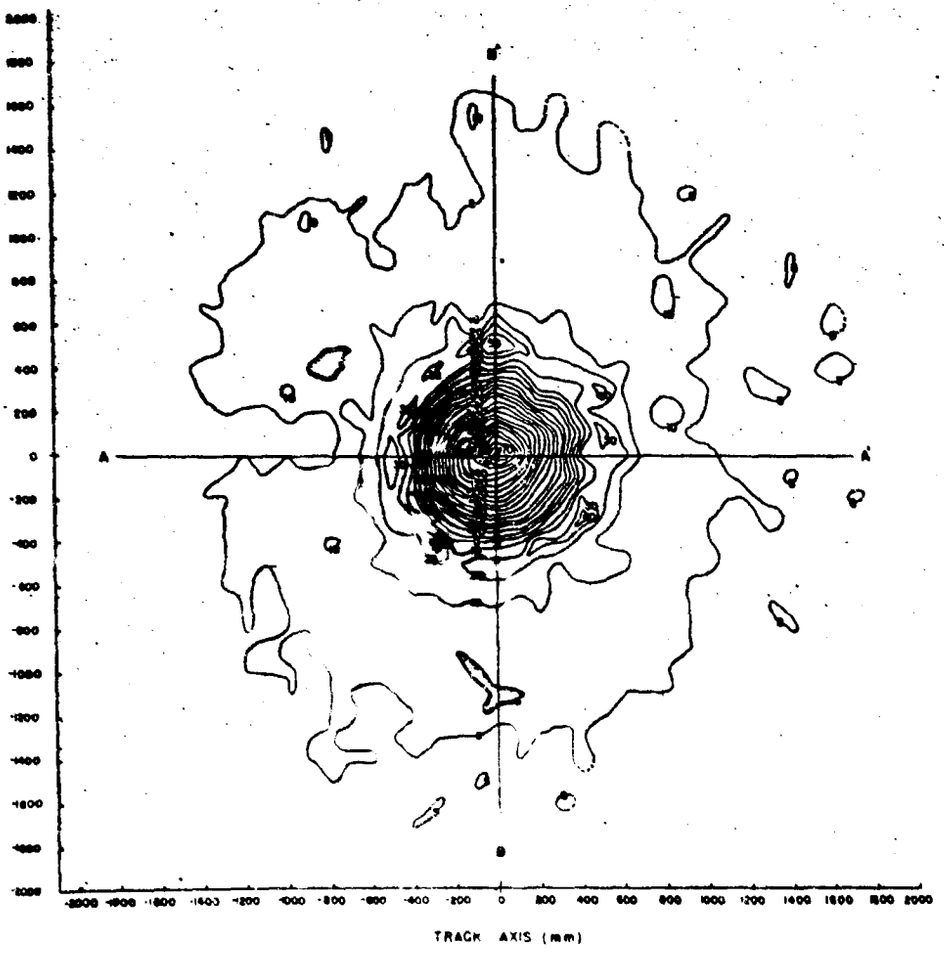

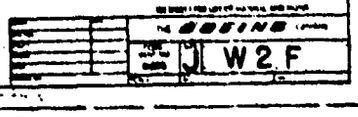

Figure C. 23 Crater Map and Profile for Shot W2F

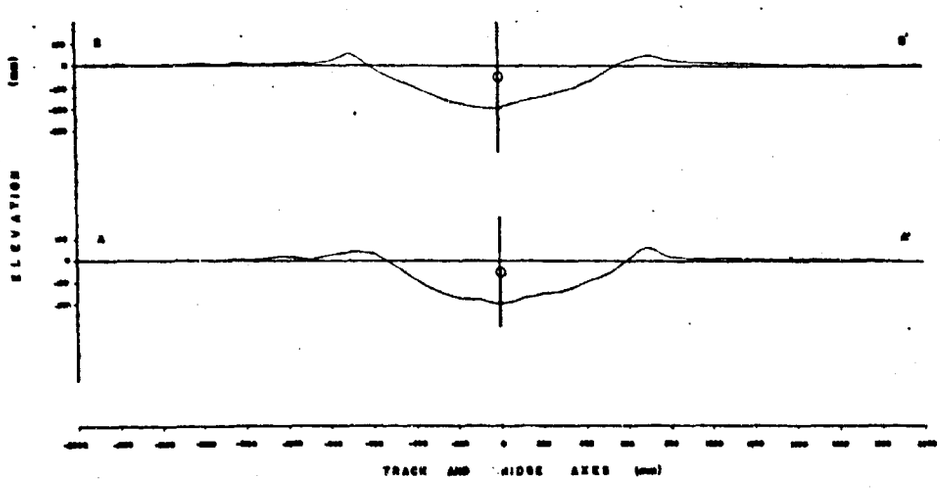
B
B'
A
A'
ELEVATION (mm)
TRACK AND RIDGE AXES (mm)

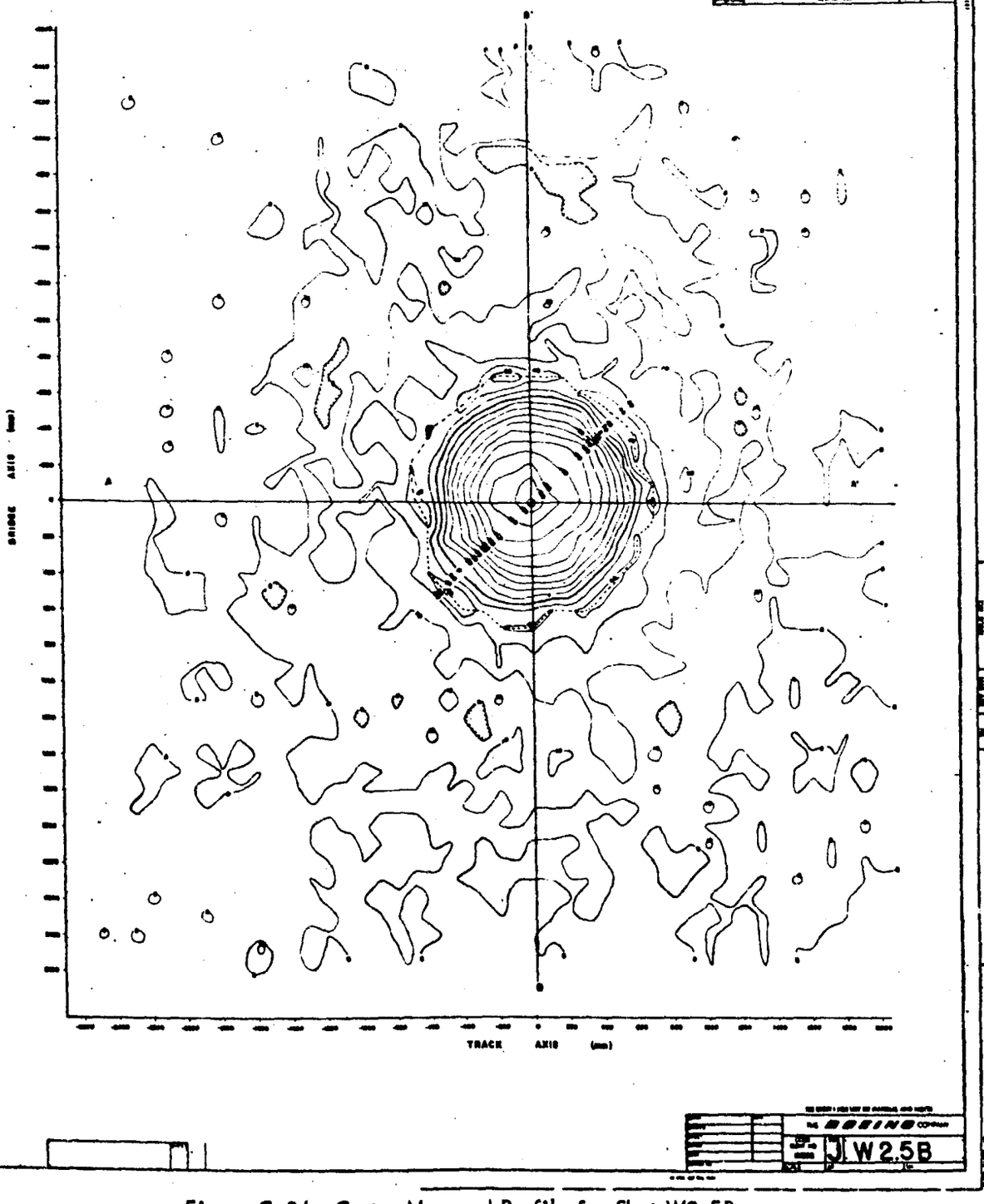

Figure C. 24 Crater Map and Profile for Shot W2.5B

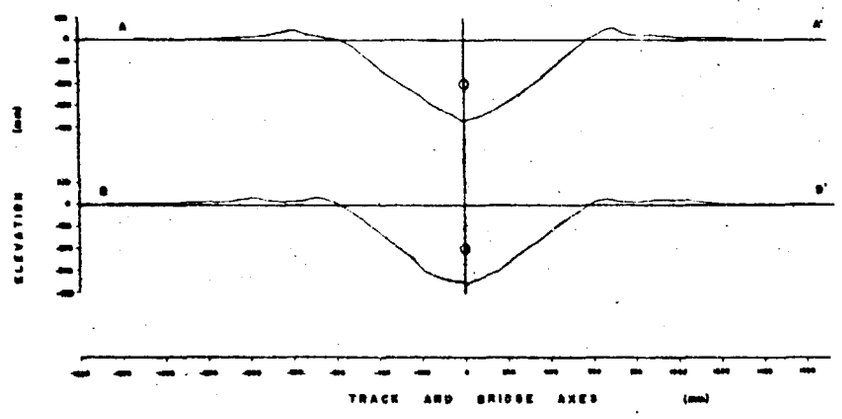
A
A'
B
B'
ELEVATION (mm)
TRACK AND BRIDGE AXES (mm)

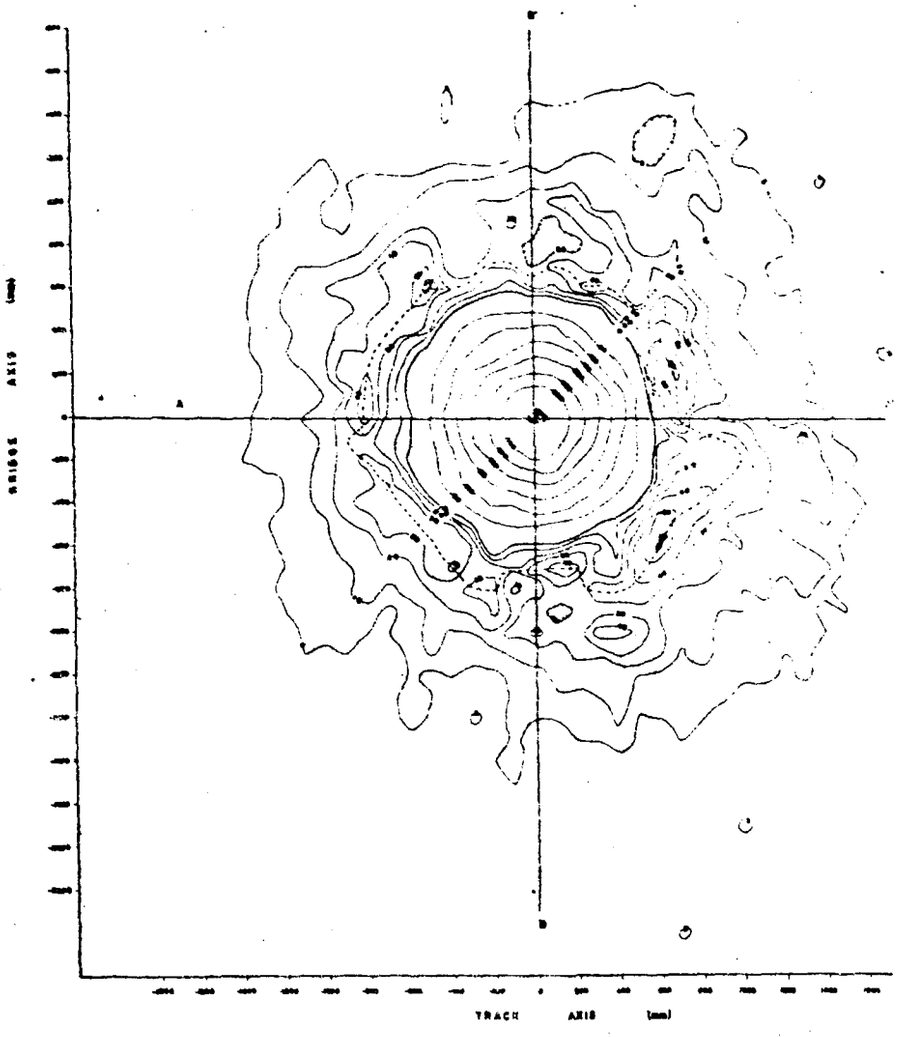

Figure C. 25 Crater Map and Profile for Shot W3. 5B

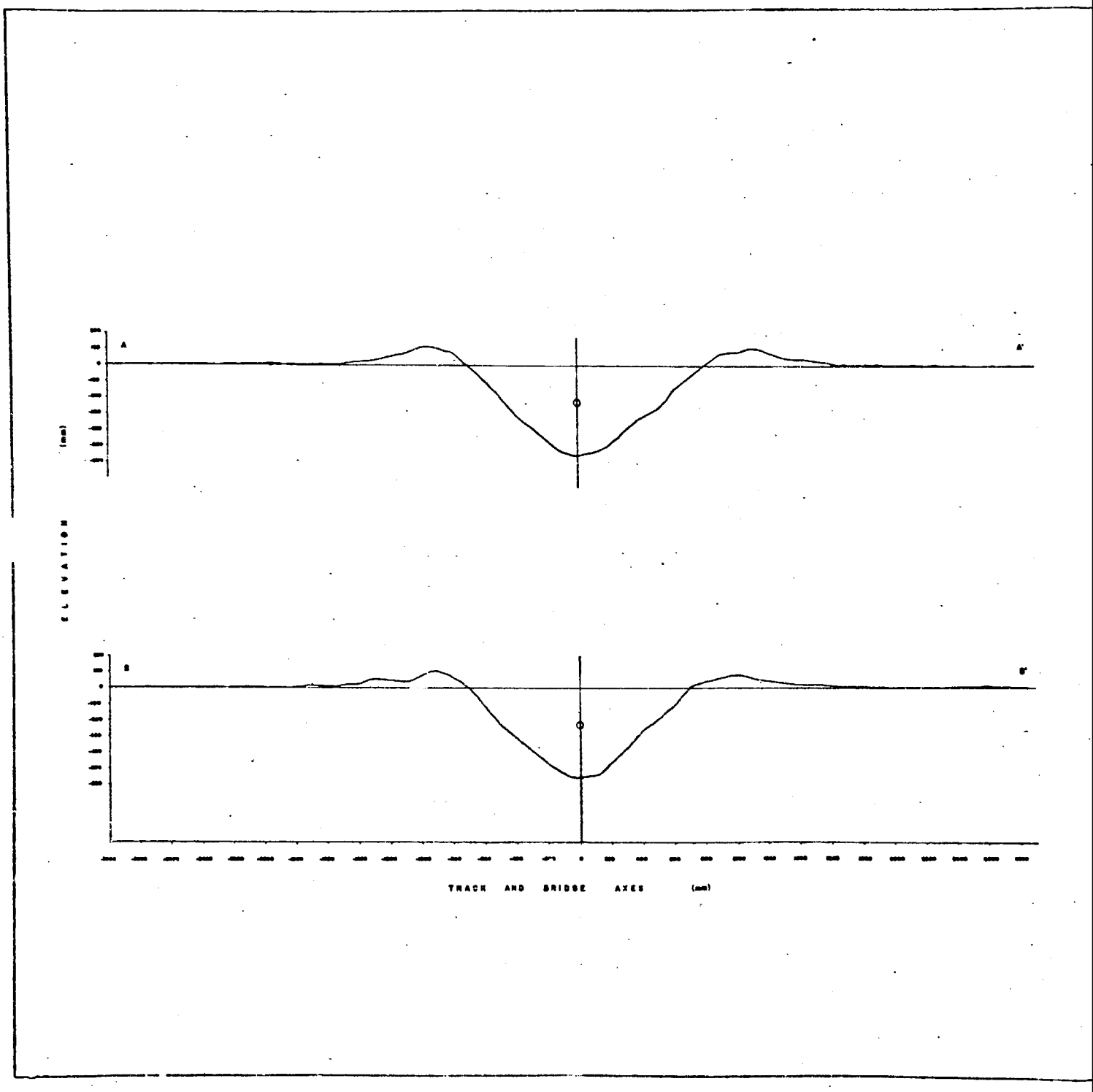
A
A'
B
B'
ELEVATION
(mm)
TRACK AND BRIDGE AXES (mm)

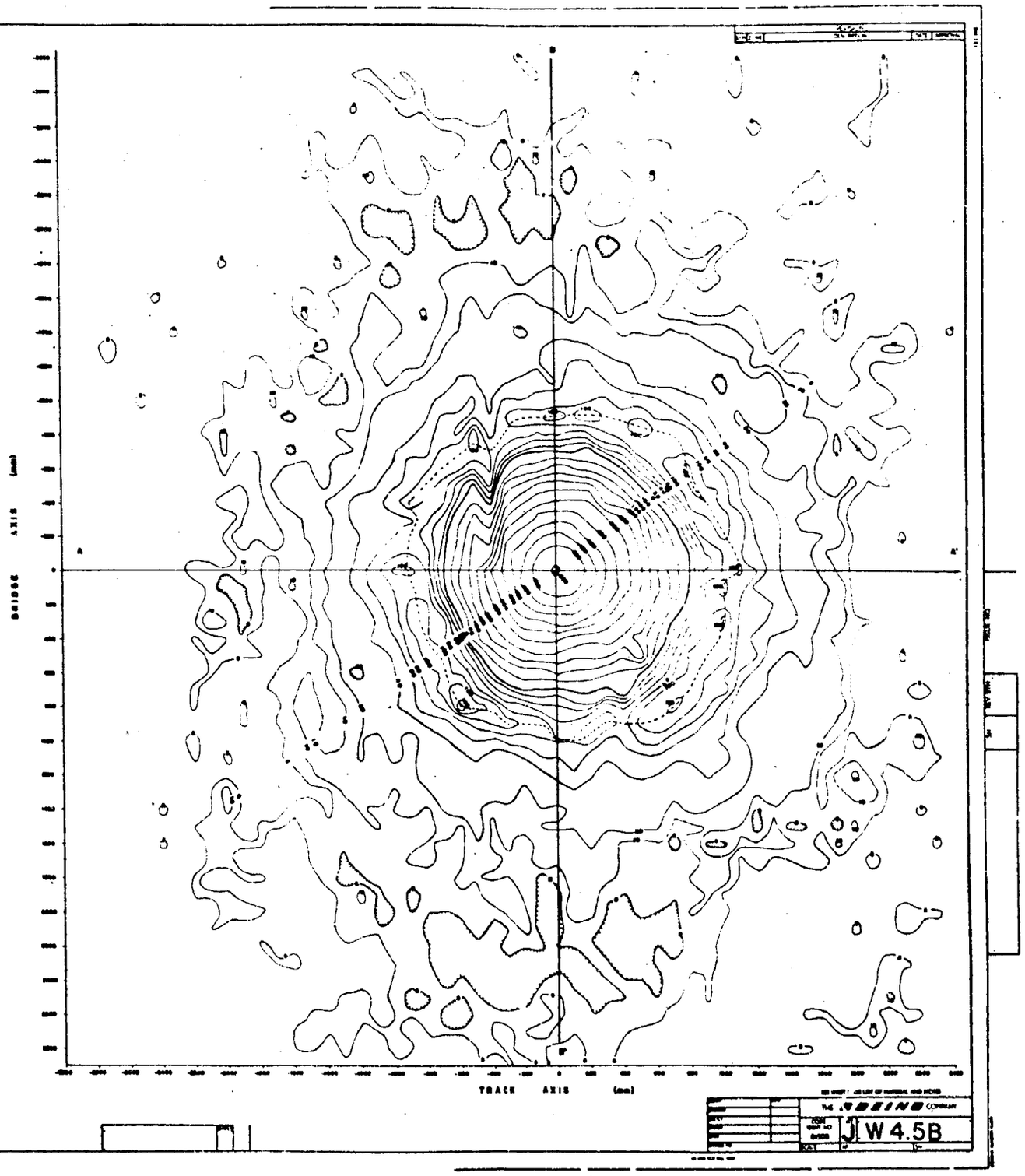

Figure C. 26 Crater Map and Profile for Shot W4. 5B

2

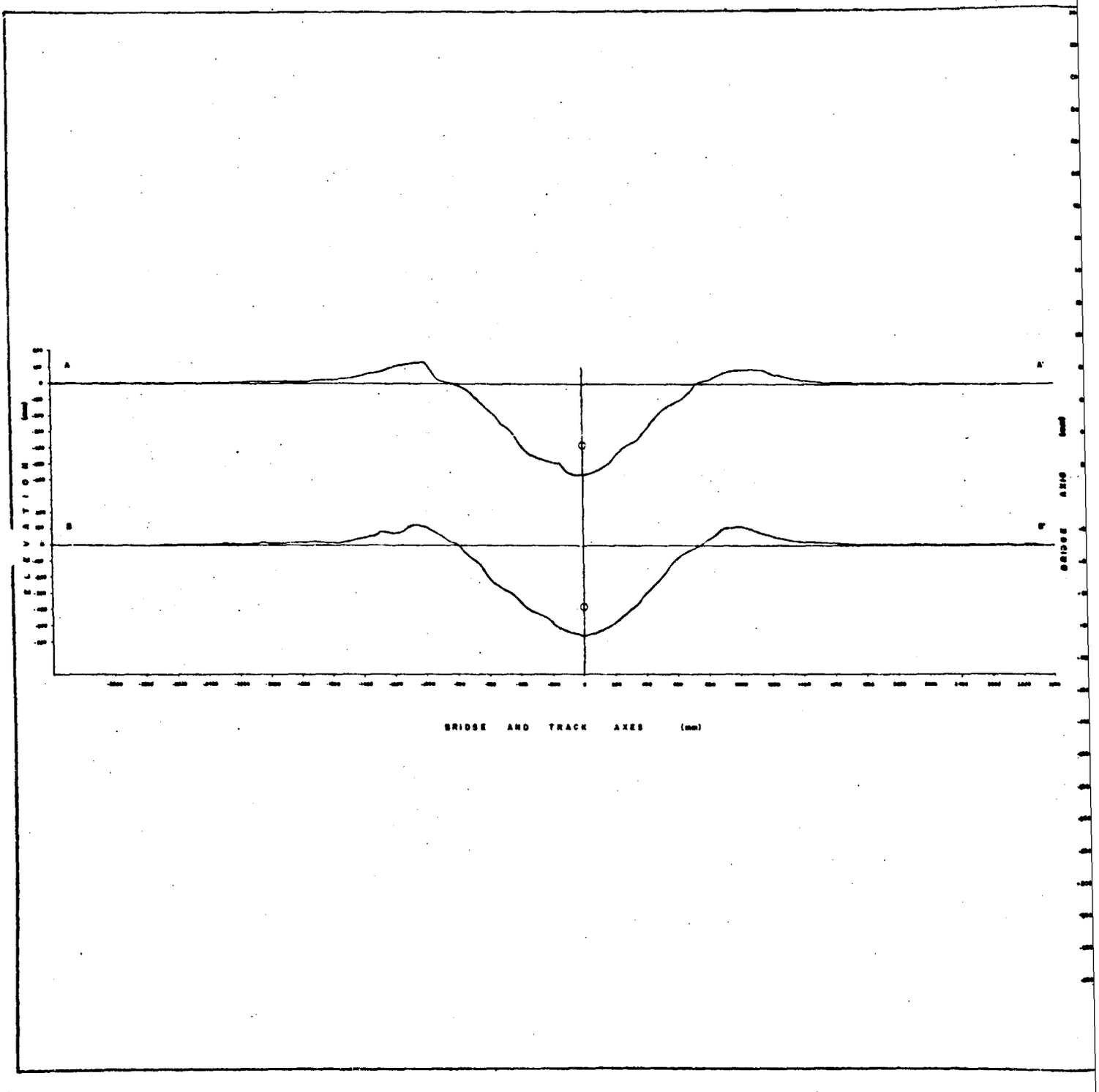
A
A'
B
B'
ELEVATION (mm)
BRIDGE AND TRACK AXES (mm)

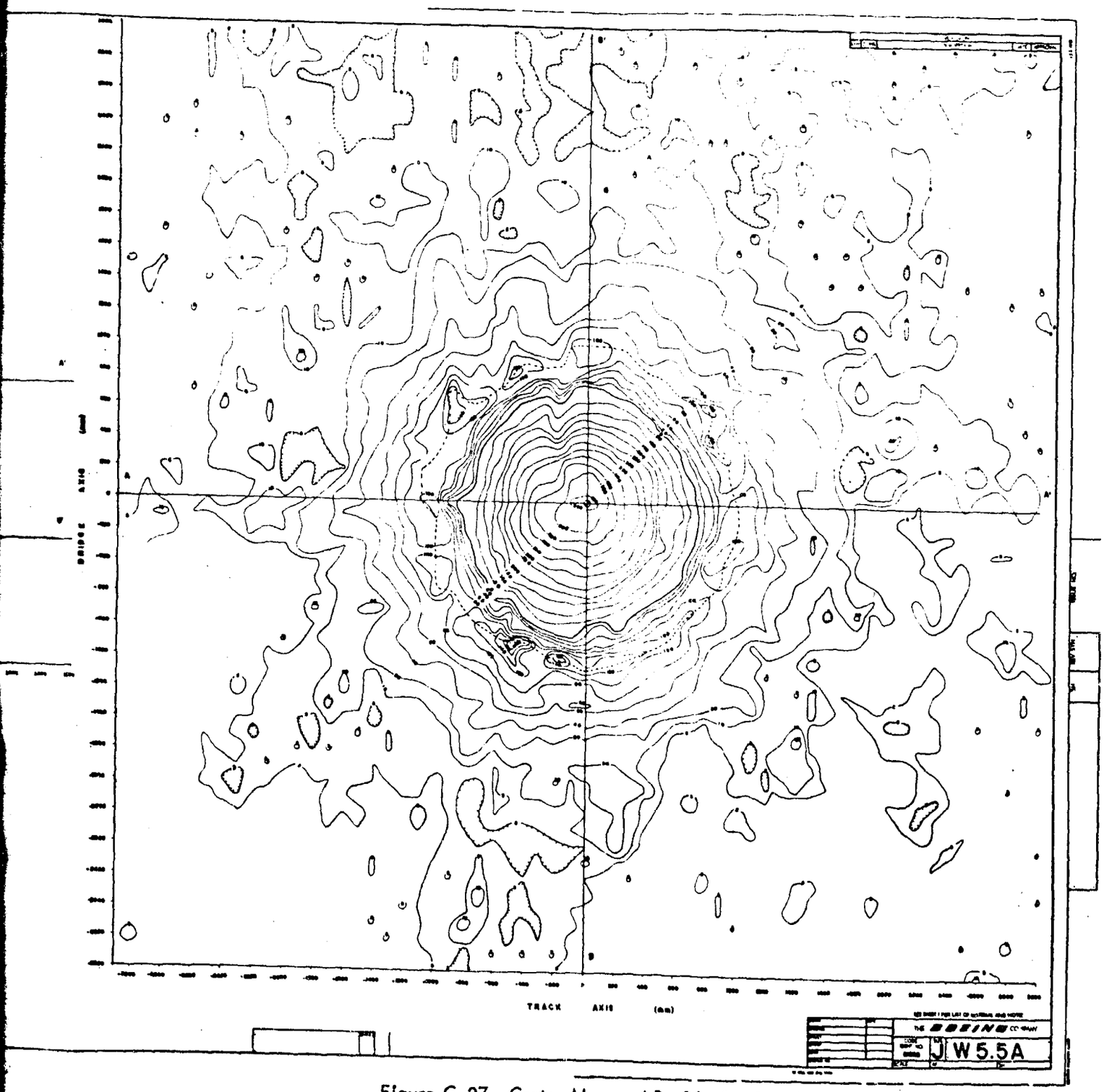

Figure C. 27 Crater Map and Profile for Shot W5. 5A

2

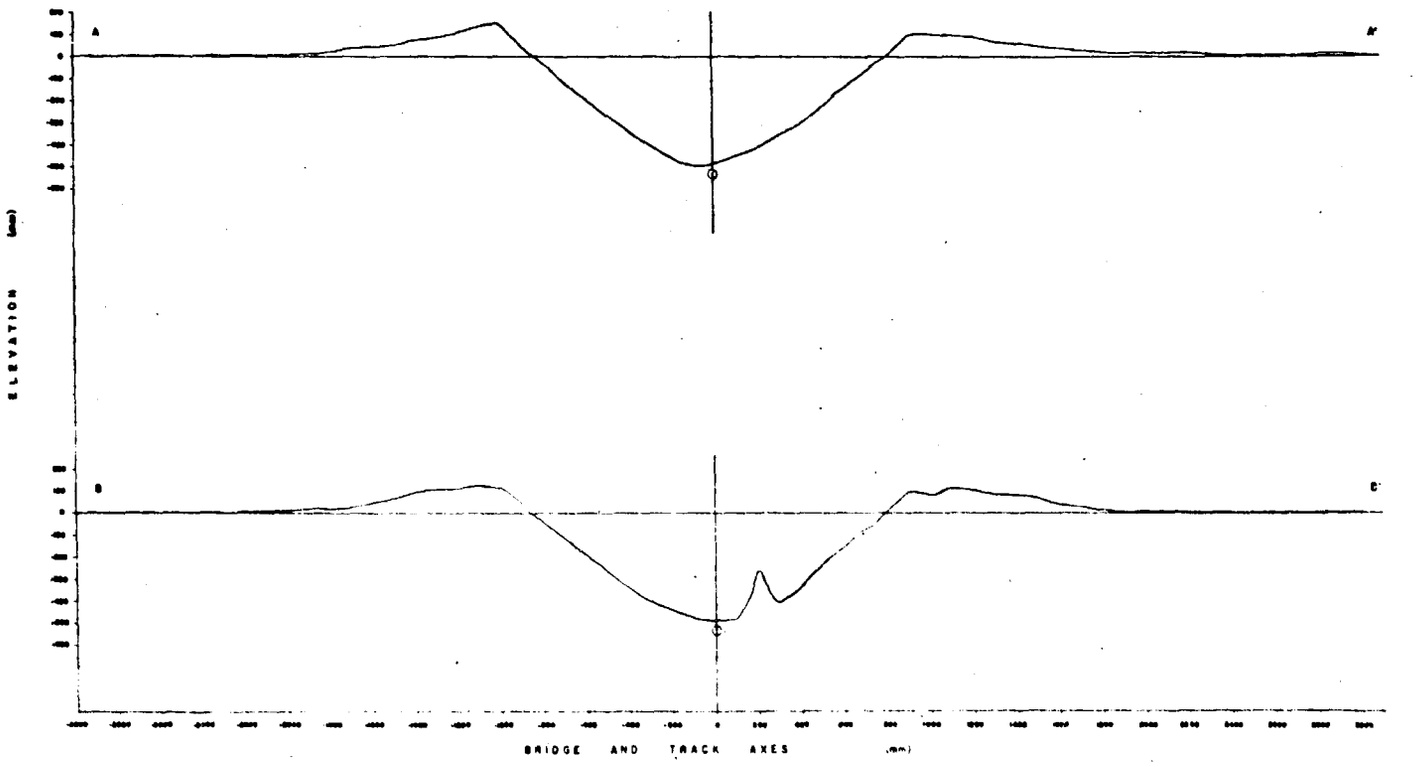
A
A'
B
B'
ELEVATION (mm)
BRIDGE AXIS (mm)
BRIDGE AND TRACK AXES (mm)

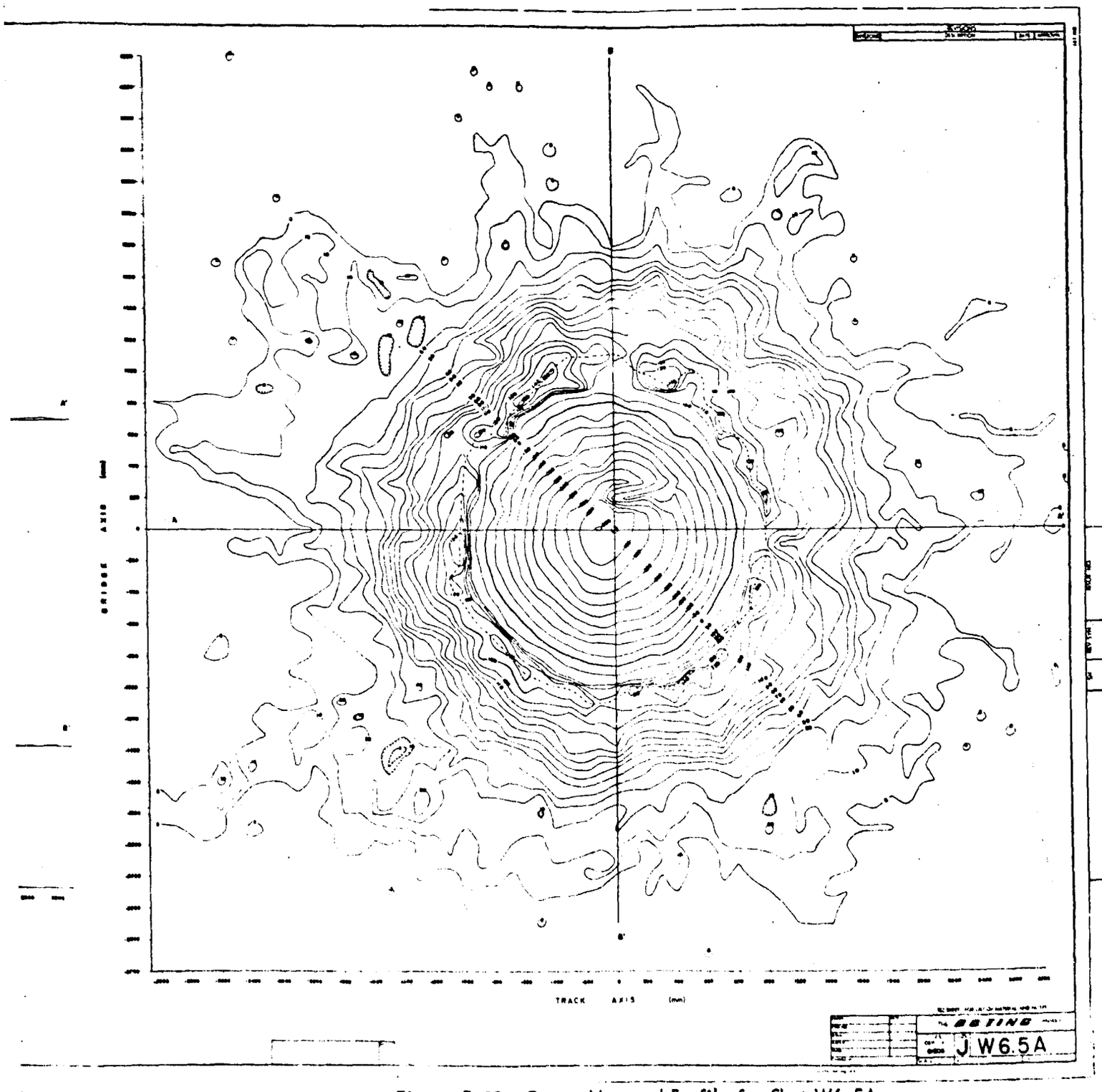

Figure C. 28 Crater Map and Profile for Shot W6.5A

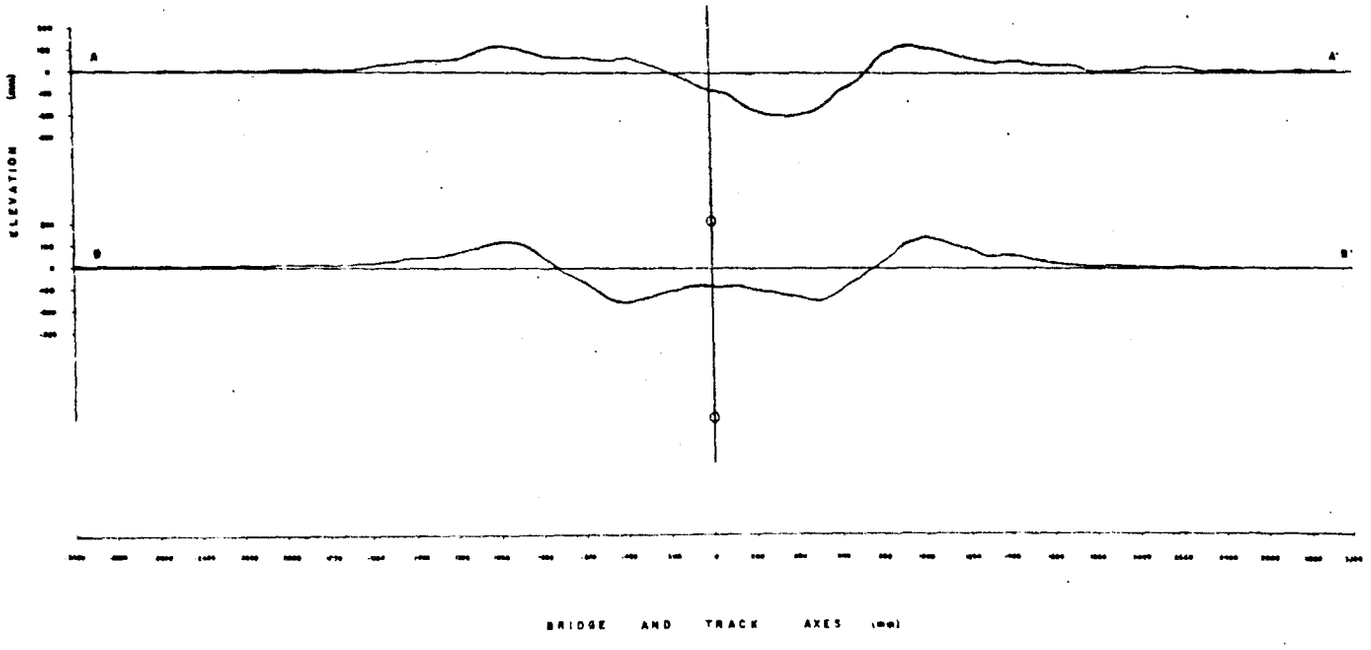
ELEVATION (mm)
A
A'
B
B'
BRIDGE AND TRACK AXES (mm)

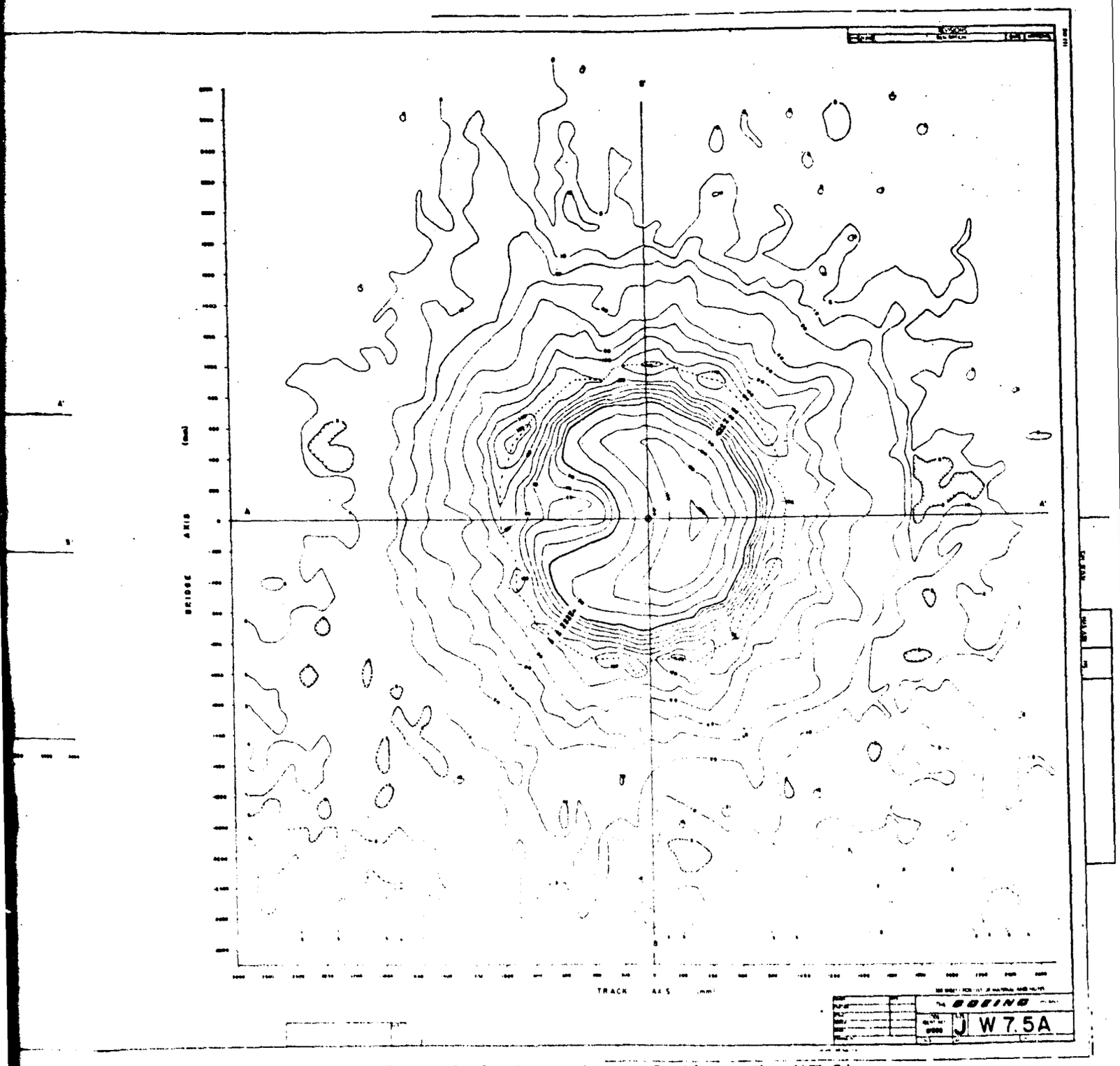

Figure C. 29 Crater Map and Profile for Shot W7.5A

REFERENCES

1. C. W. Lampson, Effects of Atomic Weapons, Combat Forces Press, 1950, p. 410.

2. M. D. Nordyke, "Nuclear Craters and Preliminary Theory of Mechanics of Explosive Crater Formation," Jour. of Geophysical Res., Vol. 66, No. 10, 1961, pp. 3439-3459.

3. B. F. Murphey and L. J. Vortman, "High-Explosive Craters in Desert Alluvium, Tuff and Basalt," Jour. Geophysical Res., Vol. 66, No. 10, 1961, pp. 3389-3404.

4. M. D. Nordyke, Recommended Crater Nomenclature, Univ. Calif. Lawrence Radiation Laboratory, Contract No. W-7405eng-48, March 1964, pp. 1-3.

5. W. A. Roberts, The Crater Lip Crest, Boeing Document D2-90298, 1963.

6. R. B. Baldwin, The Measure of the Moon, University of Chicago Press, Chicago, Illinois, 1963.

7. U. S. Army Engineer Waterways Experiment Station, Effects of a Soil-Rock Interface on Cratering, Technical Report 2-478, AFSWP-1059, 1958.

8. R. H. Carlson and G. D. Jones, Ejecta Distribution Studies, Boeing Document D2-90575, November 1964.

9. R. H. Carlson and W. A. Roberts, Mass Distribution and Throwout Studies, Project Sedan, Boeing Document D2-90457, November 1963.

LIMITATIONS

This document is controlled by Nuclear and Space Physics, 2-7900

All revisions to this document shall be approved by the above noted organization prior to release.

DDC AVAILABILITY NOTICE

☐ Qualified requesters may obtain copies of this document from DDC.

☐ Foreign announcement and dissemination of this report by DDC is not authorized.

☒ U. S. Government agencies may obtain copies of this document directly from DDC. Other qualified DDC users shall request through The Boeing Company, Seattle, Wn.

☐ U. S. military agencies may obtain copies of this document directly from DDC. Other users shall request through The Boeing Company, Seattle, Wn.

☐ All distribution of this document is controlled. Qualified DDC users shall request through The Boeing Company, Seattle, Wn.

PROPRIETARY NOTES

ACTIVE SHEET RECORD

SHEET NUMBER	REV LTR	ADDED SHEETS				SHEET NUMBER	REV LTR	ADDED SHEETS			
		SHEET NUMBER	REV LTR	SHEET NUMBER	REV LTR			SHEET NUMBER	REV LTR	SHEET NUMBER	REV LTR
1						40					
2						41					
3						42					
4						43					
5						44					
6						45					
7						46					
8						47					
9						48					
10						49					
11						50					
12						51					
13						52					
14						53					
15						54					
16						55					
17						56					
18						57					
19						58					
20						59					
21						60					
22						61					
23						62					
24						63					
25						64					
26						65					
27						66					
28						67					
29						68					
30						69					
31						70					
32						71					
33						72					
34						73					
35						74					
36						75					
37						76					
38						77					
39						78					

ACTIVE SHEET RECORD

SHEET NUMBER	REV LTR	ADDED SHEETS				SHEET NUMBER	REV LTR	ADDED SHEETS			
		SHEET NUMBER	REV LTR	SHEET NUMBER	REV LTR			SHEET NUMBER	REV LTR	SHEET NUMBER	REV LTR
79											
80											
81											
82											
83											
84											
85											
86											
87											
88											
89											
90											
91											
92											
93											
94											
95											
96											
97											
98											

REVISIONS

LTR	DESCRIPTION	DATE	APPROVAL

U3 4802 1432 ORIG. 4/65

DOCUMENT DISTRIBUTION RECORDS

CARD 2 OF ___ | DOC. NO. D2- 13-1

TITLE

MODEL: CLASSIFICATION

ORIGINATOR: UNIT: TEL. EXT:

REMARKS

NEW RELEASE ☐
PARTIAL REVISION ☐
COMPLETE REVISION ☐
REVISION SYMBOL

QTY / TYPE	NAME	ADDS DATE	LOCATION OR MAIL STOP	QTY / TYPE	NAME	ADDS DATE	LOCATION OR MAIL STOP
1	DR. F.M. SAUER STANFORD RESEARCH INSTITUTE MENLO PARK, CALIF.						
1	DR. R.B. VAILE STANFORD RESEARCH INSTITUTE MENLO PARK, CALIF.						
1	CHIEF SUPER. ATTEN: MR. O.A.H. JONES SUFFIELD EXPERIMENTAL STATION RALSTON, ALBERTA, CANADA						
1	LIBRARY (7)		13-84				

X 8802C ORIG. 1/65

NOTICE: PLEASE NOTIFY ENGINEERING DOCUMENT DISTRIBUTION RECORDS CLERK, ORGN. 2-2275 M/S 22-72 WHEN KEEP-UP-TO-DATE OF YOUR COPY(S) ARE NO LONGER REQUIRED

DOCUMENT DISTRIBUTION RECORDS

CARD 1 OF 2 | DOC. NO. D2-90633-1

TITLE: CRATERING CHARACTERISTICS OF WET AND DRY SAND

MODEL:

CLASSIFICATION: UNCLASSIFIED

ORIGINATOR: G.L. KEISTER UNIT: 2-7900 TEL. EXT: 5-5374

REMARKS:

NEW RELEASE ☐
PARTIAL REVISION ☐
COMPLETE REVISION ☐
REVISION SYMBOL

QTY / TYPE	NAME	ADDS DATE	LOCATION OR MAIL STOP	QTY / TYPE	NAME	ADDS DATE	LOCATION OR MAIL STOP
1	D.J.BECKER		2-7900 23-72	1	C.R. WAUCHOPE		2-7940 23-81
1	J.A. BLAYLOCK		2-7940 23-81	1	E.N. YORK		2-7920 47-24
1	D.D. COX		2-1605 47-26	1	D.M. YOUNG		2-7940 23-51
1	W.E. CHIST		2-7941 23-81	10	R.J. CARLSON - BOEING CO. SUITE 1707 5310 CENTRAL AVE. NE ALBUQUERQUE, N.M. 87108		
1	T.P. DAY		2-7940 23-81	1	DR. H. COOMBS GEOLOGY DEPT. U. OF W.		
10	C.V. FULMER		2-7930 23-82	1	DR. F. DANES DEPT. OF PHYSICS U. OF PUGET SOUND TACOMA, WN		
1	F.O. GRAY		2-5742 31-01	1	ALTON FRANDSEN NUCLEAR CRATERING GROUP USAC OF ENG. LAWRENCE RADIATION LAB. LIVERMORE, CALIF.		
1	J.R. HIGHLANDER		2-7940 23-81	1	E.B. AHLERS IIT RESEARCH INSTITUTE 10 WEST 35 ST. CHICAGO, 16, ILL.		
1	W.D. HODGE		2-5865 35-45	1	J.N. STRANGE USAE WATERWAYS EXP. STATION CORP. OF ENG. VICKSBURG, MISS.		
1	G.D. JONES		2-7940 23-81	1	DR. E. KAARSBURG DEPT. OF GEOPHYSICS GEORGIA TECH. ATLANTA, GEORGIA		
1	H. LIN		2-5500 47-23	1	DR. H.J. MOORE U.S. GEOLOGICAL SURVEY MENLO PARK, CALIF.		
1	J.H. LINCOLN		2-5412 32-36	1	DR. A.H. NAREVSKY AEROSPACE CORP. SAN BERNARDINO, CALIF.		
1	N.S.P. TECH INFO CENTER		2-7920 23-81	1	A.D. ROOKE, JR. USAE WATERWAYS EXP. STA. CORP. OF ENG. VICKSBURG, MISS.		
1	N.S.P. DOCUMENT GROUP		2-7900 23-72	1	M.L. MERRITT SANDIA CORP., SANDIA BASE 5232 ALBUQUERQUE, NEW MEXICO		
1	W.A. ROBERTS		2-7930 23-82	1	L.J. VORTMAN SANDIA CORP. SANDIA BASE 5232 ALBUQUERQUE, NEW MEXICO		
1	T.P. RONA		2-1605 47-19	1	DDC, ALEXANDRIA, VA.		
1	G.M. ROUZE		2-5865 35-45	1	DR. E.M. SHOEMAKER U.S. GEOLOGICAL SURVEY ASTROGEOLOGICAL LAB. FLAGSTAFF, ARIZONA		
1	A.N. SAKAMOTO		2-5742 31-01	1	DR. R.B. BALDWIN 1745 ALEXANDER RD. SE EAST GRAND RAPIDS, MICHIGAN		

X 5302C ORIG. 1 '65

NOTICE: PLEASE NOTIFY ENGINEERING DOCUMENT DISTRIBUTION RECORDS CLERK, ORGN. 2-2225 M.S. 2-22 WHEN KEEP-UP-TO-DATE OF YOUR COPY(S) ARE NO LONGER REQUIRED.

2-5153

Unclassified

Security Classification

DOCUMENT CONTROL DATA - R&D

(Security classification of title, body of abstract and indexing annotation must be entered when the overall report is classified)

1 ORIGINATING ACTIVITY (Corporate author)

The Boeing Company

2a REPORT SECURITY CLASSIFICATION

Unclassified

2b GROUP

3 REPORT TITLE

(6) (upper case)

Cratering Characteristics of Wet and Dry Sand,

4 DESCRIPTIVE NOTES (type of report and inclusive dates)

(9) Final Report,

5 AUTHOR(S) (Last name, first name, initial)

[redacted] (10) Charles V. Fulmer.

(11)

6 REPORT DATE

7 Oct [redacted] 65,

7a TOTAL NO. OF PAGES

(12) 94p.

7b NO. OF REFS

9

8a CONTRACT OR GRANT NO.

None

b PROJECT NO.

c

d

9a ORIGINATOR'S REPORT NUMBER(S)

(14) D2-90683-1

9b OTHER REPORT NO(S) (Any other numbers that may be assigned this report)

None

10 AVAILABILITY/LIMITATION NOTICES

U. S. Government agencies may obtain copies of this document directly from DDC. Other users shall request through The Boeing Company, Seattle, Wn.

11 SUPPLEMENTARY NOTES

12 SPONSORING MILITARY ACTIVITY

None

13 ABSTRACT

Thirty-seven 1-pound (lb) spheres of TNT were individually exploded at various depths of burst in a sand test pad. Of these, 19 detonations were conducted in a dry sand-medium and 18 in a wet-sand medium at comparable depths of burst. The craters produced were accurately surveyed by using a bridge and probe assembly. The results of these crater surveys are shown on topographic maps. In addition to topographic measurements, volumetric measurements of the craters, ejecta measurements, and medium density, moisture content, grain size distributions are presented. The experimental procedures, equipment test area, and sand medium are discussed in detail. The comparison of crater characteristics of wet- and dry-sand environments are discussed and the results presented in tables and graphs. In addition to the crater characteristics, the formation of intracone structures, shock-agglutinated missiles, and the reduction in size of the sand grains composing the medium are discussed.

DD FORM 1 JAN 64 1473

U3 4802 1030 ORIG. 12 64

PART 1 OF 2

REV LTR _____

Security Classification

D2-90683-1

BOEING NO.

SH 59600

14 KEY WORDS	LINK A		LINK B		LINK C	
	ROLE	WT	ROLE	WT	ROLE	WT
High Explosive						
Mass distribution						
True Crater						
Fallback Material						
Intrasone structure						
Lip crest						
Apparent lip crest height						
Surface burst						
Uplifted ground surface						
Original ground surface						
Ejecta						
Crater characteristics						

INSTRUCTIONS

1. ORIGINATING ACTIVITY: Enter the name and address of the contractor, subcontractor, grantee, Department of Defense activity or other organization (corporate author) issuing the report.

2a. REPORT SECURITY CLASSIFICATION: Enter the overall security classification of the report. Indicate whether "Restricted Data" is included. Marking is to be in accordance with appropriate security regulations.

2b. GROUP: Automatic downgrading is specified in DoD Directive 5200.10 and Armed Forces Industrial Manual. Enter the group number. Also, when applicable, show that optional markings have been used for Group 3 or Group 4 as authorized.

3. REPORT TITLE: Enter the complete report title in all capital letters. Titles in all cases should be unclassified. If a meaningful title cannot be selected without classification, show title classification in all capitals in parenthesis immediately following the title.

4. DESCRIPTIVE NOTES: If appropriate, enter the type of report, e.g., interim, progress, summary, annual, or final. Give the inclusive dates when a specific reporting period is covered.

5. AUTHOR(S): Enter the name(s) of author(s) as shown on or in the report. Enter last name, first name, middle initial. If military, show rank and branch of service. The name of the principal author is an absolute minimum requirement.

6. REPORT DATE: Enter the date of the report as day, month, year, or month, year. If more than one date appears on the report, use date of publication.

7. TOTAL NUMBER OF PAGES: The total page count should follow normal pagination procedures, i.e., enter the number of pages containing information.

7b. NUMBER OF REFERENCES: Enter the total number of references cited in the report.

8a. CONTRACT OR GRANT NUMBER: If appropriate, enter the applicable number of the contract or grant under which the report was written.

8b, &c, & &d. PROJECT NUMBER: Enter the appropriate military department identification, such as project number, subproject number, system numbers, task number, etc.

9a. ORIGINATOR'S REPORT NUMBER(S): Enter the official report number by which the document will be identified and controlled by the originating activity. This number must be unique to this report.

9b. OTHER REPORT NUMBER(S): If the report has been assigned any other report numbers (either by the originator or by the sponsor), also enter this number(s).

10. AVAILABILITY LIMITATION NOTICES: Enter any limitations on further dissemination of the report, other than those imposed by security classification, using standard statements such as:

(1) "Qualified requesters may obtain copies of this report from DDC."

(2) "Foreign announcement and dissemination of this report by DDC is not authorized."

(3) "U.S. Government agencies may obtain copies of this report directly from DDC. Other qualified DDC users shall request through _____."

(4) "U.S. military agencies may obtain copies of this report directly from DDC. Other qualified users shall request through _____."

(5) "All distribution of this report is controlled. Qualified DDC users shall request through _____."

If the report has been furnished to the Office of Technical Services, Department of Commerce, for sale to the public, indicate this fact and enter the price, if known.

11. SUPPLEMENTARY NOTES: Use for additional explanatory notes.

12. SPONSORING MILITARY ACTIVITY: Enter the name of the departmental project office or laboratory sponsoring (paying for) the research and development. Include address.

13. ABSTRACT: Enter an abstract giving a brief and factual summary of the document indicative of the report, even though it may also appear elsewhere in the body of the technical report. If additional space is required, a continuation sheet shall be attached.

It is highly desirable that the abstract of classified reports be unclassified. Each paragraph of the abstract shall end with an indication of the military security classification of the information in the paragraph, represented as (TS), (S), (C), or (U).

There is no limitation on the length of the abstract. However, the suggested length is from 150 to 225 words.

14. KEY WORDS: Key words are technically meaningful terms or short phrases that characterize a report and may be used as index entries for cataloging the report. Key words must be selected so that no security classification is required. Identifiers, such as equipment model designation, trade name, military project code name, geographic location, may be used as key words but will be followed by an indication of technical context. The assignment of links, roles, and weights is optional.